AALBORG UNIVERSITY

Master's thesis

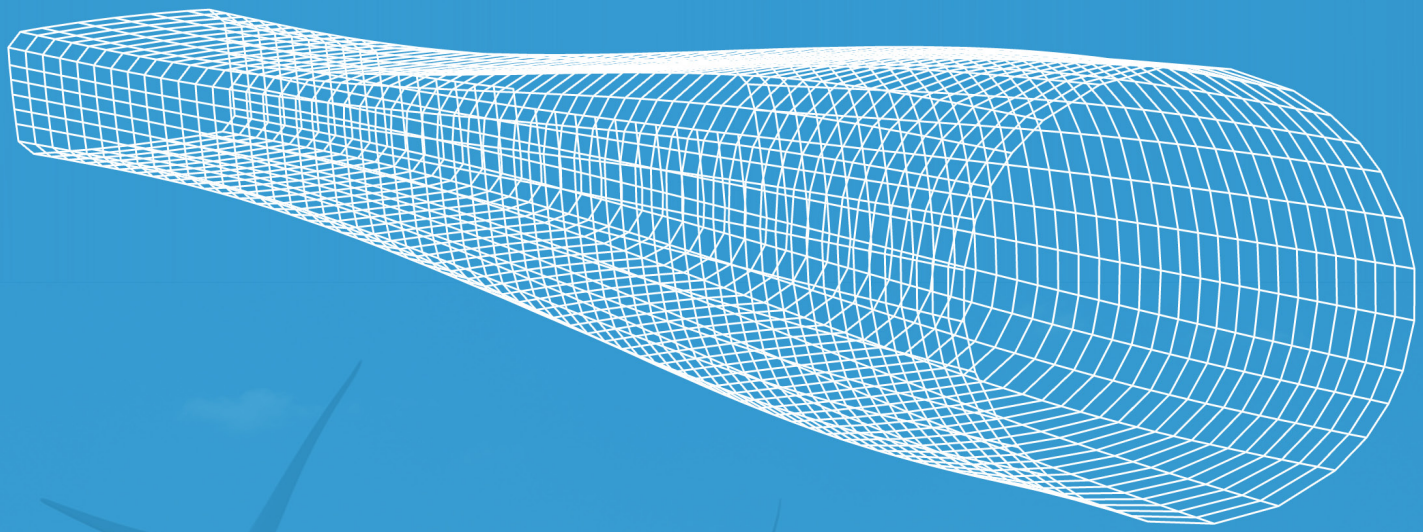

Optimisation of Composite Structures Using Lamination Parameters in a Finite Element Application

Spring 2011
Design of Mechanical Systems
Department of Mechanical & Manufacturing Engineering

Group 29a, DMS10
René Sørensen
Jesper Kann

AALBORG UNIVERSITY

Aalborg University
Department of Mechanical
& Manufacturing Engineering
Pontoppidanstræde 105
9220 Aalborg Ø
Tel (+45) 9940 9300
Fax (+45) 9815 1675
http://www.m-tech.aau.dk/

Title:

Optimisation of Composite Structures Using Lamination Parameters in a Finite Element Application

Semester theme:
Industrial development work

Project period:
The M-sectors tenth semester
February 1st 2011 – May 31st 2011

Project Group:
29a, DMS10

Participants:
René Sørensen
Jesper Kann

Supervisors:
Professor, Ph.D. Erik Lund
Assistant Professor, Ph.D. Esben Lindgaard

Copies: 5

Number of Pages: 92

René Sørensen

Jesper Kann

Abstract

This Master's thesis deals with mathematical optimisation of composite structures. A new method is presented, in which it is attempted to overcome the non-convex nature often associated with optimisation of composite structures modelled with finite elements.

First of all, the underlying theory is presented. The brief overview of shell theory is given, and the formulations needed in order to incorporate it into a finite element analysis application are derived. That is, the geometric representations needed are established, followed by an expression for the strain-displacement matrix. From this the layer-wise thickness integration needed to obtain the stiffness for a laminate structures is studied and used to derive an expression for performing *explicit thickness integration* instead, which involves slight approximations of the element Jacobian. Further approximations can, however, be made resulting in an expression for doing *approximate explicit thickness integration*. On top of the stiffness formulations the constitutive relations are addressed. Aided by the lamina invariants, the constitutive relations are rephrased to include the *lamination parameters* assuming that the laminate under inspection is composed of only a single material through all layers (with different orientations though). The result of this, in combination with the formulation of explicit thickness integration, is that the element stiffness matrix is seen to be linear in the lamination parameters. The above reformulations are at last verified numerically and seen to give accurate results. Furthermore it is seen that the expression of explicit thickness integration is especially efficient when working with laminates consisting of many layers.

Based on the presented theory the newly developed method is presented. First of all, the focus is brought to maximum stiffness optimisation with reference to the standard model, which is done by minimising the compliance. With the expressions of explicit thickness in hand the sensitivities needed for such an optimisation can be determined analytically, which is verified numerically to give accurate results.

The method of optimisation is based on a patch-compatible parameterisation where lamination parameters play an essential role. In order to overcome the non-convex nature of the optimisation problem some characteristics of lamination parameters are studied, namely the problem of feasibility and the question of convexity of the objective function. If the objective function is optimised with lamination parameters as design variables the strain energy is in fact convex. However, this approach would give problems with ensuring feasibility of the final result. Hence the problems are sought solved by keeping the fibre orientations of the laminate as design variables and then overcoming the non-convex nature of the problem by designing the optimisation method as a *two-step approach*. Thus some of the ideas from the *two-step approach* presented by [Foldager, 1999] are utilised in combination with results from [Kann and Sørensen, 2010] in order to develop a new and more robust two-step method. The method developed includes an *identification process* where an *identification function* based on a local linearisation is minimised by the use of a genetic algorithm.

The developed method have been implemented in MUST with the ability to switch between different numbers of applied lamination parameters in the identification process as well as both a full and an approximate method.

In order to test the new method numeric experiments have been conducted. Three simple problems of "academic character" are presented - a cantilever beam with a distributed load, a flat plate with a uniform pressure normal to the surface, and a pinched hemisphere with different curvature-to-thickness ratios. The three examples show that successful identification is indeed found in several instances, meaning that a local minimum can be overcome. However, the success is dependent on a *several-to-one* relationship between the number of design variables and the number of lamina-

tion parameters. Furthermore the results indicate that one of the first problems arising, when doing stiffness optimisation of composite structures, seems to be that the design variables get stuck at the bounds of the design space.

Asides from the experiments of "academic character", a more "industrial/practical" experiment has been conducted as well. The geometry under inspection is a *generic main spar* from a wind turbine blade. The conclusion from this experiment is first and foremost that the method can indeed be used on large industrial structures. Furthermore the results are close to what would be expected, however, there are small differences. These differences can be explained by the patch breakdown and effects of so small magnitude that they cannot be captured numerically. Finally, there is a strong indication that post-processing of the optimised structure is indeed necessary, as the design typically contains features which cannot be realised, or maybe is too complicated or too impractical for the manufacturer to fully realise the optimised structural design. The amount of time needed for post-processing may be reduced by incorporating restrictions associated with the manufacturing process into the numerical optimisation routines.

Preface

This Master's thesis is written by group 29a on the tenth semester of the *Design of Mechanical Systems*-programme at Aalborg University, spring 2011. The semester theme is *Industrial development work* and the title of the project is:

> *Optimisation of Composite Structures Using Lamination Parameters in a Finite Element Application*

The project group would like to thank Professor Krister Svanberg for help with providing articles which seemed hard to find using the universities library service.
The report consists of a main report and additional documentation given in appendices. In appendix C a CD is found with the following content:

- Electronic copy of the report.
- Electronic copies of some articles which have been hard to get hold of, and therefore is provided in order to help along the reader doing the same job.
- The developed edition of MUST. The software is provided both as executable files as well as source code.
- Relevant FE-examples used in the report.

Citations and references are done in accordance with the Harvard Style where the last name of the author and year of publication are given in square brackets. The bibliography is found on page 92.

Figures and equations are numbered according to the chapter in which they are presented—for instance: *figure 1.2* is the 2nd figure in chapter 1. Appendices are labelled with capital letters followed by a section number—for instance: *A.1* is the 1st section in appendix A.

The following mathematical notation is used throughout the text:

Vectors:	$\vec{x}$
Matrices:	$\underline{K}$

The following notation is used for specifying the lay-ups of composite laminates:

Four ply laminate:	$(\theta_1, \theta_2, \theta_3, \theta_4)$
A symmetric laminate:	$(\theta_1, \theta_2, \theta_2, \theta_1) \Rightarrow (\theta_1, \theta_2)_S$
An antisymmetric laminate:	$(\theta_1, \theta_2, -\theta_2, -\theta_1) \Rightarrow (\theta_1, \theta_2)_A$
Unequal ply thickness:	$(\theta_1 @ t_1, \theta_2 @ t_2, \theta_3 @ t_3)$

Unless otherwise stated all plies of a laminate are of equal thickness and have the same orthotropic material properties.

Further notation and nomenclature is given where relevant and a general list of nomenclature is found on page 94.

Contents

Chapter

1

Introduction

In recent years the world agenda has really been set on care for climate and environment as well as efficient use of raw materials. In terms of efficient use of materials composite structures are a key player. The idea behind building structures from composite materials is focused around efficient use of materials. The world of composites has thus drawn quite a lot of attention in recent years, and the result is that composite materials are being used to a larger and larger extent. Composite materials are in particular used in high-performance structures due their high stiffness-to-weight as well as strength-to-weight ratios. Thus composite materials are today a key player in the production of boats, rackets, aircrafts, space shuttles, bicycles, race cars, wind turbine blades, and many others. The many applications of composite materials have naturally given many stakeholders within research and development of such materials which again has resulted in an enormous on-going development within the area.

The main idea of composite structures is to utilise the materials in the best possible way by *tailoring* the material to the application. A composite material is thus not just used in an immediate form but designed to meet the specified requirements. From mechanics of materials it is well known that the maximum stresses occur in a certain direction. Thus, having uniform strength of the material in all directions leads to a natural "oversizing" in the non-maximum directions. This oversizing is strongly reduced in laminated composite structures as the material is designed to have directional strength where needed.

Directional strength is not the only possibility of tailoring a composite material to the application. A wide variety of properties can be improved by the use of composite materials. Some of these properties are [Jones, 1999]:

- Strength
- Stiffness
- Corrosion resistance
- Wear resistance
- Attractiveness
- Weight
- Fatigue life
- Temperature-dependent behaviour
- Thermal insulation
- Thermal conductivity
- Acoustical insulation

Design of such property-improved structures is often done with inclusion of the finite element method in one way or the other. The challenge here though is to obtain an efficient mathematical formulation in order to reduce calculation time. Finite element analysis has nowadays been a central part of research and development of mechanical engineering for quite some years, and as such efficient finite element formulations are in general obtained for a lot of applications and scenarios. However, efficient modelling of composite materials in finite element applications does lag some

years behind. One of the areas that has been under research for the last couple of decades, and still is, is the modelling and analysis of thin-walled structures. Thus efficient plate and shell formulations are of great interest, and hence that is exactly one of the main areas of this thesis - to do efficient plate/shell modelling of composite laminates.

Though the inclusion of composite materials in a plate or shell formulation can give both accurate and effective analyses, the design phase also becomes quite complex. Thus a powerful synthesis tool such as mathematical optimisation now becomes even more complicated when working with composite materials. Actually, to do efficient optimisation of the above is not possible offhand. A traditional gradient-based optimisation algorithm is prone to get stuck in a local minimum, whereby the result of the process becomes a non-optimal structure. The solution could be to do a more complete scan of the design space, but with the inclusion of a finite element analysis this usually gets too computationally heavy. This issue is sought solved in this thesis. The proposed solution is based on a stiffness formulation incorporating the so-called lamination parameters. These lamination parameters are mathematical quantities that arise from the physical variables describing the composite material, namely the fibre orientation and the thicknesses of each ply in the material. The lamination parameters themselves do not give any physical meaning, but they do carry some characteristics which make them well-suited as a tool for optimisation. However, though the lamination parameters bring some nice and convenient aspects to the optimisation they also bring several challenges that has to be overcome, but that are still not solved. In the following subsection a brief exposition of the current status on optimisation of composite structures is given with a special weight on research regarding lamination parameters.

1.1 State-of-the-art

In recent years much effort has been put on developing an efficient method for optimisation of composite structures in such a way that the non-convex nature of the problem is overcome. This has lead to many new methods within the area. Examples of such methods could be those presented by [Stegmann and Lund, 2005], [Hammer et al., 1997], [Foldager, 1999], [Setoodeh et al., 2006], and [Bloomfield et al., 2009], where the latter four included lamination parameters in one way or the other. Though these methods represent state of the art within the field they are all designed for a specific application which gives limitations when used in another context. E.g. the method presented by [Hammer et al., 1997] is as presented restricted to laminates with three layers which quickly becomes insufficient. Examples of more generally applicable methods are given by [Stegmann and Lund, 2005], who used *discrete material optimisation* to determine the optimal material from a predefined set of possibilities, and [Bloomfield et al., 2009], who established the *feasibility constraints* of the lamination parameters for a set of laminates with homogenous material but different angular orientations of each layer. Though both of these methods are general in terms of the allowed loading scenarios, they do have that in common that they are restricted in terms of the design variables as these are treated discretely. On the contrary e.g. the method presented by [Hammer et al., 1997] and [Setoodeh et al., 2006] has no restrictions on the design variables as these are treated continuously, but do impose restrictions on the loading scenario and how the laminate must be designed. As it is today, to the knowledge of the authors, the only restriction free method with continuously treated design variables and the potential to overcome the non-convex nature of the problem is the method by [Foldager, 1999]. However, as shall be clarified later in this thesis this method is not at all flawless.

In the attempt to draw general optimisation of composite structures closer, several people have contributed with various partial results and/or characteristics of lamination parameters. Among these, the first to mention should naturally be [Tsai and Pagano, 1968] who introduced the lamination parameters. The first to establish anything concrete about the feasibility of the lamination parameters were [Miki, 1982] who determined the bounds of the feasible domain for an orthotropic laminate sub-

jected to either in-plane or out-of-plane loads. After this many people have contributed with other special cases of bounds on the feasible domain, though still without any achieving the bound for the general case. Among other results worth noticing are [Fukunaga and Sekine, 1992] who determined the relationship between the four in-plane parameters and also for the four out-of-plane parameters, [Grenestedt and Gudmundson, 1993] who showed that the feasible domain of the general case is convex, and [Svanberg, 1984] who proved that if the finite element stiffness matrix is linear in the design variables, then the problem of optimising w.r.t. maximum stiffness is in fact convex. This was later verified by [Grenestedt and Gudmundson, 1993], who also determined that the application of lamination parameters as design variables in stiffness related optimisation would produce a convex design space.

With regards to efficient shell formulations [Kumar and Palaninathan, 1997] developed the basis for the method of explicit thickness integration, whereas [Hvejsel and Hansen, 2007] implemented a formulation of such a method in the finite element program MUST. Later [Laustsen and Vestergaard, 2010] expanded the implementation in MUST to include non-linear behaviour. However, none of these implementations included the use of lamination parameters.

Asides from this, the authors of the current thesis have done some preliminary work before the work accounted for in this thesis [Kann and Sørensen, 2010] (an electronic copy of the report is found on the CD in appendix C). This previous work studied the possibilities of utilising some of the preliminary ideas of the method presented by [Foldager, 1999] in combination with a newly developed and more robust formulation. The previous studies were based on plate theory which was treated in Matlab without the use of finite elements. Thus only a uniform plate with uniform loads could be handled.

In this thesis it is attempted to utilise some of the results from the previous work in order to obtain a more generally applicable method [Kann and Sørensen, 2010]. Thus earlier results are combined and utilised to develop and implement a generally applicable optimisation procedure for laminated composite shells with the use of the efficient finite element formulations in MUST.

1.2 Outline of Report

The method presented in this thesis is based on the idea presented by [Foldager, 1999] and some of the results presented in [Kann and Sørensen, 2010]. The thesis enables optimisation of composite laminates in a formulation where the angular orientations of the plies in the laminate are used as design variables without any restrictions. The method is applicable to both plate and shell formulations of composite laminates where both of these are treated with efficient finite element formulations. Finite element analysis is thus an integrated part of the method.

The thesis documents the development of the formulations as well as a brief exposition of the current implementation in MUST. Following the implementation several numerical experiments have been performed in order to study the performance of the method. These results are presented in the thesis as well.

The report is divided into seven chapters which are organised as follows:

Chapter 1: Introduction and outline of the thesis.

Chapter 2: A theoretical exposition of efficient shell modelling of composite laminates in finite element analysis.

Chapter 3: Presentation of the developed optimisation method.

Chapter 4: Brief overview of how the developed method has been incorporated into MUST.

Chapter 5: Presentation of results from the performed numerical experiments.

Chapter 6: Discussions and conclusions of the thesis in general.

Chapter 7: Suggestions for further work with the method.

Chapter

2

Shell Element Theory

This chapter serves to introduce the theoretical foundation of shell theory in a finite element context. Thus the basic concepts of shell theory are briefly presented. Next necessary quantities such as geometric representations and a strain-displacement matrix are derived in order to incorporate the shell theory into a finite element analysis. Given this, some effort is made into reformulating the expression for the element stiffness matrix in order to obtain a more efficient formulation with what is called explicit thickness integration *and as well* approximated explicit thickness integration. *At last, the constitutive relations are briefly outlined and a reformulation is made implementing the so-called* lamination parameters *which shall be used later on for performing optimisation. The chapter is based on [Stegmann and Lund, 2002], [Hvejsel and Hansen, 2007], [Laustsen and Vestergaard, 2010], [Jones, 1999] and [Tsai and Pagano, 1968].*

2.1 Basic Concepts of Shell Elements

A shell is geometrically characterised as a curved or doubly curved solid structure where the extent in one of the dimensions is negligible when compared to the other two. The geometric characteristic of the shell makes it possible to represent the shell by a reference surface and a thickness, thus obtaining a 2D representation of the structure. Resulting from the geometry is that the ideal way to load a shell structure is to load it with purely membrane stresses.

The shell in mechanics of materials can be understood as a generalisation of a plate (or the plate as a specific case of a shell). The difference is, as already implicitly stated, the permission of curved or doubly curved surfaces. If the structure in fact was properly loaded a full and exhaustive 3D description would not at all be necessary — actually a simple 2D description with kinematic assumptions allowing the structure to carry loads in pure membrane and pure bending stresses only would be sufficient. However, due to external loads, supports, and the slightly curved geometry, this idealisation is seldom sufficient. The Kirchhoff-Love assumptions known from classical plate theory are thus too restrictive for a shell. Instead a *first order shear deformation theory (FSDT)* is applied by allowing the transverse normals of the reference surface to rotate following the Reissner-Mindlin assumptions:

- The shell is thin when compared to the radius of curvature ($t/R \ll 1$).
- The linear and angular deformations of the shell are small.
- The transverse normal stress is negligible.
- Normals to the reference plane before deformation remain straight and inextensible after deformation, but are allowed to rotate.

The first assumption is the most basic, since if this is violated the other three assumptions are also violated. The second assumption ensures that the governing equations become linear since the deformed geometry can be related directly to the non-deformed geometry. The third assumption is the assumption of a state of plane stress which is reasonable for a thin shell. The fourth assumption is where the distinction from the Kirchhoff-Love assumptions is found. The transverse normal strains are assumed negligible as they also are in the Kirchhoff-Love assumptions, but the transverse normals are allowed to rotate. Thus the FSDT accounts for transverse shear strains while it still neglects transverse normal strains.

An effect of the Reissner-Mindlin assumptions is that too much shear deformation energy is absorbed as the shear strains are modelled as a constant contribution through the thickness when in fact they should be modelled as varying through the thickness. For an isotropic plate a shear correction factor of 5/6 can be determined analytically to be appropriate. The choice of shear correction factor is, however, strongly dependent on geometry and loading conditions. For a laminated plate 5/6 is often used as compensation, although in fact the distributions should be piecewise parabolic.

The 2D description of the model is obtained by relating the geometry of the shell to the mid-surface as a reference surface, as indicated in the shell element sketched in figure 2.1. The fundamental assumptions, as explained above, are applicable only for thin to moderately thick structures. In this connection it should furthermore be emphasised that for layered composite structures the term "thin" is a question of both thickness and stiffness of the layers.

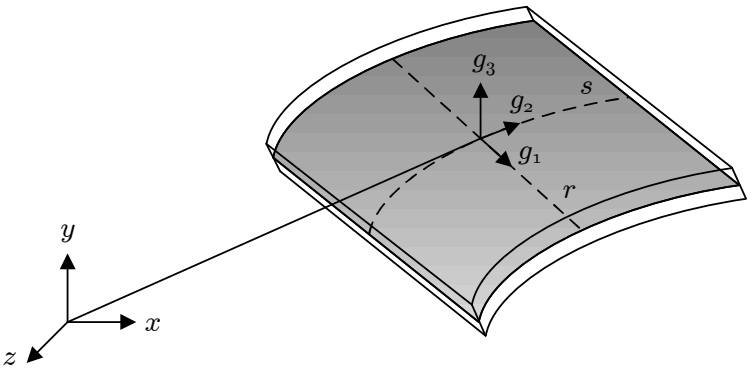

Figure 2.1: *Illustration of the reference surface of a shell. The shaded area is the reference surface.*

2.2 Geometric Representation

In order to model anything with shell elements a proper geometric representation is needed. That is, appropriate coordinate systems as well as a reliable shell element formulation need to be established.

2.2.1 Coordinate Systems

When modelling with shell elements the need for different coordinate systems quickly arises. The geometric characteristics can be most conveniently defined in one coordinate system while the material properties are defined in another. Hence, in order to do a proper and exhaustive analysis different local coordinate systems must be defined.

The element is, as illustrated in figure 2.1, attached a set of *natural coordinates* r, s, and t, which all attain values within ± 1 thus mapping the physical geometry in a global space to the natural space, as illustrated in figure 2.2. The natural coordinates do not necessarily constitute a Cartesian base.

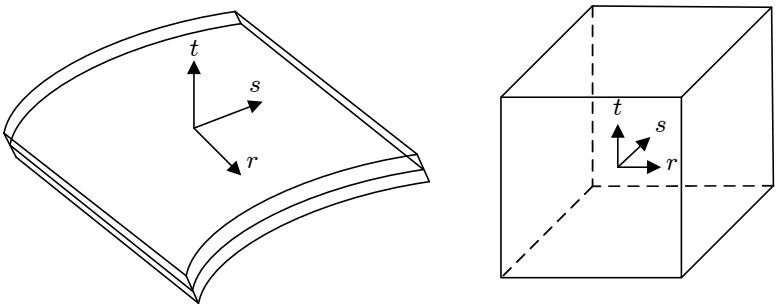

Figure 2.2: *Mapping of shell element geometry from (a) global space to (b) natural space.*

2.2.1.1 Element Coordinate System

In order to fully describe the geometry of the shell a parameterisation is made based on the natural surface coordinates r and s, and the natural thickness coordinate t. Provided that the thickness direction unit vector, $\vec{v}_3$ is given, any point in the structure can then be described as:

$$\vec{x}(r,s,t) = \vec{x}_0(r,s) + t\frac{h}{2}\vec{v}_3 \tag{2.1}$$

where:

$\vec{x}$	Any point in the structure.
$\vec{x}_0$	The point on the reference surface.
r, s, t	Natural curvilinear coordinates.
h	The thickness of the shell.
$\vec{v}_3$	The thickness direction unit vector.

Here the thickness direction unit vector is defined based on the *covariant tangent base vectors* $\vec{g}_i$. The covariant tangent base vectors are in general defined as:

$$\vec{g}_i = \frac{\partial \vec{x}}{\partial r_i} \tag{2.2}$$

where:

r_i	Denotes r, s, and t, respectively

The thickness direction unit vector is then determined as the unit normal to the tangent plane spanned by the two base vectors $\vec{g}_1$ and $\vec{g}_2$. The thickness direction unit vector is thus determined as:

$$\vec{v}_3 = \frac{\vec{g}_1 \times \vec{g}_2}{|\vec{g}_1 \times \vec{g}_2|} \tag{2.3}$$

The thickness direction unit vector is also referred to as *the node director*. It should be noted that $\vec{v}_3$ is normal to $\vec{g}_1$ and $\vec{g}_2$, whereas $\vec{g}_3$ not necessarily is. Also, the r, s, and t axes constitute *the element coordinate system* (ECS) which not necessarily is a Cartesian coordinate system.

2.2.1.2 Material Coordinate System

Constitutive relations are normally defined in a Cartesian coordinate system. Hence the ECS is inappropriate. A new Cartesian coordinate system, *the material coordinate system* (MCS) is thus defined in order to handle the constitutive relations efficiently. The MCS has three unit base vectors $\vec{m}_1$, $\vec{m}_2$,

and $\vec{m}_3$. The two base vectors lie in the tangent plane of the reference surface whereas the last, $\vec{m}_3$, is normal to the reference surface. Hence $\vec{m}_3$ is equal to $\vec{v}_3$, cf. equation (2.3).

In order to determine $\vec{m}_1$ and $\vec{m}_2$ two auxiliary vectors, $\vec{a}$ and $\vec{b}$, are constructed from the covariant tangent base. $\vec{a}$ and $\vec{b}$ are defined as:

$$\vec{a} = \frac{\vec{g}_1 + \vec{g}_2}{\left|\vec{g}_1 + \vec{g}_2\right|} \quad , \quad \vec{b} = \frac{\vec{m}_3 \times \vec{a}}{|\vec{m}_3 \times \vec{a}|} \tag{2.4}$$

From the two auxiliary vectors $\vec{m}_1$ and $\vec{m}_2$ are defined as:

$$\vec{m}_1 = \frac{\sqrt{2}}{2}(\vec{a} - \vec{b}) \quad , \quad \vec{m}_2 = \frac{\sqrt{2}}{2}(\vec{a} + \vec{b}) \tag{2.5}$$

Hereby the three base vectors $\vec{m}_i$ are uniquely defined and the constitutive relations can be stated according to this. Obviously, with one coordinate system being Cartesian and the other not necessarily, the two coordinate systems (ECS and MCS) cannot always be coincident. However, with the method accounted for here, the angle between $\vec{g}_1$ and $\vec{m}_1$ is identical to the angle between $\vec{g}_2$ and $\vec{m}_2$ which ensures that the MCS-base is as close to the ECS-base as possible.

If only isotropic materials were used, the MCS would be sufficient to fully describe the constitutive relations. However, with the use of orthotropic materials a need for *principal material directions* (PMD) arises. The PMD are normally described using a single angle θ. The angle is to be interpreted as a rotation of the $\vec{m}_i$-base around the $\vec{m}_3$ axis. Thus the first principal direction of the orthotropic material is found rotated an angle θ around the $\vec{m}_3$-axis from $\vec{m}_1$, and the second principal direction is found rotated an angle $\theta + \frac{\pi}{2}$ around the $\vec{m}_3$-axis from $\vec{m}_1$. The third principal direction is coincident with $\vec{m}_3$.

2.2.1.3 Director Coordinate System

In each node, a, a *director coordinate system* (DCS) with a Cartesian base $\vec{v}_i$ is attached. The DCS is used for defining the axes of the rotational degrees of freedom of *the node director* which is a vector indicating the thickness direction of the element. The third axis of the DCS-base is the node director defined above. To complete the local Cartesian base two other base vectors must be established. These can in principle be chosen arbitrarily as long as the definition is unique. In different literature many different schemes for this task exist. In MUST the approach is first to check if $\vec{v}_3^a$ coincides with $\vec{j}$. If this is the case then the remaining two base vectors are simply chosen as $\vec{v}_1^a = \vec{i}$ and $\vec{v}_2^a = \vec{k}$. Otherwise the two remaining base vectors are defined as:

$$\vec{v}_1^a = \frac{\vec{j} \times \vec{v}_3^a}{\left|\vec{j} \times \vec{v}_3^a\right|} \quad , \quad \vec{v}_2^a = \vec{v}_1^a \times \vec{v}_3^a \tag{2.6}$$

2.2.2 Degenerated Shell Element

The shell element is a special type of element developed by eliminating nodes from a solid element imposing the kinematic assumptions described in section 2.1. The process of removing nodes is called *degeneration*. A general 20-node solid element is able to interpolate displacements quadratically in all three directions for all nodes. However, this is unnecessary for a shell as the normals in the thickness direction are assumed to remain straight and inextensible. Hence, some nodes can be removed without losing notable accuracy.

The degeneration process is done in two steps, as sketched in figure 2.3. First the mid-nodes in the thickness direction are removed as with linear interpolation functions they can just as well be interpolated from the two corner nodes, thus removing four nodes from the element. The next

step is to utilise the fact that normals to the reference surface are assumed to be inextensible. When this is the case, the relative information extracted from two corresponding corner nodes is simply the direction of the thickness, as the distance between them is kept constant. This can be done "cheaper" by having a single node where the rotation of the node director is accounted for. The latter step requires two additional degrees of freedom for the shell element though. So even though the number of nodes is reduced from 16 to 8, the number of degrees of freedom is only reduced from 48 to 40. The result is a shell element with 8 nodes on the reference surface and 40 degrees of freedom which encompasses the kinematic assumptions of shell theory presented in section 2.1.

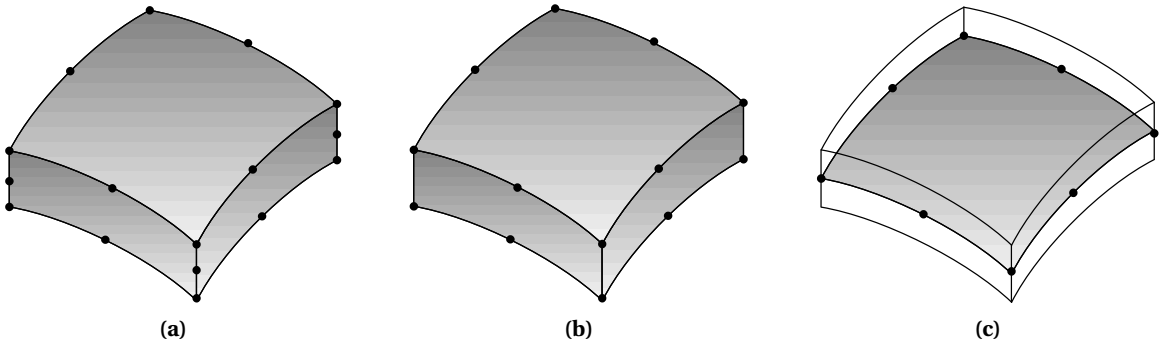

Figure 2.3: *Degeneration of (a) a 20-node solid element into first (b) a 16-node solid element with interpolated midnodes and next into (c) an 8-node shell element.*

2.2.3 Interpolation Functions

Following the development of a degenerated shell element, the interpolation of coordinates between the nodes must also be rephrased. Traditionally any point within a solid element given in natural curvilinear (r,s,t)-coordinates can be transformed to global Cartesian (x,y,x)-coordinates as:

$$\vec{x} = \sum_{a=1}^{n_{solid}} N_a^{3D}\, \vec{x}_a^{3D} \tag{2.7}$$

where:

	$\vec{x}$	Global Cartesian coordinates of arbitrary point.
	n_{solid}	Number of nodes in a solid element.
	N_a^{3D}	Interpolation function for node a — is a function of the natural (r,s,t)-coordinates.
	$\vec{x}_a^{3D}$	Global Cartesian coordinates of node a in the solid element.

In order to reduce the equations to hold for a 8-node shell element, the trick is to divide the interpolation functions $N_a^{3D}(r,s,t) = \frac{1}{8}(1\pm r)(1\pm s)(1\pm t)$ into a plane part $N_a^{2D} = \frac{1}{2}(1\pm r)(1\pm s)$ and a thickness part $N_a^t = \frac{1}{2}(1\pm t)$, with the interpolation functions being linear. The interpolation of coordinates can

then be rephrased as:

$$\begin{aligned}\vec{x} &= \sum_{a=1}^{n_{solid}} N_a^{3D}\vec{x}_a^{3D} = \sum_{a=1}^{n_{solid}} N_a^t N_a^{2D}\vec{x}_a^{3D} \\ &= \sum_{a=1}^{n_{solid}} \frac{1}{2}(1\pm t)N_a^{2D}\vec{x}_a^{3D} \\ &= \sum_{a=1}^{n_{shell}} \left(\frac{1}{2}(1+t)N_a^{2D}\vec{x}_a^{top} + \frac{1}{2}(1-t)N_a^{2D}\vec{x}_a^{bottom}\right) \\ &= \sum_{a=1}^{n_{shell}} \left(N_a^{2D}\frac{1}{2}\left(\vec{x}_a^{top} + \vec{x}_a^{bottom}\right) + \frac{t}{2}\left(\vec{x}_a^{top} - \vec{x}_a^{bottom}\right)\right)\end{aligned} \tag{2.8}$$

where: n_{shell} $= \frac{1}{2}(n_{solid} - n_{midnodes})$. The number of nodes in a shell element. Hence a for a 16-node element refers to a "virtual" node on the reference surface.

$\vec{x}_a^{top}$ Global Cartesian coordinates of the top nodes of a 16-node element as sketched in figure 2.3b.

$\vec{x}_a^{bottom}$ Global Cartesian coordinates of the bottom nodes of a 16-node element as sketched in figure 2.3b.

Now the coordinates of the nodes on the reference surface are expressed in terms of the top and bottom nodes as:

$$\vec{x}_a = \frac{1}{2}\left(\vec{x}_a^{top} + \vec{x}_a^{bottom}\right) \tag{2.9}$$

where: $\vec{x}_a$ Global Cartesian coordinates of the nodes on the reference surface of a shell element.

Furthermore the node director defining the thickness direction in each node can be expressed as:

$$\vec{v}_3^a = \frac{1}{h_a}\left(\vec{x}_a^{top} - \vec{x}_a^{bottom}\right) \tag{2.10}$$

where: h_a The height of the shell.

Substituting equations (2.9) and (2.10) into equation (2.8) now gives a new expression for the interpolation of coordinates:

$$\vec{x} = \sum_{a=1}^{n_{shell}} N_a^{2D}\left(\vec{x}_a + \frac{t}{2}h_a\vec{v}_3^a\right) \tag{2.11}$$

The displacements are by definition given as the change in coordinates. Thus, the displacements can be derived from equation (2.11) as:

$$\begin{aligned}\vec{u} &= \sum_{a=1}^{n_{shell}} N_a^{2D}\left(\Delta\vec{x}_a + \frac{t}{2}h_a\Delta\vec{v}_3^a\right) \\ &= \sum_{a=1}^{n_{shell}} N_a^{2D}\left(\vec{u}_a + \frac{t}{2}h_a\Delta\vec{v}_3^a\right)\end{aligned} \tag{2.12}$$

where: $\vec{u}$ Global Cartesian displacements.

$\vec{u}_a$ Global Cartesian displacements of node a.

$\Delta\vec{v}_3^a$ Relative displacements of the node director in node a.

As normals to the reference surface remain inextensible after deformation, only the orientation of $\vec{v}_3^a$ changes, the length does not. This change in orientation can, as earlier mentioned, be described by two rotations α and β. These are illustrated in figure 2.4.

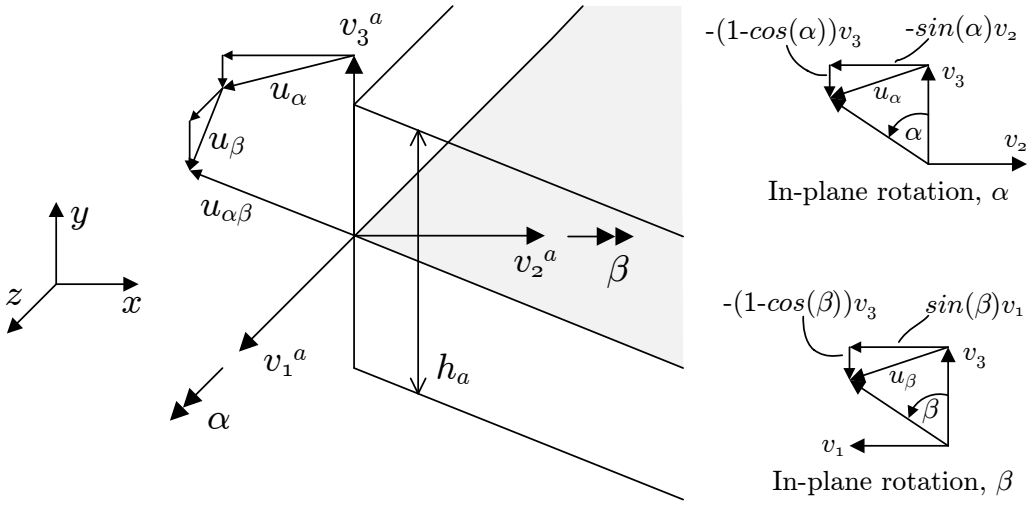

Figure 2.4: *Global displacements due to nodal rotations of the node director. Vector arrows are omitted in the figure.*

Considering the figure, the change in rotation angles α and β can be described as:

$$\vec{u}_\alpha = -\vec{v}_2 \sin(\alpha) - \vec{v}_3(1-\cos(\alpha)) \tag{2.13a}$$

$$\vec{u}_\beta = \vec{v}_1 \sin(\beta) - \vec{v}_3(1-\cos(\beta)) \tag{2.13b}$$

Recalling that the rotations are assumed to be small, in order to obtain a linear formulation, the above reduces to:

$$\vec{u}_\alpha = -\vec{v}_2\alpha \tag{2.14a}$$

$$\vec{u}_\beta = \vec{v}_1\beta \tag{2.14b}$$

Substituting equations (2.14) into equation (2.12) now gives the final expression for the displacements:

$$\vec{u} = \sum_{a=1}^{n_{shell}} N_a^{2D}\left(\vec{u}_a + \frac{t}{2}h_a(\vec{v}_1\beta - \vec{v}_2\alpha)\right) \tag{2.15}$$

which for the sake of simplicity is rephrased to:

$$\vec{u} = \sum_{a=1}^{n} N_a\left(\vec{u}_a + \frac{t}{2}h_a(\vec{v}_1\beta - \vec{v}_2\alpha)\right) \tag{2.16}$$

where: $n = n_{shell}$

$N_a = N_a^{2D}$

Thus the displacements of all points within the element are related to five degrees of freedom of each node. In matrix notation this can be written as:

$$\vec{u} = \begin{Bmatrix} u \\ v \\ w \end{Bmatrix} = \underline{N}\vec{d} \tag{2.17}$$

where *the shape function matrix,* $\underline{N}$, is:

$$\underline{N} = \begin{bmatrix} \dots & \begin{bmatrix} N_a & 0 & 0 & -\frac{t}{2}h_a\vec{v}_2\cdot\vec{i} & \frac{t}{2}h_a\vec{v}_1\cdot\vec{i} \\ 0 & N_a & 0 & -\frac{t}{2}h_a\vec{v}_2\cdot\vec{j} & \frac{t}{2}h_a\vec{v}_1\cdot\vec{j} \\ 0 & 0 & N_a & -\frac{t}{2}h_a\vec{v}_2\cdot\vec{k} & \frac{t}{2}h_a\vec{v}_1\cdot\vec{k} \end{bmatrix} & \dots \end{bmatrix} \tag{2.18}$$

and the nodal degrees of freedom, $\vec{d}$, are assembled in a vector:

$$\vec{d} = \begin{bmatrix} \dots & \begin{bmatrix} u_a & v_a & w_a & \alpha_a & \beta_a \end{bmatrix} & \dots \end{bmatrix}^T \tag{2.19}$$

2.2.4 Strain-displacement Matrix

Now that expressions for the displacements are obtained the next step is to take the derivatives in order to get the strains, and thereby the relation between strains and displacements known as *the strain-displacement matrix*. As known from the theory of elasticity the strains are, according to Cauchy's definition of the strain tensor, expressed in terms of displacements as:

$$\begin{aligned} \vec{\varepsilon} &= \begin{bmatrix} \varepsilon_x & \varepsilon_y & \varepsilon_z & \gamma_{xy} & \gamma_{yz} & \gamma_{zx} \end{bmatrix}^T = \begin{bmatrix} \varepsilon_x & \varepsilon_y & \varepsilon_z & 2\varepsilon_{xy} & 2\varepsilon_{yz} & 2\varepsilon_{zx} \end{bmatrix}^T \\ &= \begin{bmatrix} u_{,x} & v_{,y} & w_{,z} & u_{,y}+v_{,x} & v_{,z}+w_{,y} & u_{,z}+w_{,x} \end{bmatrix}^T \\ &= \underline{\partial}\,\vec{u} \\ &= \underline{\partial}\,\underline{N}\,\vec{d} \end{aligned} \tag{2.20}$$

where: $\underline{\partial}$ Differential operator matrix.

whereby the strain-displacement matrix can be stated as:

$$\underline{B} = \underline{\partial}\,\underline{N} \tag{2.21}$$

where: $\underline{B}$ The strain-displacement matrix.

Thus what is needed is the derivative of the displacements w.r.t. the global coordinates. This is determined by use of the chain rule where the derivative of the displacements w.r.t. the natural coordinates are found first, and secondly multiplied with the derivative of the natural coordinates w.r.t. the global coordinates, i.e.:

$$\frac{\partial\vec{u}}{\partial\vec{x}} = \frac{\partial\vec{u}}{\partial\vec{r}}\frac{\partial\vec{r}}{\partial\vec{x}} \tag{2.22}$$

The first term on the right-hand side of this equation is obtained by taking the derivative of equation (2.17) as:

$$\begin{Bmatrix} u_{,r} \\ u_{,s} \\ u_{,t} \\ v_{,r} \\ v_{,s} \\ v_{,t} \\ w_{,r} \\ w_{,s} \\ w_{,t} \end{Bmatrix} = \begin{bmatrix} \dots & \begin{bmatrix} N_{a,r} & 0 & 0 & -N_{a,r}\frac{t}{2}h_a\vec{v}_2\cdot\vec{i} & N_{a,r}\frac{t}{2}h_a\vec{v}_1\cdot\vec{i} \\ N_{a,s} & 0 & 0 & -N_{a,s}\frac{t}{2}h_a\vec{v}_2\cdot\vec{i} & N_{a,s}\frac{t}{2}h_a\vec{v}_1\cdot\vec{i} \\ 0 & 0 & 0 & -N_a\frac{h_a}{2}\vec{v}_2\cdot\vec{i} & N_a\frac{h_a}{2}\vec{v}_1\cdot\vec{i} \\ 0 & N_{a,r} & 0 & -N_{a,r}\frac{t}{2}h_a\vec{v}_2\cdot\vec{j} & N_{a,r}\frac{t}{2}h_a\vec{v}_1\cdot\vec{j} \\ 0 & N_{a,s} & 0 & -N_{a,s}\frac{t}{2}h_a\vec{v}_2\cdot\vec{j} & N_{a,s}\frac{t}{2}h_a\vec{v}_1\cdot\vec{j} \\ 0 & 0 & 0 & -N_a\frac{h_a}{2}\vec{v}_2\cdot\vec{j} & N_a\frac{h_a}{2}\vec{v}_1\cdot\vec{j} \\ 0 & 0 & N_{a,r} & -N_{a,r}\frac{t}{2}h_a\vec{v}_2\cdot\vec{k} & N_{a,r}\frac{t}{2}h_a\vec{v}_1\cdot\vec{k} \\ 0 & 0 & N_{a,s} & -N_{a,s}\frac{t}{2}h_a\vec{v}_2\cdot\vec{k} & N_{a,s}\frac{t}{2}h_a\vec{v}_1\cdot\vec{k} \\ 0 & 0 & 0 & -N_a\frac{h_a}{2}\vec{v}_2\cdot\vec{k} & N_a\frac{h_a}{2}\vec{v}_1\cdot\vec{k} \end{bmatrix} & \dots \end{bmatrix} \begin{Bmatrix} \vdots \\ u_a \\ v_a \\ w_a \\ \alpha_a \\ \beta_a \\ \vdots \end{Bmatrix} = \underline{F}\,\vec{d} \tag{2.23}$$

where: $u_{,p}, v_{,p}, w_{,p}$ The partial derivative of the displacements w.r.t. the variable p.

$N_{a,p}$ The partial derivative of N_a w.r.t. the variable p.

The second right-hand term in equation (2.22) is the derivative of the natural coordinates w.r.t. the global coordinates, which can be found by first determining the derivative of the global coordinates w.r.t. the natural coordinates and next inverting it. The first step is completed by differentiating equation (2.11) w.r.t. the natural coordinates:

$$\frac{\partial \vec{x}}{\partial r} = \sum_{a=1}^{n} \left(N_{a,r}\, \vec{x}_a + N_{a,r} \frac{t}{2} h_a\, \vec{v}_3^a \right) \tag{2.24a}$$

$$\frac{\partial \vec{x}}{\partial s} = \sum_{a=1}^{n} \left(N_{a,s}\, \vec{x}_a + N_{a,s} \frac{t}{2} h_a\, \vec{v}_3^a \right) \tag{2.24b}$$

$$\frac{\partial \vec{x}}{\partial t} = \sum_{a=1}^{n} \frac{h_a}{2} N_a\, \vec{v}_3^a \tag{2.24c}$$

Assembling these derivatives in a matrix gives what is known as *the Jacobian matrix* for the element:

$$\begin{aligned} \underline{J} &= \begin{bmatrix} \frac{\partial x}{\partial r} & \frac{\partial y}{\partial r} & \frac{\partial z}{\partial r} \\ \frac{\partial x}{\partial s} & \frac{\partial y}{\partial s} & \frac{\partial z}{\partial s} \\ \frac{\partial x}{\partial t} & \frac{\partial y}{\partial t} & \frac{\partial z}{\partial t} \end{bmatrix} \\ &= \sum_{a=1}^{n} \begin{bmatrix} N_{a,r} x_a + N_{a,r} \frac{t}{2} h_a\, \vec{v}_3^a \cdot \vec{i} & N_{a,r} y_a + N_{a,r} \frac{t}{2} h_a\, \vec{v}_3^a \cdot \vec{j} & N_{a,r} z_a + N_{a,r} \frac{t}{2} h_a\, \vec{v}_3^a \cdot \vec{k} \\ N_{a,s} x_a + N_{a,s} \frac{t}{2} h_a\, \vec{v}_3^a \cdot \vec{i} & N_{a,s} y_a + N_{a,s} \frac{t}{2} h_a\, \vec{v}_3^a \cdot \vec{j} & N_{a,s} z_a + N_{a,s} \frac{t}{2} h_a\, \vec{v}_3^a \cdot \vec{k} \\ \frac{h_a}{2} N_a\, \vec{v}_3^a \cdot \vec{i} & \frac{h_a}{2} N_a\, \vec{v}_3^a \cdot \vec{j} & \frac{h_a}{2} N_a\, \vec{v}_3^a \cdot \vec{k} \end{bmatrix} \end{aligned} \tag{2.25}$$

where: $\underline{J}$ The Jacobian matrix.

The right-hand side of equation (2.22) is now given as a simple product (where the inverse of the Jacobian is used three times as three global displacements need to be treated):

$$\begin{Bmatrix} u_{,x} \\ u_{,y} \\ u_{,z} \\ v_{,x} \\ v_{,y} \\ v_{,z} \\ w_{,x} \\ w_{,y} \\ w_{,z} \end{Bmatrix} = \begin{bmatrix} \underline{J}^{-1} & \underline{0} & \underline{0} \\ \underline{0} & \underline{J}^{-1} & \underline{0} \\ \underline{0} & \underline{0} & \underline{J}^{-1} \end{bmatrix} \begin{Bmatrix} u_{,r} \\ u_{,s} \\ u_{,t} \\ v_{,r} \\ v_{,s} \\ v_{,t} \\ w_{,r} \\ w_{,s} \\ w_{,t} \end{Bmatrix} = \underline{\Gamma}_{uvw} \begin{Bmatrix} u_{,r} \\ u_{,s} \\ u_{,t} \\ v_{,r} \\ v_{,s} \\ v_{,t} \\ w_{,r} \\ w_{,s} \\ w_{,t} \end{Bmatrix} \tag{2.26}$$

Thus the derivatives of the displacements w.r.t. the global coordinates are obtained. What is needed in order to get the strains as listed in equation (2.20) is now only to keep track of the bookkeeping. This is done by pre-multiplying with an *auxiliary summation matrix* $\underline{H}$:

$$\underline{H} = \begin{bmatrix} 1 & 0 & 0 & 0 & 0 & 0 & 0 & 0 & 0 \\ 0 & 0 & 0 & 0 & 1 & 0 & 0 & 0 & 0 \\ 0 & 0 & 0 & 0 & 0 & 0 & 0 & 0 & 1 \\ 0 & 1 & 0 & 1 & 0 & 0 & 0 & 0 & 0 \\ 0 & 0 & 0 & 0 & 0 & 1 & 0 & 1 & 0 \\ 0 & 0 & 1 & 0 & 0 & 0 & 1 & 0 & 0 \end{bmatrix} \tag{2.27}$$

Hence the expression for the strains becomes:

$$\vec{\varepsilon} = \underline{\partial}\,\underline{N}\,\vec{d} = \underline{H}\,\underline{\Gamma}_{uvw}\,\underline{F}\,\vec{d} \equiv \underline{H}\,\underline{G}\,\vec{d} \equiv \underline{B}\,\vec{d} \tag{2.28}$$

where: $\underline{G}$ Matrix containing shape function derivatives with respect to global coordinates.

2.2.5 Thickness Dependency

In order to establish *explicit thickness integration* the thickness dependency of the strain-displacement matrix needs to be expressed explicitly. That is, the z-dependency of $\underline{B}$ needs to be identified. To reach this identification two reformulations are done. First of all $\underline{F}$ is split into two z-independent matrices, which enables an explicit formulation of its thickness dependency. Second the variation of the inverse Jacobian matrix, $\underline{\Gamma}_{uvw}$, over the thickness is approximated by a linear function as done by [Kumar and Palaninathan, 1997], which is known to be a good approximation for thin shells with $\left|\frac{h}{R} \ll 1\right|$.
Before decomposing $\underline{F}$ into two submatrices a change of variable is first made. The physical thickness coordinate z' is introduced by substituting it with $\frac{h_a}{2}t$. Next, $\underline{F}$ is decomposed into two submatrices $\underline{F}_1$ and $\underline{F}_2$ that are independent of z'. Simultaneously the shell thickness h_a is assumed to be constant within the element and therefore just denoted by h. $\underline{F}$ can thus be rewritten as:

$$\underline{F} = \underline{F}_1 + z'\,\underline{F}_2 \tag{2.29}$$

with

$$\underline{F}_1 = \begin{bmatrix} & \cdots & & \cdots \\ \cdots & \begin{bmatrix} N_{a,r} & 0 & 0 & 0 & 0 \\ N_{a,s} & 0 & 0 & 0 & 0 \\ 0 & 0 & 0 & -N_a\frac{h}{2}\vec{v}_2\cdot\vec{i} & N_a\frac{h}{2}\vec{v}_1\cdot\vec{i} \\ 0 & N_{a,r} & 0 & 0 & 0 \\ 0 & N_{a,s} & 0 & 0 & 0 \\ 0 & 0 & 0 & -N_a\frac{h}{2}\vec{v}_2\cdot\vec{j} & N_a\frac{h}{2}\vec{v}_1\cdot\vec{j} \\ 0 & 0 & N_{a,r} & 0 & 0 \\ 0 & 0 & N_{a,s} & 0 & 0 \\ 0 & 0 & 0 & -N_a\frac{h}{2}\vec{v}_2\cdot\vec{k} & N_a\frac{h}{2}\vec{v}_1\cdot\vec{k} \end{bmatrix} & \cdots \\ & \cdots & & \cdots \end{bmatrix} \tag{2.30}$$

$$\underline{F}_2 = \begin{bmatrix} & \cdots & & \cdots \\ \cdots & \begin{bmatrix} 0 & 0 & 0 & -N_{a,r}\vec{v}_2\cdot\vec{i} & N_{a,r}\vec{v}_1\cdot\vec{i} \\ 0 & 0 & 0 & -N_{a,s}\vec{v}_2\cdot\vec{i} & N_{a,s}\vec{v}_1\cdot\vec{i} \\ 0 & 0 & 0 & 0 & 0 \\ 0 & 0 & 0 & -N_{a,r}\vec{v}_2\cdot\vec{j} & N_{a,r}\vec{v}_1\cdot\vec{j} \\ 0 & 0 & 0 & -N_{a,s}\vec{v}_2\cdot\vec{j} & N_{a,s}\vec{v}_1\cdot\vec{j} \\ 0 & 0 & 0 & 0 & 0 \\ 0 & 0 & 0 & -N_{a,r}\vec{v}_2\cdot\vec{k} & N_{a,r}\vec{v}_1\cdot\vec{k} \\ 0 & 0 & 0 & -N_{a,s}\vec{v}_2\cdot\vec{k} & N_{a,s}\vec{v}_1\cdot\vec{k} \\ 0 & 0 & 0 & 0 & 0 \end{bmatrix} & \cdots \\ & \cdots & & \cdots \end{bmatrix} \tag{2.31}$$

The inverse Jacobian matrix is approximated linearly as done by [Kumar and Palaninathan, 1997] as:

$$\begin{aligned} \underline{J}^{-1} &\simeq \underline{J}_A^{-1} + t\,\underline{J}_V^{-1} \\ &= \underline{J}_A^{-1} + z'\frac{2}{h}\,\underline{J}_V^{-1} \end{aligned} \tag{2.32}$$

with

$$\underline{J}_A^{-1} = \frac{1}{2}\left(\underline{J}^{-1}|_{t=1} + \underline{J}^{-1}|_{t=-1}\right) \tag{2.33a}$$

$$\underline{J}_V^{-1} = \frac{1}{2}\left(\underline{J}^{-1}|_{t=1} - \underline{J}^{-1}|_{t=-1}\right) \tag{2.33b}$$

Next the two reformulations are substituted into the $\underline{G}$-matrix in order to give an approximate explicit thickness dependency of both $\underline{G}$ and $\underline{B}$. As seen by equations (2.26) and (2.28) $\underline{G}$ consist of three similar parts dealing with each of the three displacements u, v and w. That is:

$$\underline{G} = \begin{Bmatrix} \underline{G}^u \\ \underline{G}^v \\ \underline{G}^w \end{Bmatrix} \tag{2.34}$$

In order to shorten the following derivations these are only conducted for the $\underline{G}^u$-part. For the other two parts the derivations are quite similar and thus in a way redundant.
Substituting the two new expressions into $\underline{G}^u$ and rearranging gives:

$$\begin{aligned} \underline{G}^u &= \underline{J}^{-1}\,\underline{F}^u \\ &= \left(\underline{J}_A^{-1} + z'\,\tfrac{2}{h}\,\underline{J}_V^{-1}\right)\left(\underline{F}_1^u + z'\,\underline{F}_2^u\right) \\ &= \underbrace{\underline{J}_A^{-1}\,\underline{F}_1^u}_{\underline{G}_1^u} + z'\underbrace{\left(\tfrac{2}{h}\,\underline{J}_V^{-1}\,\underline{F}_1^u + \underline{J}_A^{-1}\,\underline{F}_2^u\right)}_{\underline{G}_2^u} + z'^2\underbrace{\tfrac{2}{h}\,\underline{J}_V^{-1}\,\underline{F}_2^u}_{\underline{G}_3^u} \end{aligned} \tag{2.35}$$

which can be done similarly for $\underline{G}^v$ and $\underline{G}^w$.
Hereby the expression for $\underline{G}$ with approximate explicit thickness dependency can be stated as:

$$\underline{G} = \underline{G}_1 + z'\,\underline{G}_2 + z'^2\,\underline{G}_3 \tag{2.36}$$

Recalling that $\underline{B} = \underline{H}\,\underline{G}$ this also gives an expression for the strain-displacement matrix with its thickness dependency explicitly stated:

$$\underline{B} = \underline{B}_1 + z'\,\underline{B}_2 + z'^2\,\underline{B}_3 \tag{2.37}$$

Hereby the strain-displacement matrix is decomposed into three thickness independent submatrices. This gives the approximate explicit thickness dependency. The matrices shall be used for developing an expression for explicit thickness integration of shell elements.

2.3 Thickness Integration

In order to obtain a stiffness matrix for a shell element it must be integrated through the thickness. In this section an efficient way of performing this integration is introduced namely the *explicit thickness integration*. However, first "traditional" layer-wise thickness integration is described.
The stiffness matrix for a shell element, as sketched in figure 2.5, can according to [Cook et al., 2002] be derived to:

$$\underline{k}_e = \int_{-1}^{1}\int_{-1}^{1}\int_{-1}^{1} \underline{B}^T \, \underline{C} \, \underline{B} |\, \underline{J}| dr ds dt \tag{2.38}$$

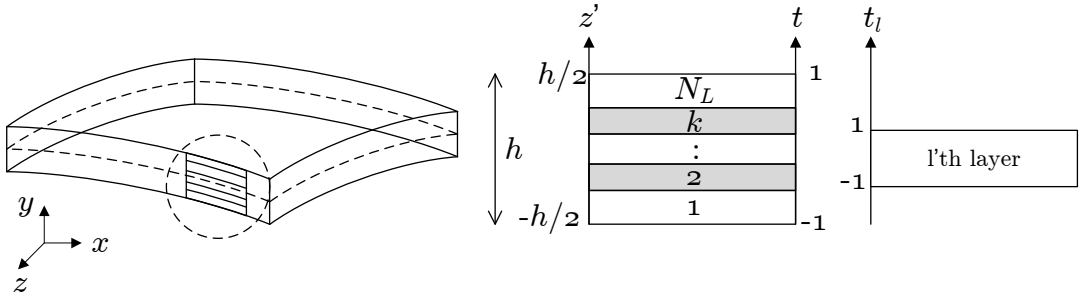

Figure 2.5: *Layered shell element.*

2.3.1 Layer-wise Thickness Integration

In traditional layer-wise thickness integration each layer is integrated separately and the results for each layer are summed. In order to do this, a *natural layer-wise thickness coordinate* t_l is constructed for each layer. t_l runs from -1 to 1 for each layer. The correlation between the natural layer-wise thickness coordinate and the natural thickness coordinate for the element can be stated as:

$$t = -1 + \frac{1}{h}\left(2\sum_{k=1}^{N_l} h_k - h_l(1-t_l)\right) \tag{2.39}$$

where: h_k The summed thicknesses of the preceding layers.

h_l The thickness of the l'th layer.

Before integration of the element stiffness matrix in equation (2.38) the new natural layer-wise thickness coordinate is substituted into the equation to replace the natural thickness coordinate. Equation (2.39) yields:

$$dt = \frac{h_l}{h} dt_l \tag{2.40}$$

which substituted into the stiffness matrix, remembering the summation over the layers, gives:

$$\underline{k}_e = \sum_{l=1}^{N_L}\int_{-1}^{1}\int_{-1}^{1}\int_{-1}^{1} \underline{B}^T \, \underline{C} \, \underline{B} |\, \underline{J}| \frac{h_l}{h} dr ds dt_l \tag{2.41}$$

Even though Gauss quadrature is used to perform the integration, this kind of integration requires $3 \cdot 3 \cdot 2N_L$ evaluations of shape functions and their derivatives. For structures with many layers this becomes computationally expensive.

2.3.2 Explicit Thickness Integration

A more computationally inexpensive integration can be obtained by use of an approximate explicit thickness integration. This section serves to derive the necessary equations. In order to do so, the approximate thickness dependencies from section 2.2.5 are employed in the stiffness matrix from equation (2.38). However, first the natural thickness coordinate from the stiffness matrix must be substituted for the z'-variable used in section 2.2.5:

$$z' = t\frac{h}{2} \qquad \Rightarrow \tag{2.42a}$$

$$dt = \frac{2}{h}dz' \tag{2.42b}$$

which inserted in the stiffness matrix gives:

$$\begin{aligned}\underline{k}_e &= \int_{-1}^{1}\int_{-1}^{1}\int_{-1}^{1} \underline{B}^T\,\underline{C}\,\underline{B}|\,\underline{J}|drdsdt \\ &= \int_{-1}^{1}\int_{-1}^{1}\int_{\frac{-h}{2}}^{\frac{h}{2}} \underline{B}^T\,\underline{C}\,\underline{B}|\,\underline{J}|\tfrac{2}{h}dz'drds\end{aligned} \tag{2.43}$$

Next the Jacobian determinant is rephrased by an approach used by [Kumar and Palaninathan, 1999]. First the square root of the Jacobian determinant is expressed at the top and bottom of the shell:

$$\Delta_{top} = \sqrt{|\,\underline{J}|_{t=1}} \tag{2.44a}$$

$$\Delta_{bottom} = \sqrt{|\,\underline{J}|_{t=-1}} \tag{2.44b}$$

The thickness average and slope of the determinant are then given by:

$$\Delta_A = \frac{1}{2}\left(\Delta_{top} + \Delta_{bottom}\right) \tag{2.45a}$$

$$\Delta_V = \frac{1}{2}\left(\Delta_{top} - \Delta_{bottom}\right) \tag{2.45b}$$

Hereby the square root of the Jacobian can be expressed as:

$$\Delta = \Delta_A + \frac{2}{h}z'\Delta_V \tag{2.46}$$

and the Jacobian can then be expressed as:

$$\begin{aligned}|\,\underline{J}| = \Delta^2 &= \left(\Delta_A + \frac{2}{h}z'\Delta_V\right)^2 \\ &= \Delta_A^2 + 2\frac{2}{h}z'\Delta_V\Delta_A + \frac{4}{h^2}z'^2\Delta_V^2 \\ &= \Delta_A^2\left(1 + 2z'\frac{2\Delta_V}{h\Delta_A} + z'^2\frac{4\Delta_V^2}{h^2\Delta_A^2}\right) \\ &= \Delta_A^2\left(1 + 2z'\gamma + z'^2\gamma^2\right)\end{aligned} \tag{2.47}$$

where: $\gamma = \frac{2\Delta_V}{h\Delta_A}$

The Jacobian matrix is thus set up for the reference surface and extrapolated from there based on evaluations at the top and bottom surface. For structures with many layers this can save significant computational time. It should be noted that for a plate (which has no curvature) the Jacobian is identical at top and bottom. Hence $\Delta_V = 0$ and $\gamma = 0$ meaning that the Jacobian is simply $|\underline{J}| = \Delta_A^2$
Now the new expressions for the Jacobian matrix and the strain-displacement matrix are inserted into the element stiffness matrix — that is, equations (2.47) and (2.37) are substituted into equation (2.43):

$$\begin{aligned}
\underline{k}_e &= \int_{-1}^{-1}\int_{-1}^{-1}\int_{\frac{-h}{2}}^{\frac{h}{2}} \left(\underline{B}_1^T + z'\,\underline{B}_2^T + z'^2\,\underline{B}_3^T\right)\underline{C}\left(\underline{B}_1 + z'\,\underline{B}_2 + z'^2\,\underline{B}_3\right)\frac{2}{h}\Delta^2 dz'drds \\
&= \int_{-1}^{-1}\int_{-1}^{-1}\int_{\frac{-h}{2}}^{\frac{h}{2}} \Big(\underline{B}_1^T\,\underline{C}\,\underline{B}_1 + z'\,\underline{B}_1^T\,\underline{C}\,\underline{B}_2 + z'^2\,\underline{B}_1^T\,\underline{C}\,\underline{B}_3 \\
&\qquad + z'\,\underline{B}_2^T\,\underline{C}\,\underline{B}_1 + z'^2\,\underline{B}_2^T\,\underline{C}\,\underline{B}_2 + z'^3\,\underline{B}_2^T\,\underline{C}\,\underline{B}_3 \\
&\qquad + z'^2\,\underline{B}_3^T\,\underline{C}\,\underline{B}_1 + z'^3\,\underline{B}_3^T\,\underline{C}\,\underline{B}_2 + z'^4\,\underline{B}_3^T\,\underline{C}\,\underline{B}_3\Big) \\
&\qquad \Delta_A^2\left(1 + 2z'\gamma + z'^2\gamma^2\right)\frac{2}{h}dz'drds
\end{aligned} \tag{2.48}$$

Remembering that $\underline{B}_1$, $\underline{B}_2$, and $\underline{B}_3$ are thickness independent and the constitutive properties constant for each layer, the strain-displacement matrices can be put outside the integral and the thickness integration thereby conducted separately for each term. This yield:

$$\begin{aligned}
\underline{k}_e = \int_{-1}^{-1}\int_{-1}^{-1} \Big(&\underline{B}_1^T\,\underline{E}_1\,\underline{B}_1 + \underline{B}_1^T\,\underline{E}_2\,\underline{B}_2 + \underline{B}_1^T\,\underline{E}_3\,\underline{B}_3 \\
&+ \underline{B}_2^T\,\underline{E}_2\,\underline{B}_1 + \underline{B}_2^T\,\underline{E}_3\,\underline{B}_2 + \underline{B}_2^T\,\underline{E}_4\,\underline{B}_3 \\
&+ \underline{B}_3^T\,\underline{E}_3\,\underline{B}_1 + \underline{B}_3^T\,\underline{E}_4\,\underline{B}_2 + \underline{B}_3^T\,\underline{E}_5\,\underline{B}_3\Big)\Delta_A^2\frac{2}{h}drds
\end{aligned} \tag{2.49}$$

with the thickness integrated constitutive properties $\underline{E}_1, \ldots, \underline{E}_5$ given as:

$$\underline{E}_1 = \sum_{k=1}^{N_L}\underline{C}_k\int_{z'_{k-1}}^{z'_k}\left(1 + 2z'\gamma + z'^2\gamma^2\right)dz' = \sum_{k=1}^{N_L}\underline{C}_k\left(\mathrm{var}_1 + 2\gamma\mathrm{var}_2 + \gamma^2\mathrm{var}_3\right)_k \tag{2.50a}$$

$$\underline{E}_2 = \sum_{k=1}^{N_L}\underline{C}_k\int_{z'_{k-1}}^{z'_k} z'\left(1 + 2z'\gamma + z'^2\gamma^2\right)dz' = \sum_{k=1}^{N_L}\underline{C}_k\left(\mathrm{var}_2 + 2\gamma\mathrm{var}_3 + \gamma^2\mathrm{var}_4\right)_k \tag{2.50b}$$

$$\underline{E}_3 = \sum_{k=1}^{N_L}\underline{C}_k\int_{z'_{k-1}}^{z'_k} z'^2\left(1 + 2z'\gamma + z'^2\gamma^2\right)dz' = \sum_{k=1}^{N_L}\underline{C}_k\left(\mathrm{var}_3 + 2\gamma\mathrm{var}_4 + \gamma^2\mathrm{var}_5\right)_k \tag{2.50c}$$

$$\underline{E}_4 = \sum_{k=1}^{N_L}\underline{C}_k\int_{z'_{k-1}}^{z'_k} z'^3\left(1 + 2z'\gamma + z'^2\gamma^2\right)dz' = \sum_{k=1}^{N_L}\underline{C}_k\left(\mathrm{var}_4 + 2\gamma\mathrm{var}_5 + \gamma^2\mathrm{var}_6\right)_k \tag{2.50d}$$

$$\underline{E}_5 = \sum_{k=1}^{N_L}\underline{C}_k\int_{z'_{k-1}}^{z'_k} z'^4\left(1 + 2z'\gamma + z'^2\gamma^2\right)dz' = \sum_{k=1}^{N_L}\underline{C}_k\left(\mathrm{var}_5 + 2\gamma\mathrm{var}_6 + \gamma^2\mathrm{var}_7\right)_k \tag{2.50e}$$

where: $\text{var}_j \quad = \frac{1}{j}(z'^j_k - z'^j_{k-1})$

In this way, the stiffness matrix for each element can be determined by explicit integration in the thickness direction. Obtaining the stiffness matrix in this way requires $3 \cdot 3 \cdot 2$ evaluations where the last two are evaluations of the inverse Jacobian at the bottom and top of the shell cf. equations (2.33). As stated by [Kumar and Palaninathan, 1999] further approximations of the stiffness matrix can be done by neglecting $\underline{G}_3$, and thus $\underline{B}_3$, as these matrices merely contain entrances that are of negligible magnitude due to the multiplication of higher order terms of the shell thickness. Hence by removing these terms the number of integrand terms in the stiffness matrix is reduced from 9 to 4, i.e:

$$\underline{k}_e = \int_{-1}^{-1}\int_{-1}^{-1} \Big(\underline{B}_1^T \underline{E}_1 \underline{B}_1 + \underline{B}_1^T \underline{E}_2 \underline{B}_2 + \underline{B}_2^T \underline{E}_2 \underline{B}_1 + \underline{B}_2^T \underline{E}_3 \underline{B}_2 \Big) \Delta_A^2 \frac{2}{h} dr ds \tag{2.51}$$

For a laminate consisting of the same orthotropic material (with different orientations) through the thickness, these constitutive properties can be expressed in terms of *lamination parameters*. Naturally this holds for both the method of explicit thickness integration, c.f. equation (2.49) and for the method of explicit thickness integration with further approximations, c.f. equation (2.51). This reformulation is shown in section 2.4.3.

2.4 Constitutive Relations

This section serves to describe the constitutive relations for a composite laminate. The focus is based on laminates consisting of plies with orthotropic behaviour. The approach for obtaining constitutive relations for a laminate is first to determine the relations for a single ply at a macroscopic level, and next combining the constitutive relations for all plies into a general governing equation for the entire laminate.

2.4.1 Single Layers

For a linear homogeneous material the general constitutive law is (using Einstein's index notation):

$$\sigma_{ij} = C_{ijkl}\varepsilon_{kl} \tag{2.52}$$

where:

σ_{ij}	The stress tensor.
C_{ijkl}	The constitutive tensor.
ε_{kl}	The strain tensor.

The 81 unknown components can, using tensorial symmetry and thermodynamic considerations, be reduced to 21 independent components. For a material with anisotropic behaviour the constitutive law can thus be written in matrix form as:

$$\begin{Bmatrix} \sigma_{11} \\ \sigma_{22} \\ \sigma_{33} \\ \sigma_{12} \\ \sigma_{23} \\ \sigma_{13} \end{Bmatrix} = \begin{bmatrix} Q_{11} & Q_{12} & Q_{13} & Q_{14} & Q_{15} & Q_{16} \\ & Q_{22} & Q_{23} & Q_{24} & Q_{25} & Q_{26} \\ & & Q_{33} & Q_{34} & Q_{35} & Q_{36} \\ & & & Q_{44} & Q_{45} & Q_{46} \\ & sym. & & & Q_{55} & Q_{56} \\ & & & & & Q_{66} \end{bmatrix} \begin{Bmatrix} \varepsilon_{11} \\ \varepsilon_{22} \\ \varepsilon_{33} \\ 2\varepsilon_{12} \\ 2\varepsilon_{23} \\ 2\varepsilon_{13} \end{Bmatrix} \tag{2.53}$$

where: Q_{ij} The components of the constitutive tensor, which traditionally is denoted as $\underline{Q}$ instead of $\underline{C}$ when dealing with laminaes.

A material with three planes of material symmetry is said to have *orthotropic* behaviour. For such a material equation (2.53) can, when described in the PMD, be reduced to:

$$\begin{Bmatrix} \sigma_{11} \\ \sigma_{22} \\ \sigma_{33} \\ \sigma_{12} \\ \sigma_{23} \\ \sigma_{13} \end{Bmatrix} = \begin{bmatrix} Q_{11} & Q_{12} & Q_{13} & 0 & 0 & 0 \\ & Q_{22} & Q_{23} & 0 & 0 & 0 \\ & & Q_{33} & 0 & 0 & 0 \\ & & & Q_{44} & 0 & 0 \\ & sym. & & & Q_{55} & 0 \\ & & & & & Q_{66} \end{bmatrix} \begin{Bmatrix} \varepsilon_{11} \\ \varepsilon_{22} \\ \varepsilon_{33} \\ 2\varepsilon_{12} \\ 2\varepsilon_{23} \\ 2\varepsilon_{13} \end{Bmatrix} \tag{2.54}$$

The assumptions of FSDT were introduced in section 2.1. The third assumption stated was that normal strains are negligible, i.e. $\varepsilon_{33} = 0$. At the same time an assumption of plane stress is presumed for thin to moderately thick shells. When accounting for the Poisson effect these two assumptions are obviously conflicting. This can be corrected by modifying the stiffness matrix into what is referred to as the *reduced stiffness matrix* of a shell.

The relationship between σ_{33} and ε_{33} is, according to equation (2.54):

$$\sigma_{33} = Q_{13}\varepsilon_{11} + Q_{23}\varepsilon_{22} + Q_{33}\varepsilon_{33} = 0 \tag{2.55}$$

The only solution to this expression, which is fulfilled for all combinations of strains, is the trivial solution, i.e. $Q_{13} = Q_{23} = Q_{33} = 0$. The *reduced constitutive relations* for a shell with FSDT assumptions thus become:

$$\begin{Bmatrix} \sigma_{11} \\ \sigma_{22} \\ \sigma_{33} \\ \sigma_{12} \\ \sigma_{23} \\ \sigma_{13} \end{Bmatrix} = \begin{bmatrix} Q_{11} & Q_{12} & 0 & 0 & 0 & 0 \\ & Q_{22} & 0 & 0 & 0 & 0 \\ & & 0 & 0 & 0 & 0 \\ & & & Q_{44} & 0 & 0 \\ & sym. & & & Q_{55} & 0 \\ & & & & & Q_{66} \end{bmatrix} \begin{Bmatrix} \varepsilon_{11} \\ \varepsilon_{22} \\ \varepsilon_{33} \\ 2\varepsilon_{12} \\ 2\varepsilon_{23} \\ 2\varepsilon_{13} \end{Bmatrix} \tag{2.56}$$

As previously mentioned, the FSDT assumptions incorporate a constant through the thickness distribution of the shear strains γ_{13}, γ_{23}. These distributions should in fact be shaped more like a parabola within each layer. In order to obtain a more correct strain energy, the shear stiffnesses Q_{55} and Q_{66} are correlated with a *shear correction factor k*. The magnitude of the shear correction factor is in fact dependent on both geometry and loading. Using energy considerations it can be derived that a factor of $\frac{5}{6}$ gives a reasonable compensation for isotropic materials. For sandwich structures on the other hand, a factor of 1 should be used. However, what to do for laminates in general is dependent on both the material properties, the number of layers etc. and thus it can be a laborious task to determine the correct value. The result is that simplifications often are made. In MUST the strategy implemented is simply to use a factor of 1 for sandwich structures and a factor of $\frac{5}{6}$ for all other applications.

2.4.2 Multiple Layers

When the laminaes are assembled into a laminate the PMD's are not necessarily equal. Hence a plane rotation of the constitutive relations of each lamina into the MCS (which is common to all layers) is thus required. This is conducted as:

$$\underline{\overline{Q}} = \underline{T}_\theta^T \, \underline{Q} \, \underline{T}_\theta \tag{2.57}$$

where the *rotation tensor* is given as:

$$\underline{T}_\theta = \begin{bmatrix} \cos^2(\theta) & \sin^2(\theta) & 0 & \sin(\theta)\cos(\theta) & 0 & 0 \\ \sin^2(\theta) & \cos^2(\theta) & 0 & -\sin(\theta)\cos(\theta) & 0 & 0 \\ 0 & 0 & 1 & 0 & 0 & 0 \\ -2\sin(\theta)\cos(\theta) & 2\sin(\theta)\cos(\theta) & 0 & \cos^2(\theta)-\sin^2(\theta) & 0 & 0 \\ 0 & 0 & 0 & 0 & \cos(\theta) & -\sin(\theta) \\ 0 & 0 & 0 & 0 & \sin(\theta) & \cos(\theta) \end{bmatrix} \tag{2.58}$$

Hereby the reduced stiffnesses of a lamina in the MCS yields:

$$\underline{\overline{Q}} = \begin{bmatrix} \overline{Q}_{11} & \overline{Q}_{12} & 0 & \overline{Q}_{14} & 0 & 0 \\ & \overline{Q}_{22} & 0 & \overline{Q}_{24} & 0 & 0 \\ & & 0 & 0 & 0 & 0 \\ & & & \overline{Q}_{44} & 0 & 0 \\ & sym. & & & \overline{Q}_{55} & \overline{Q}_{56} \\ & & & & & \overline{Q}_{66} \end{bmatrix} \tag{2.59}$$

2.4.2.1 Lamina invariants

Another way of expressing the reduced stiffnesses is by use of *lamina invariants*. Lamina invariants are material properties that are invariant to coordinate transformations. The lamina invariants U_1 to U_6 are in fact just reformulations of the reduced stiffnesses where trigonometric identities and several rearrangements have been employed. The invariants are given as [Tsai and Pagano, 1968]:

$$U_1 = \frac{3Q_{11} + 3Q_{22} + 2Q_{12} + 4Q_{66}}{8} \tag{2.60a}$$

$$U_2 = \frac{Q_{11} - Q_{22}}{2} \tag{2.60b}$$

$$U_3 = \frac{Q_{11} + Q_{22} - 2Q_{12} - 4Q_{66}}{8} \tag{2.60c}$$

$$U_4 = \frac{Q_{11} + Q_{22} + 6Q_{12} - 4Q_{66}}{8} \tag{2.60d}$$

$$U_5 = \frac{Q_{55} + Q_{66}}{2} \tag{2.60e}$$

$$U_6 = \frac{Q_{55} - Q_{66}}{2} \tag{2.60f}$$

Using these invariants the reduced stiffnesses, stored in a vector $\overline{\overline{Q}}$, can be expressed as:

$$\overline{\overline{Q}} = \begin{Bmatrix} \overline{Q}_{11} \\ \overline{Q}_{22} \\ \overline{Q}_{12} \\ \overline{Q}_{55} \\ \overline{Q}_{66} \\ \overline{Q}_{56} \\ \overline{Q}_{44} \\ \overline{Q}_{14} \\ \overline{Q}_{24} \end{Bmatrix} = \begin{bmatrix} U_1 & U_2 & 0 & U_3 & 0 \\ U_1 & -U_2 & 0 & U_3 & 0 \\ U_4 & 0 & 0 & -U_3 & 0 \\ U_5 & U_6 & 0 & 0 & 0 \\ U_5 & -U_6 & 0 & 0 & 0 \\ 0 & 0 & -U_6 & 0 & 0 \\ \frac{1}{2}(U_1 - U_4) & 0 & 0 & -U_3 & 0 \\ 0 & 0 & \frac{1}{2}U_2 & 0 & U_3 \\ 0 & 0 & \frac{1}{2}U_2 & 0 & -U_3 \end{bmatrix} \begin{Bmatrix} 1 \\ \cos(2\theta) \\ \sin(2\theta) \\ \cos(4\theta) \\ \sin(4\theta) \end{Bmatrix} = \underline{U} \begin{Bmatrix} 1 \\ \cos(2\theta) \\ \sin(2\theta) \\ \cos(4\theta) \\ \sin(4\theta) \end{Bmatrix} \tag{2.61}$$

As such the latter is simply a reformulation of how to determine the reduced stiffness components for a lamina and the immediate application of this does actually not provide anything new. However, it paves the road for the use of so-called lamination parameters, which can be incorporated in the formulation when the laminate consists of only a single material (with different orientations in each layer). This shall be elaborated in the following subsection.

2.4.3 Lamination Parameters

As shown in section 2.3 a product of the strain-displacement matrix and the constitutive matrix has to be integrated through the thickness in order to get the stiffness matrix. If all layers in the lay-up are of the same material (but possibly with different angular orientation), this product can be rephrased in terms of *the lamination parameters*. The 28 lamination parameters are defined as:

$$\xi^A_{[1,2,3,4]} = \frac{1}{2}\int_{-1}^{1} \left[\cos(2\theta_k) \quad \sin(2\theta_k) \quad \cos(4\theta_k) \quad \sin(4\theta_k)\right]^T dt \tag{2.62a}$$

$$\xi^B_{[1,2,3,4]} = \frac{2}{2}\int_{-1}^{1} t\left[\cos(2\theta_k) \quad \sin(2\theta_k) \quad \cos(4\theta_k) \quad \sin(4\theta_k)\right]^T dt \tag{2.62b}$$

$$\xi^D_{[1,2,3,4]} = \frac{3}{2}\int_{-1}^{1} t^2\left[\cos(2\theta_k) \quad \sin(2\theta_k) \quad \cos(4\theta_k) \quad \sin(4\theta_k)\right]^T dt \tag{2.62c}$$

$$\xi^E_{[1,2,3,4]} = \frac{4}{2}\int_{-1}^{1} t^3\left[\cos(2\theta_k) \quad \sin(2\theta_k) \quad \cos(4\theta_k) \quad \sin(4\theta_k)\right]^T dt \tag{2.62d}$$

$$\xi^F_{[1,2,3,4]} = \frac{5}{2}\int_{-1}^{1} t^4\left[\cos(2\theta_k) \quad \sin(2\theta_k) \quad \cos(4\theta_k) \quad \sin(4\theta_k)\right]^T dt \tag{2.62e}$$

$$\xi^G_{[1,2,3,4]} = \frac{6}{2}\int_{-1}^{1} t^5\left[\cos(2\theta_k) \quad \sin(2\theta_k) \quad \cos(4\theta_k) \quad \sin(4\theta_k)\right]^T dt \tag{2.62f}$$

$$\xi^H_{[1,2,3,4]} = \frac{7}{2}\int_{-1}^{1} t^6\left[\cos(2\theta_k) \quad \sin(2\theta_k) \quad \cos(4\theta_k) \quad \sin(4\theta_k)\right]^T dt \tag{2.62g}$$

Now changing the thickness coordinate to the physical thickness coordinate z' and performing the integration gives:

$$\xi^A_{[1,2,3,4]} = \frac{1}{2}\int_{-\frac{h}{2}}^{\frac{h}{2}} \begin{bmatrix}\cos(2\theta_k) & \sin(2\theta_k) & \cos(4\theta_k) & \sin(4\theta_k)\end{bmatrix}^T \tfrac{2}{h} dz'$$

$$= \frac{1}{h}\sum_{k=1}^{N_L} (\text{var}_1)_k \begin{bmatrix}\cos(2\theta_k) & \sin(2\theta_k) & \cos(4\theta_k) & \sin(4\theta_k)\end{bmatrix}^T \tag{2.63a}$$

$$\xi^B_{[1,2,3,4]} = \frac{2}{2}\int_{-\frac{h}{2}}^{\frac{h}{2}} \left(\tfrac{2}{h}z'\right) \begin{bmatrix}\cos(2\theta_k) & \sin(2\theta_k) & \cos(4\theta_k) & \sin(4\theta_k)\end{bmatrix}^T \tfrac{2}{h} dz'$$

$$= \frac{4}{h^2}\sum_{k=1}^{N_L} (\text{var}_2)_k \begin{bmatrix}\cos(2\theta_k) & \sin(2\theta_k) & \cos(4\theta_k) & \sin(4\theta_k)\end{bmatrix}^T \tag{2.63b}$$

$$\xi^D_{[1,2,3,4]} = \frac{3}{2}\int_{-\frac{h}{2}}^{\frac{h}{2}} \left(\tfrac{2}{h}z'\right)^2 \begin{bmatrix}\cos(2\theta_k) & \sin(2\theta_k) & \cos(4\theta_k) & \sin(4\theta_k)\end{bmatrix}^T \tfrac{2}{h} dz'$$

$$= \frac{12}{h^3}\sum_{k=1}^{N_L} (\text{var}_3)_k \begin{bmatrix}\cos(2\theta_k) & \sin(2\theta_k) & \cos(4\theta_k) & \sin(4\theta_k)\end{bmatrix}^T \tag{2.63c}$$

$$\xi^E_{[1,2,3,4]} = \frac{4}{2}\int_{-\frac{h}{2}}^{\frac{h}{2}} \left(\tfrac{2}{h}z'\right)^3 \begin{bmatrix}\cos(2\theta_k) & \sin(2\theta_k) & \cos(4\theta_k) & \sin(4\theta_k)\end{bmatrix}^T \tfrac{2}{h} dz'$$

$$= \frac{32}{h^4}\sum_{k=1}^{N_L} (\text{var}_4)_k \begin{bmatrix}\cos(2\theta_k) & \sin(2\theta_k) & \cos(4\theta_k) & \sin(4\theta_k)\end{bmatrix}^T \tag{2.63d}$$

$$\xi^F_{[1,2,3,4]} = \frac{5}{2}\int_{-\frac{h}{2}}^{\frac{h}{2}} \left(\tfrac{2}{h}z'\right)^4 \begin{bmatrix}\cos(2\theta_k) & \sin(2\theta_k) & \cos(4\theta_k) & \sin(4\theta_k)\end{bmatrix}^T \tfrac{2}{h} dz'$$

$$= \frac{80}{h^5}\sum_{k=1}^{N_L} (\text{var}_5)_k \begin{bmatrix}\cos(2\theta_k) & \sin(2\theta_k) & \cos(4\theta_k) & \sin(4\theta_k)\end{bmatrix}^T \tag{2.63e}$$

$$\xi^G_{[1,2,3,4]} = \frac{6}{2}\int_{-\frac{h}{2}}^{\frac{h}{2}} \left(\tfrac{2}{h}z'\right)^5 \begin{bmatrix}\cos(2\theta_k) & \sin(2\theta_k) & \cos(4\theta_k) & \sin(4\theta_k)\end{bmatrix}^T \tfrac{2}{h} dz'$$

$$= \frac{192}{h^6}\sum_{k=1}^{N_L} (\text{var}_6)_k \begin{bmatrix}\cos(2\theta_k) & \sin(2\theta_k) & \cos(4\theta_k) & \sin(4\theta_k)\end{bmatrix}^T \tag{2.63f}$$

$$\xi^H_{[1,2,3,4]} = \frac{7}{2}\int_{-\frac{h}{2}}^{\frac{h}{2}} \left(\tfrac{2}{h}z'\right)^6 \begin{bmatrix}\cos(2\theta_k) & \sin(2\theta_k) & \cos(4\theta_k) & \sin(4\theta_k)\end{bmatrix}^T \tfrac{2}{h} dz'$$

$$= \frac{448}{h^7}\sum_{k=1}^{N_L} (\text{var}_7)_k \begin{bmatrix}\cos(2\theta_k) & \sin(2\theta_k) & \cos(4\theta_k) & \sin(4\theta_k)\end{bmatrix}^T \tag{2.63g}$$

Next, the strategy is to utilise the results with thickness integrated constitutive properties of section 2.3. To do so the constitutive properties should be transformed from the MCS to the global coordinate system. This is done by multiplication with the transformation matrix $\underline{T}_{MG}$ as (where the general idea

is illustrated by just one of the matrices):

$$\begin{aligned}\underline{E}_1 &= \sum_{k=1}^{N_L} \underline{C}_k \int_{z_{k-1}}^{z_k} (1+2z'\gamma+z'^2\gamma^2)dz' \\ &= \sum_{k=1}^{N_L} \underline{T}_{MG}^T \overline{\underline{Q}}_k \underline{T}_{MG} \int_{z_{k-1}}^{z_k} (1+2z'\gamma+z'^2\gamma^2)dz' \\ &= \underline{T}_{MG}^T \sum_{k=1}^{N_L} \left(\overline{\underline{Q}}_k \int_{z_{k-1}}^{z_k} (1+2z'\gamma+z'^2\gamma^2)dz' \right) \underline{T}_{MG} \end{aligned} \tag{2.64}$$

where: $\underline{T}_{MG}$ Transformation matrix from MCS to global coordinate system.

Realising that if all layers are made of the same material then the constitutive matrix for the different layers are identical, except for the orientations. Thus the relationship developed in equation (2.61) can be applied where the invariant matrix, $\underline{U}$, can be placed outside the summation due to the material being identical through the thickness. However, a problem arises as $\overline{\overline{Q}}$ in equation (2.61) is a 1×9 vector, whereas $\overline{\underline{Q}}$ in equation (2.59) is a 6×6 matrix, meaning that the vector needs to be transformed into the matrix-form. This can in principle be done by use of two bookkeeping matrices $\underline{T}_1$ and $\underline{T}_2$ (with the dimensions of the matrices noted below) as:

$$\underset{6\times 6}{\overline{\underline{Q}}} = \underset{6\times 9}{\underline{T}_1} \left(\underset{9\times 1}{\overline{\overline{Q}}} \; \underset{1\times 6}{\underline{T}_2} \right) \tag{2.65}$$

However, in the current implementation this task is instead done by simply placing the entrances of the vector at the correct locations in the matrix (which in practice is both easier and also saves computational time). So ignoring the need for transformation from vector into matrix, equation (2.64) can be further rewritten into:

$$\begin{aligned}\underline{E}_1 &= \underline{T}_{MG}^T \underline{U} \left(\sum_{k=1}^{N_L} \begin{bmatrix} 1 & \cos(2\theta_k) & \sin(2\theta_k) & \cos(4\theta_k) & \sin(4\theta_k) \end{bmatrix}^T \int_{z_{k-1}}^{z_k} (1+2z'\gamma+z'^2\gamma^2)dz' \right) \underline{T}_{MG} \\ &= \underline{T}_{MG}^T \underline{U} \Big(h \begin{bmatrix} 1 & \xi_1^A & \xi_2^A & \xi_3^A & \xi_4^A \end{bmatrix}^T + 2\gamma \tfrac{h^2}{4} \begin{bmatrix} 0 & \xi_1^B & \xi_2^B & \xi_3^B & \xi_4^B \end{bmatrix}^T \\ &\quad + \gamma^2 \tfrac{h^3}{12} \begin{bmatrix} 1 & \xi_1^D & \xi_2^D & \xi_3^D & \xi_4^D \end{bmatrix}^T \Big) \underline{T}_{MG} \end{aligned} \tag{2.66}$$

Correspondingly the matrices $\underline{E}_2$ to $\underline{E}_5$ can be reformulated to give:

$$\begin{aligned}\underline{E}_2 &= \underline{T}_{MG}^T \underline{U} \Big(\tfrac{h^2}{4} \begin{bmatrix} 0 & \xi_1^B & \xi_2^B & \xi_3^B & \xi_4^B \end{bmatrix}^T + 2\gamma \tfrac{h^3}{12} \begin{bmatrix} 1 & \xi_1^D & \xi_2^D & \xi_3^D & \xi_4^D \end{bmatrix}^T \\ &\quad + \gamma^2 \tfrac{h^4}{32} \begin{bmatrix} 0 & \xi_1^E & \xi_2^E & \xi_3^E & \xi_4^E \end{bmatrix}^T \Big) \underline{T}_{MG} \end{aligned} \tag{2.67a}$$

$$\begin{aligned}\underline{E}_3 &= \underline{T}_{MG}^T \underline{U} \Big(\tfrac{h^3}{12} \begin{bmatrix} 1 & \xi_1^D & \xi_2^D & \xi_3^D & \xi_4^D \end{bmatrix}^T + 2\gamma \tfrac{h^4}{32} \begin{bmatrix} 0 & \xi_1^E & \xi_2^E & \xi_3^E & \xi_4^E \end{bmatrix}^T \\ &\quad + \gamma^2 \tfrac{h^5}{80} \begin{bmatrix} 1 & \xi_1^F & \xi_2^F & \xi_3^F & \xi_4^F \end{bmatrix}^T \Big) \underline{T}_{MG} \end{aligned} \tag{2.67b}$$

$$\begin{aligned}\underline{E}_4 &= \underline{T}_{MG}^T \underline{U} \Big(\tfrac{h^4}{32} \begin{bmatrix} 0 & \xi_1^E & \xi_2^E & \xi_3^E & \xi_4^E \end{bmatrix}^T + 2\gamma \tfrac{h^5}{80} \begin{bmatrix} 1 & \xi_1^F & \xi_2^F & \xi_3^F & \xi_4^F \end{bmatrix}^T \\ &\quad + \gamma^2 \tfrac{h^6}{192} \begin{bmatrix} 0 & \xi_1^G & \xi_2^G & \xi_3^G & \xi_4^G \end{bmatrix}^T \Big) \underline{T}_{MG} \end{aligned} \tag{2.67c}$$

$$\begin{aligned}\underline{E}_5 &= \underline{T}_{MG}^T \underline{U} \Big(\tfrac{h^5}{80} \begin{bmatrix} 1 & \xi_1^F & \xi_2^F & \xi_3^F & \xi_4^F \end{bmatrix}^T + 2\gamma \tfrac{h^6}{192} \begin{bmatrix} 0 & \xi_1^G & \xi_2^G & \xi_3^G & \xi_4^G \end{bmatrix}^T \\ &\quad + \gamma^2 \tfrac{h^7}{448} \begin{bmatrix} 1 & \xi_1^H & \xi_2^H & \xi_3^H & \xi_4^H \end{bmatrix}^T \Big) \underline{T}_{MG} \end{aligned} \tag{2.67d}$$

Thus expressions for the thickness integrated constitutive properties in terms of the lamination parameters have been obtained. Hence the stiffness matrix in equation (2.49) may also be expressed in terms of lamination parameters, and accordingly it must as well be linear in those.

As previously mentioned in section 2.3.2 the explicit thickness integration can also be formulated in an approximate form where the strain displacement matrix $\underline{B}_3$ is set to zero, and thus reducing the number of integration terms when determining the element stiffness matrix. As a consequence the stiffness contributions from $\underline{E}_4$ and $\underline{E}_5$ are neglected. Hence the number of active lamination parameters is reduced from 28 to 20. Further reductions occur for flat shells i.e. plates due to the parameter $\gamma = 0$ which results in 12 active lamination parameters: ξ_i^A, ξ_i^B, and ξ_i^D. These 12 parameters are identical to those known from classical laminate plate theory.

2.5 Numerical Verification & Performance

Having obtained new formulations of the stiffness this section serves to verify that the new formulations give meaningful results. In particular it is desirable to know whether stiffnesses obtained by explicit thickness integration as well as approximated explicit thickness integration give accurate results. Furthermore it is desirable to investigate the difference in performance between full layer-wise integration, explicit thickness integration and approximated explicit thickness integration. Such numerical experiments testing the accuracy and performance of the above-mentioned methods have been conducted by [Hvejsel and Hansen, 2007], wherefrom the results are reproduced. However, as large parts of the code have been redesigned in order to activate and deactivate the use of lamination parameters in the calculations of the stiffnesses, it has been found necessary to test whether the results obtained by [Hvejsel and Hansen, 2007] still hold. As this has in fact been verified, what is presented in the following subsections are results produced by [Hvejsel and Hansen, 2007] with the remark that the same experiments conducted with the use of laminations parameters give identical results. The two characteristics, accuracy and performance, are addressed separately using two standard examples.

2.5.1 Accuracy — Pinched Hemisphere

In order to test the shell elements' behaviour in a mixed membrane and bending situation, the example used is the double curved *pinched hemisphere* sketched in figure 2.6. The hemisphere has a hole in the top in order to avoid triangular elements. As also can be seen in the figure symmetric boundary conditions are used and hence only a quarter of the geometry is analysed.

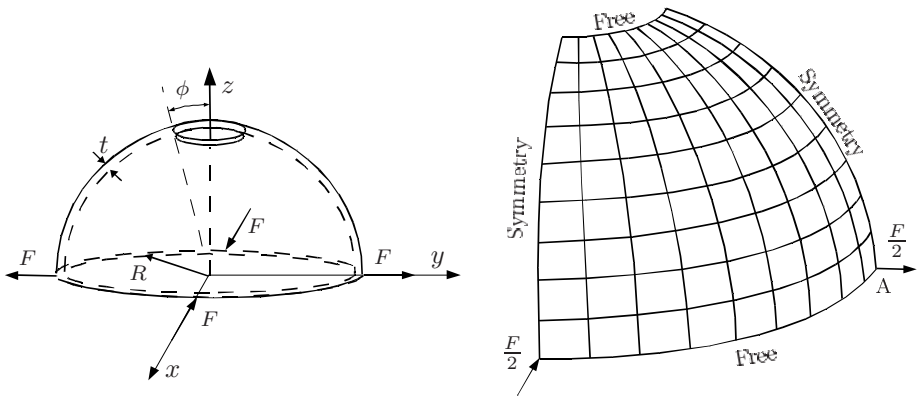

Figure 2.6: *Geometry and boundary conditions for the pinched hemisphere. Load* $F = 2$. *Dimensions:* $R = 10.0, t = 0.04, \phi = 18.0°$. *Isotropic material properties:* $E = 6.825 \cdot 10^7, \nu = 0.3$. *Reproduced from [Hvejsel and Hansen, 2007].*

When developing the formulation of the explicit thickness integration the radius of curvature was assumed to be significantly larger than the shell thickness. Hence, what is interesting to investigate is the precision of this assumption when varying the ratio of radius of curvature to shell thickness. The pinched hemisphere is thus analysed for a series of $\frac{R}{t}$ ratios. This task is done using both regular layer-wise thickness integration, explicit thickness integration and approximated explicit thickness integration. For comparison the radial displacement of point A is monitored for all analyses.

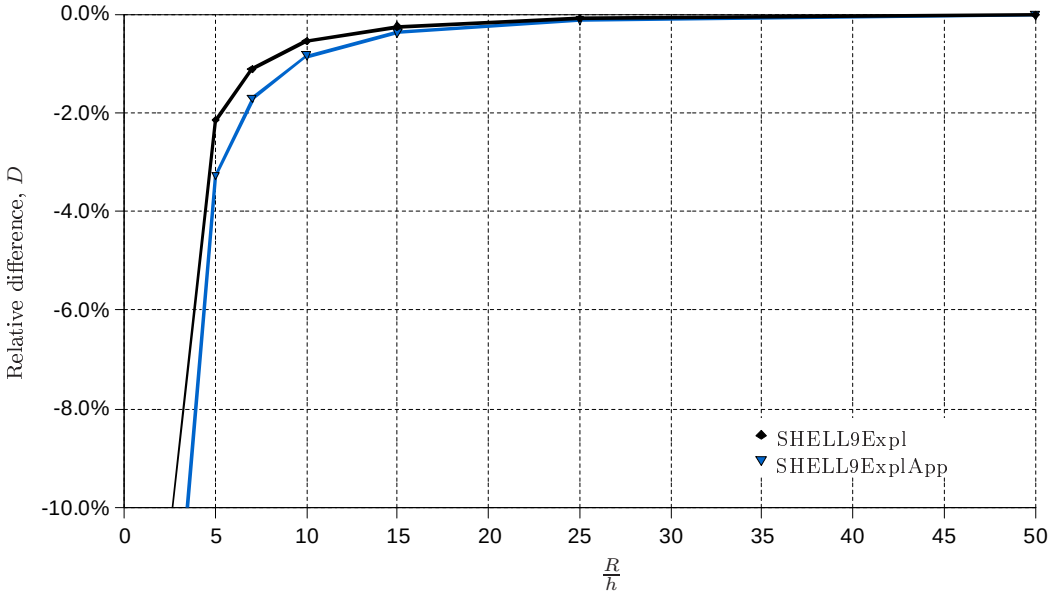

Figure 2.7: *Relative difference in displacement of point A for both analyses conducted with explicit thickness integration and analyses conducted with approximated explicit thickness integration when compared to analyses conducted with regular layer-wise integration. Reproduced from [Hvejsel and Hansen, 2007].*

The results of the investigation are plotted in figure 2.7. As can be seen from the figure, when the $\frac{R}{t}$ ratio is above ~ 25 both explicit thickness integration and approximated explicit thickness integration give results that are almost identical to the layer-wise thickness integration. For ratios in the other end of the scale, below ~ 15, a slight difference between the explicit thickness integration and the approximated explicit thickness integration is observed. This may be explained by the fact that the approximate explicit integration was derived upon the notion that the $\underline{B_3}$ contains higher order terms of the shell thickness. Thus as the thickness is increased the difference between the two formulations must be expected to likewise increase. Results from analyses with $\frac{R}{t} < 10$ are also shown in the plot. However, it might be questioned if such structures should be modelled with shell assumptions (FSDT). In general it is seen that the explicit thickness integration give accurate results, that only differ with around 1% when at its most. Also the approximated explicit thickness integration give good results. A slightly larger relative difference must be expected here though, especially for thick and curved structures.

The reformulations of this project regarding the use of lamination parameters have been tested to give the exact same results as the formulations implemented by [Hvejsel and Hansen, 2007]. The accuracy of the implemented stiffness calculations is thus ensured.

2.5.2 Performance — Rectangular elements

Now knowing that the explicit thickness integration as well as the approximated explicit thickness integration give reasonably accurate results, the next interesting question is whether the methods actually give any decrease in calculation time. This question is sought investigated by assembling the element stiffness matrices of 100 rectangular plates as a function of the number of layers. Since plate elements are used, the variation of the Jacobian in theory vanishes making a lot of the entrances in the $\underline{E}_i$-matrices zero. However, in the experiment these entrances are still present so it should be representable. The results are shown in figure 2.8.

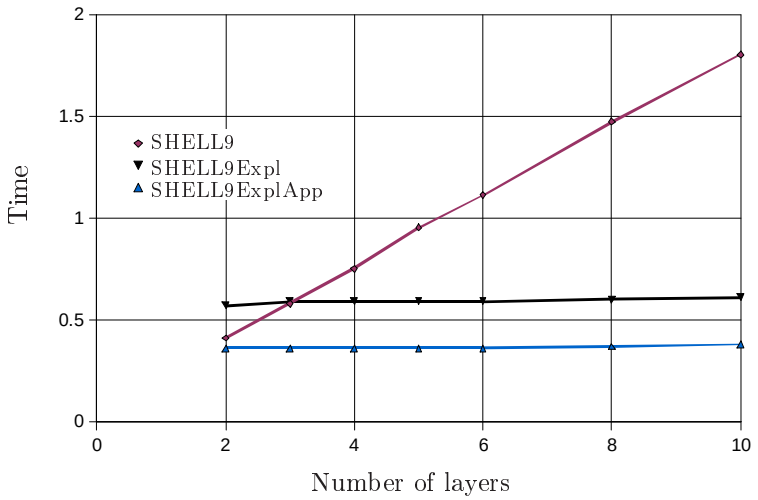

Figure 2.8: *Time of formulation and assembly of stiffness matrix for 100 elements bye the three distinct methods. Reproduced from [Hvejsel and Hansen, 2007].*

As can be seen from the plot, the time consumption for regular layer-wise integration is proportional to the number of layers, whereas the time consumption for both the explicit thickness integration and the approximated explicit thickness integration seem almost constant (or at least have a much lower proportionality constant). The conclusion is that for structures consisting of only a few layers a regular layer-wise integration is preferred, whereas for structures with many layers the two explicit methods are much more efficient, and as more layers are present in the geometry, the larger is the gain in performance. In the industry structures with several hundred layers are not unusual. Hence the explicit methods are considered a remarkable improvement. It could, however, be questioned whether the increase in computational performance with the approximated explicit thickness integration when compared to the explicit thickness integration is worth the loss in accuracy. This judgment is related to both geometry and the desired results for which reason it must be assessed for each individual problem.

2.6 Summary

This chapter has introduced the basic concepts of shell element theory. Given both a geometric representation and the FSDT assumptions the required strain-displacement relations have been derived as seen in equation (2.41). The thickness dependency has been explicitly noted as a first step in order to obtain the derived methods of explicit thickness integration and approximated explicit thickness integration. These methods are basically constituted by equations (2.49) and (2.51).

Furthermore the constitutive relations have been examined in order to obtain a formulation where the so-called *lamination parameters* are incorporated. This has been obtained in the form of equa-

tions (2.66) and (2.67) which when all comes to all renders the stiffness matrix linear in the lamination parameters. Namely this last property is what is sought utilised in the following parts of the thesis.

At last the derived formulations have been investigated w.r.t. accuracy and performance. The conclusions of this investigation are that both explicit thickness integration and approximated explicit thickness integration gives reasonable results when the shell is thin compared to the radius of curvature, which is in correspondence with the assumptions of FSDT, and that the two explicit methods give a noticeable increase in computational efficiency.

The next chapter serves to utilise some of the aspects derived in this chapter, in order to overcome a common problem associated with optimisation of composite structures, namely the presence of local minima solutions in the design space.

Chapter

3

Optimisation with Lamination Parameters

In this chapter a new method for optimising layered composite structures is presented. The method is based upon preliminary ideas presented by [Foldager, 1999] which were revised by [Kann and Sørensen, 2010]. The method utilises lamination parameters to overcome the non-convex nature of the design space associated with applying fibre orientations as design variables. At first, however, some preliminary concepts are presented regarding optimisation in general and optimisation where lamination parameters are applied as design variables. Afterwards the optimisation technique used in this thesis is presented — a technique where the properties of lamination parameters are used but the fibre orientations are kept as design variables.

3.1 Concept of Optimisation

The purpose of performing optimisation is either to maximise or to minimise the performance of a given problem. In structural mechanics, this is done by reformulating the physical problem into a mathematical problem, also called an objective function. The purpose of this function is to grade the performance of the problem by a single value. In structural mechanics the variables of the objective function are generally based upon the values of the physical parameters i.e. geometric design, fibre orientation, thicknesses, and material. These variables thus reflect the design of the structure, hence they are also referred to as design variables. Besides the objective function, constraint functions can also be formulated. These functions ensure that the criteria which they represent are fulfilled during the optimisation process by dividing the design space into allowable and inadmissible parts. In general two types of constraint functions exist, equality and inequality constraints. Typically, the above mentioned functions are formulated in a manner which is referred to as *The Standard Model*. According to [Arora, 2004] this formulation is defined as:

Objective function:

$$f(\vec{x}) = f(x_1, x_2, ..., x_n) \tag{3.1a}$$

Subjected to the equality constraints:

$$h_i(\vec{x}) = h_i(x_1, x_2, ..., x_n) = 0, \quad i = 1...p \tag{3.1b}$$

and the inequality constraints:

$$g_j(\vec{x}) = g_j(x_1, x_2, ..., x_n) \leq 0 \quad j = 1...m \tag{3.1c}$$

where: $x_1, x_2, ..., x_n$ Design variables.

Typically, the objective function is formulated such that the goal is to minimise the function value. However, if the goal actually is to maximise the value of the objective function, then one simply has to minimise the negative objective function. Thus for the remaining part of this thesis, optimisation is always associated with minimisation of the objective function.

The objective and constraint functions can be formulated either as *explicit* or *implicit* functions where an explicit formulation most often is faster to evaluate than an implicit formulation. In structural optimisation the objective function can rarely be formulated as an explicit function being that most types of structures are too complicated to be formulated as an explicit mathematical formula. For structures such as wind turbine blades and aircraft structures where both the geometry and the load scenarios are complicated, the objective function may rely on results from a finite element model and thus making the objective function implicit. These types of problems can be solved using a wide variety of different methods. It is though beyond the scope of this thesis to make a thorough description of all the available methods. However, in structural mechanics numerical optimisation using a gradient based method is often applied due to its versatility. This type of optimisation will also be one of the main topics for the remaining part of this thesis.

Depending upon the specific type of problem the structure may be parameterised in different ways. That is, the choice of design variables can be done in many ways. However, the diverse nature of the design space associated with different parameterisations in combination with different weaknesses of the available optimisers imply that various results might arise for optimisations performed with different parameterisations and optimisers — even though the global optimum obviously is the same for all parameterisations. Thus the performance of the optimised design is highly dependent upon the choice of parametrisation.

3.2 Maximum Stiffness Optimisation

Optimisation of mechanical structures can be performed with various objectives in mind. In the early design phase topology optimisation may be applied in order to either save material. When it comes to structures made from composite materials the designer has the ability to tailor the material which makes it possible to maximise the full potential of the structures. One of the essential properties in any load carrying structure is the overall stiffness of the structures. One method of maximising the stiffness is to minimise the compliance and thus reducing the displacements of the loaded structure. The compliance is defined as the work done by the external loads with full intensity:

$$C(\vec{x}) \equiv W(\vec{x}) = \vec{D}^T \vec{R} \tag{3.2}$$

where:

C	Compliance.
W	Work done by external loads.
$\vec{x}$	Design variable vector.
$\vec{D}$	Global displacement vector.
$\vec{R}$	Global force vector.

For an elastic and conservative material the principle of energy conservation states that the strain energy, in the state of equilibrium, is equal to the work done by the external loads when these have increased uniformly from zero [Zienkiewicz and Taylor, 1989]:

$$U = \frac{1}{2}W \qquad \Rightarrow \qquad U - \frac{1}{2}W = 0 \tag{3.3}$$

where: U Strain energy

It is thus evident that the compliance is directly related to the strain energy. If the structure is in equilibrium and the material is linear elastic then the strain energy can be determined using finite element notation as:

$$U = \frac{1}{2}\vec{D}^T \underline{K}\vec{D} = \frac{1}{2}\sum_{e=1}^{n_{elem}}\left(\vec{d}_e^T \underline{k}_e \vec{d}_e\right) \tag{3.4}$$

where: $\underline{K}$ Global stiffness matrix.

$\underline{k}_e$ Element stiffness matrix.

$\vec{d}_e$ Element displacement vector.

n_{elem} Number of elements.

Thus by minimising the strain energy one also minimises the compliance whereby the stiffness of the structure is maximised. The only requirements are that the material must be linear elastic and without damping, and the structure must be in a state of equilibrium. In the context of optimisation the objective function may be formulated cf. the standard model as:

$$f(\vec{x}) = U(\vec{x}) \tag{3.5}$$

3.2.1 Stiffness Sensitivity

As mentioned in the previous section gradient based methods are often applied in structural optimisation, thus gradient / sensitivity information is needed during the optimisation process. Determining the sensitivities of the compliance with respect to the design variable x_i can be obtained through the strain energy in equation (3.4). The first derivative of the strain energy with respect to the design variable x_i is determined as:

$$\frac{\partial U}{\partial x_i} = \frac{1}{2}\left(\frac{\partial \vec{D}^T}{\partial x_i}\underline{K}\vec{D} + \vec{D}^T\frac{\partial \underline{K}}{\partial x_i}\vec{D} + \vec{D}^T\underline{K}\frac{\partial \vec{D}}{\partial x_i}\right) \tag{3.6}$$

Due to the symmetry of the stiffness matrix the above expression can be reduced to:

$$\frac{\partial U}{\partial x_i} = \vec{D}^T\underline{K}\frac{\partial \vec{D}}{\partial x_i} + \frac{1}{2}\vec{D}^T\frac{\partial \underline{K}}{\partial x_i}\vec{D} \tag{3.7}$$

The above expression can be used directly to obtain the sensitivities. However, it is necessary to determine the quantity $\frac{\partial \vec{D}}{\partial x_i}$ whereby the equilibrium equations often have to be solved at least one additional time for each design variable. This can be a time consuming procedure. It can, however, be omitted by applying the following mathematical manipulation. Taking the first derivative of the finite element equilibrium equations with respect to the design variable x_i yields:

$$\begin{aligned} &\underline{K}\vec{D} = \vec{R} && \Rightarrow \\ &\frac{\partial \underline{K}}{\partial x_i}\vec{D} + \underline{K}\frac{\partial \vec{D}}{\partial x_i} = \frac{\partial \vec{R}}{\partial x_i} \end{aligned} \tag{3.8}$$

Now assuming that the loads are assumed to be design independent, the quantity $\frac{\partial \vec{R}}{\partial x_i} = \vec{0}$, which reduces the expression:

$$\frac{\partial \underline{\underline{K}}}{\partial x_i}\vec{D} + \underline{\underline{K}}\frac{\partial \vec{D}}{\partial x_i} = \vec{0} \qquad \Rightarrow$$
$$\underline{\underline{K}}\frac{\partial \vec{D}}{\partial x_i} = -\frac{\partial \underline{\underline{K}}}{\partial x_i}\vec{D} \tag{3.9}$$

By substituting the above expression into equation (3.7) the final expression for the strain energy sensitivity is obtained as:

$$\frac{\partial U}{\partial x_i} = -\frac{1}{2}\vec{D}^T\frac{\partial \underline{\underline{K}}}{\partial x_i}\vec{D} = -\frac{1}{2}\sum_{e=1}^{n_{elem}}\vec{d}_e^{\,T}\frac{\partial \underline{k}_e}{\partial x_i}\vec{d}_e \tag{3.10}$$

Applying the above expression the finite element equilibrium equations only have to be solved once for each optimisation step in the design space, as opposed to if equation 3.7 were used. From here it is simply a question of determining the stiffness sensitivities for those elements which the design variables have an effect on and then reuse the element displacements determined from the equilibrium equations. The stiffness sensitivities can be determined by applying a perturbation technique in the form of either a forward/backward- or a central difference approximation, depending upon the required accuracy. However, if the lamination parameters are applied as design variables then the stiffness sensitivities can be determined analytically. This is shown in the following.

3.2.2 Stiffness Sensitivity w.r.t Lamination Parameters

In section 2.3.2 the stiffness matrix of an element was derived for the case of an explicit integration through the thickness. This expression is repeated here for convenience:

$$\begin{aligned}\underline{k}_e = \int_{-1}^{1}\int_{-1}^{1}\Big(&\underline{B}_1^T\,\underline{E}_1\,\underline{B}_1 + \underline{B}_1^T\,\underline{E}_2\,\underline{B}_2 + \underline{B}_1^T\,\underline{E}_3\,\underline{B}_3\\ &+ \underline{B}_2^T\,\underline{E}_2\,\underline{B}_1 + \underline{B}_2^T\,\underline{E}_3\,\underline{B}_2 + \underline{B}_2^T\,\underline{E}_4\,\underline{B}_3\\ &+ \underline{B}_3^T\,\underline{E}_3\,\underline{B}_1 + \underline{B}_3^T\,\underline{E}_4\,\underline{B}_2 + \underline{B}_3^T\,\underline{E}_5\,\underline{B}_3\Big)\tfrac{2}{h}\Delta_A^2\,drds\end{aligned} \tag{3.11}$$

The only quantities in the above expression which are dependent upon the lamination parameters are the thickness integrated constitutive properties represented by the $\underline{E}$ matrices. Taking the first derivative of the above with respect to the lamination parameters yields:

$$\begin{aligned}\frac{\partial \underline{k}_e}{\partial \xi_i^j} = \int_{-1}^{1}\int_{-1}^{1}\Big(&\underline{B}_1^T\frac{\partial \underline{E}_1}{\partial \xi_i^j}\underline{B}_1 + \underline{B}_1^T\frac{\partial \underline{E}_2}{\partial \xi_i^j}\underline{B}_2 + \underline{B}_1^T\frac{\partial \underline{E}_3}{\partial \xi_i^j}\underline{B}_3\\ &+ \underline{B}_2^T\frac{\partial \underline{E}_2}{\partial \xi_i^j}\underline{B}_1 + \underline{B}_2^T\frac{\partial \underline{E}_3}{\partial \xi_i^j}\underline{B}_2 + \underline{B}_2^T\frac{\partial \underline{E}_4}{\partial \xi_i^j}\underline{B}_3\\ &+ \underline{B}_3^T\frac{\partial \underline{E}_3}{\partial \xi_i^j}\underline{B}_1 + \underline{B}_3^T\frac{\partial \underline{E}_4}{\partial \xi_i^j}\underline{B}_2 + \underline{B}_3^T\frac{\partial \underline{E}_5}{\partial \xi_i^j}\underline{B}_3\Big)\tfrac{2}{h}\Delta_A^2\,drds\end{aligned} \tag{3.12}$$

where: i $= 1,2,3,4.$

j $= A,B,D,E,F,G,H.$

It should be noted that the dependence of the constitutive properties upon the lamination parameters varies from E_1 – E_5. Thus the active parts of the above expression depends upon the given lamination parameter. A complete description of how to determine all the individual sensitivities is listed in appendix B.

3.2.2.1 Numerical Verification of Sensitivities

The verification of the analytically sensitivity expressions has been done by comparing results obtained from a Matlab program and the finite element program MUST. The Matlab program determines the sensitivities using a central difference approximation directly of the strain energy, whereas the analytical expressions have been implemented in MUST. The Matlab program is built around classical laminate plate theory, thus only 12 lamination parameters are subjected for comparison. The example used for the verification is a square plate clamped on one side, and pulled uniformly on the opposite side. In MUST the plate is modelled using nine equally sized nine node elements as shown in figure 3.1. The dimensions of the plate $1 \cdot 1m$, the loads is $3kN$ distributed uniformly over the indicated face. The material properties used are shown in table 3.1.

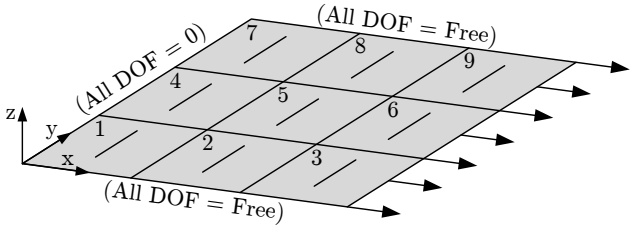

Figure 3.1: *Clamped plate subjected to uniformly distributed force. Fibre orientations are indicated as a small line in each element.*

Quantity	E_1	E_2	E_3	G_{12}	ν_{12}	ν_{23}	ν_{13}
Set to	$138MPa$	$9Mpa$	$9Mpa$	$7MPa$	0.3	0.3	0.3

Table 3.1: *Material properties for Graphite-Epoxy (AS/3501).*

The plate consists of 30 layers all with a thickness of $0.001m$ and an angular orientation of $\frac{\pi}{2}$ relative to the x-direction. In order to minimise boundary effects in the finite element model, element number 5 is selected for comparison in accordance with Saint-Venant's principle. The sensitivities are determined individually and assembled in a vector which is scaled to unit length. Comparing the results from the two models shows that they produce equal sensitivities down to the third digit, thus verifying the analytical expressions and their implementation in MUST. The results are shown in table 3.2.

	$\frac{\partial U_d}{\partial \xi_1^A}$	$\frac{\partial U_d}{\partial \xi_2^A}$	$\frac{\partial U_d}{\partial \xi_3^A}$	$\frac{\partial U_d}{\partial \xi_4^A}$
Matlab	-0.974712139750969	0	-0.223464190916772	0
MUST	-0.974706493423170	-0.000277434293206	-0.223488609380365	-0.000127224803855

	$\frac{\partial U_d}{\partial \xi_1^B}$	$\frac{\partial U_d}{\partial \xi_2^B}$	$\frac{\partial U_d}{\partial \xi_3^B}$	$\frac{\partial U_d}{\partial \xi_4^B}$
Matlab	0	0	0	0
MUST	0.000000000000001	-0.000000000000000	0.000000000000000	-0.000000000000000

	$\frac{\partial U_d}{\partial \xi_1^E}$	$\frac{\partial U_d}{\partial \xi_2^E}$	$\frac{\partial U_d}{\partial \xi_3^E}$	$\frac{\partial U_d}{\partial \xi_4^E}$
Matlab	0	0	0	0
MUST	-0.000000000000000	0.000000000000000	-0.000000000000000	0.000000000000000

Table 3.2: *Sensitivities from Matlab and MUST.*

3.3 Patches

A patch is a group of elements that share the same set of design variables. This enables the designer to use a fine mesh so as to obtain a good approximation of the displacement field, while keeping the number of design variables low so as to reduce the computational time needed for an optimisation to converge. In figure 3.2 a square plate is modelled with four patches where each patch covers nine elements.

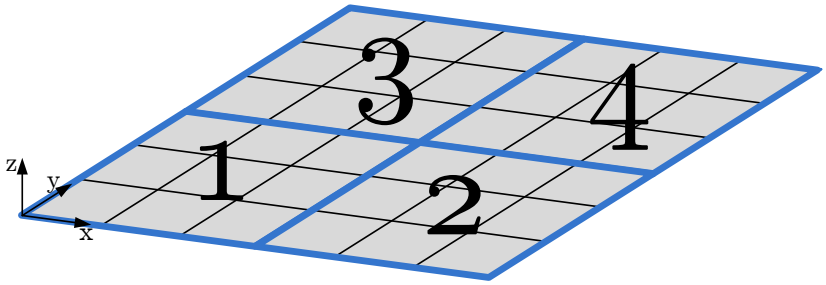

Figure 3.2: *A plate divided into four patches, each divided into nine elements.*

In this example each element contains one lamina where the fibre orientation is applied as a design variable. The patch model thus has four design variables. If the patches were removed the model would have 36 design variables which would increase the amount of time needed for convergence.

Another benefit of applying a patch formulation is that the engineer may use less time on post-processing the optimised design. This is because larger areas of the structure will have the same value of the design variable, making it easier for the engineer to translate the result into what is actually possible to build. The problem with applying a patch formulation is that each patch represents the average of the covering elements, thus some of the elements in the patch may be assigned a value of the design variable which may differ from what the optimum value is for that particular element. Thus the final design may not represent the same optimum design as would arise if the problem was solved at element level. It is thus up to the engineer to determine how small each patch has to be in order to obtain a good result, while also keeping the patch big enough so as to use less time on post-processing and waiting for the optimisation to converge. However, no matter how this ratio is scaled

the need for post-processing of the optimised design is unavoidable with the current optimisation techniques as ply continuity is not enforced between the patches.

3.4 Parametrisation

Depending on the chosen parametrisation different limitations are imposed upon the design variables. The fibre orientations, thicknesses and the lamination parameters can be utilised as continuous variables which can attain any value within their given bounds. The material properties on the other hand have to fit an existing material whereby the set of allowable values becomes a discrete set. It is also reasonable to imagine a situation where the manufacturer only has a limited set of fibre mats each with a predefined thickness and fibre orientation, thus making these properties discrete design variables. By choosing a discrete formulation the manufacturer may be able to optimise the structure according to what is possible to build. However, if the goal is to determine the best possible solution with this material, i.e. to determine the global minimum of the objective function treated with all values of the design variables possible, a discrete parametrisation of the problem may not contain this solution due to the limitations imposed on the design variables.

If continuous design variables are applied then the determination of the global minimum may be possible but certainly not guaranteed even though it may be present in the design space. It is only possible to guarantee the determination of the global minimum if the design space is convex. This especially becomes a problem when optimising composite structures using a gradient based method because both the thicknesses and fibre orientations have a strong non-linear influence on the stiffness of the structure, and as known the stiffness is an important property in structural optimisation. That is e.g. when maximising the minimum buckling load or when minimising the strain energy. This specific non-linear relation to the design variables makes the design space non-convex, and thus gradient based algorithms will typically get stuck in a local minimum. This makes the lamination parameters introduced in section 2.4.3 interesting because the element stiffness matrix of a laminate is linear with respect to these, provided that the same material is used throughout the entire thickness of the laminate. However, when applying lamination parameters as design variables one has to ensure that the parameters represent a feasible design which can be realised when the optimisation has converged. The problems of feasibility and identification are elaborated in the following.

3.5 Characteristics of Lamination Parameters

Much focus has been put on the characteristics of lamination parameters by different researchers. In particular the problems of feasibility as well as convexity have drawn the attention. These two areas of interest are elaborated on in the following.

3.5.1 Feasibility

Lamination parameters are defined on the basis of the laminate thicknesses and fibre orientations and are thus dependent parameters which reflect the laminate design rather than define it. Thus when applying lamination parameters as design variables one has to ensure that they always represent a lay-up which can be realised. To further complicate the situation the parameters are mutually dependent upon one another [Bloomfield et al., 2009]. By definition the lamination parameters can assign values within the bounds of $-1 \leq \xi_i^j \leq 1$, however, this does not provide sufficient guarantee that the parameters represent a feasible lay-up thus further constraints have to be formulated.

At the current time the research within the field of feasibility has been concentrated around classical laminate plate theory where 12 lamination parameters describe the lay-up of the plate. When applying lamination parameters to determine the stiffness of a shell in a finite element formulation, a

total of 28 lamination parameters can be used. To the knowledge of the authors no literature has been published regarding feasibility for such a formulation. In the following some research concentrated around classical laminate plate theory using 12 lamination parameters is presented.

Within the field of laminate plate theory the constraints required to ensure feasibility have still not been determined for the *general case* where all possible configurations of ply orientations and load scenarios are accounted for. However, for specific load scenarios and laminate lay-ups some constraints on the feasible domain have been determined. The first of these were presented by [Miki, 1982] who determined the bounds of the feasible domain for an orthotropic laminate subjected to either in-plane or out-of-plane loads. After [Miki, 1982] others also determined constraints for some special cases, among which are [Fukunaga and Sekine, 1992] who determined the relationship between the four in-plane parameters and also for the four out-of-plane parameters. Furthermore [Grenestedt and Gudmundson, 1993] determined a series of constraints, one of which is for an orthotropic and balanced plate subjected to coupled in- and out-of-plane loads. They further showed that the feasible domain containing the lamination parameters must be convex for the general case, where no restrictions have been made regarding laminate lay-up or loading conditions. What all of these constraint formulations have in common is that they are valid for all angular configurations, within their respective restrictions of e.g. orthotropic and/or symmetry. Attempts have also been made for describing the constraints for a discrete set of ply configurations, here [Bloomfield et al., 2009] accomplished to describe the fully constrained feasible domain for laminates with 0°, ±30°, ±45°, ±60°, 90° plies. However, the method in [Bloomfield et al., 2009] is not restricted to the presented set of configurations, but can in theory determine the constraints for any number of prefixed plies with different angular and thickness configurations. Still, at present time the full set of constraints is yet to be determined for the general case, where no restrictions are made with respect to ply orientations, lay-ups, and loads [Grenestedt and Gudmundson, 1993], [Hammer et al., 1997], [Bloomfield et al., 2009].

Thus when it comes to optimisation where lamination parameters are applied as design variables, this has only been done using 12 lamination parameters i.e. plates. In this case, the kinematics are restricted to be described by use of CLT or FSDT. Furthermore if continuous fibre orientations are desired the laminate design is restricted either in the form of its load carrying capability or lay-up. For a discrete set of ply configurations the method presented by [Bloomfield et al., 2009] can be applied. Both of these options are thus not applicable for optimisation where the laminate lay-up has to be free from restrictions and neither of them can strictly be applied if the structure has to be modelled using a shell formulation. These limitations are sought to be bypassed by use of the method presented in this thesis.

3.5.2 Convexity

Different statements regarding convexity or not of the lamination parameters and formulations of these have indeed been made. To clarify, here is given a short recap of what, to the knowledge of the authors, is known regarding lamination parameters and convexity at present time. For the sake of clarity the expression for the strain energy, in a finite element notation, is repeated from expression (3.4) here:

$$U = \frac{1}{2} \sum_{e=1}^{n_{elem}} \left(\vec{d}_e^{\,T} \, \underline{k}_e \, \vec{d}_e \right) \tag{3.13}$$

As shown in section 2.4.3 the element stiffness matrix can be expressed in terms of the lamination parameters, and it is evident that it is linear in those. Though the stiffness matrix is linear in terms of the lamination parameters, the dependency of the strain energy w.r.t. the lamination parameters are

not necessarily so simple, as the displacements are dependent upon the stiffness. For clarification the expression for the strain energy is here shown with its dependency upon the lamination parameters:

$$U = \frac{1}{2} \sum_{e=1}^{n_{elem}} \left(\vec{d}_e \left(\overrightarrow{\xi^n} \right)^T \underline{k}_e \left(\vec{\xi} \right) \vec{d}_e \left(\overrightarrow{\xi^n} \right) \right) \tag{3.14}$$

where: $X\left(\overrightarrow{\xi^n}\right)$ Indicates that X depends on ξ_i in some order n.

$X\left(\vec{\xi}\right)$ Indicates that X depends on ξ_i in first order.

As seen the strain energy is dependent upon the lamination parameters in an order of $2n+1$. Dependent on n this can obviously be very nonlinear. However, [Svanberg, 1984] showed that stiffness optimisation problems in a finite element context, can be shown to be convex if stiffness matrix is linear w.r.t the design variables and if the design variables furthermore are either linear or convex confined. This notion was later used by [Grenestedt and Gudmundson, 1993] who showed that the strain energy is convex when lamination parameters are applied as design variables. The proof utilised that the lamination parameters are confined in a convex space, as shown by [Grenestedt and Gudmundson, 1993] and by the work done by [Bloomfield et al., 2009], though this work is in fact done discretely. For the restricted case of either in- or out-of-plane loading conditions [Setoodeh et al., 2006] has proven that the complementary strain energy, which is equal to the strain energy for a linear elastic material, is convex for the given restrictions. Also in the previous work done by the authors [Kann and Sørensen, 2010], it was shown through numerical experiments that the strain energy density likewise is convex for either pure in-plane or out-of-plane loading conditions. However, all of the above proofs regarding convexity have been performed on the basis of plate theory and thus only 12 lamination parameters have been applied. To the knowledge of the authors, still no one has proven if the 20 or 28 lamination parameters applied in a shell formulation likewise are confined in a convex space, which is required for archiving the convex stiffness optimisation problem. Furthermore, in order to perform optimisation with lamination parameters as design variables the feasible domain has to be known. This has neither been determined for 12, 20 or 28 lamination parameters in a general sense and only for restricted scenarios when applying 12 lamination parameters. Thus other methods have to be applied if a restriction free lay-up is wanted.

3.6 Method for Optimisation with Lamination Parameters

As pointed out in the previous section no restriction free method exists for optimising laminated composite structures where lamination parameters are applied as design variables. However, another method exists for overcoming the non-convex nature of the design space associated with stiffness optimisation of composite structures. This method was first presented by [Foldager, 1999] and it is referred to as a *Two-Step Approach*. The concept of the method is illustrated in figure 3.3.
With this approach a conventional gradient based optimisation algorithm is utilised where the design variables are the independent parameters i.e. ply orientations and thicknesses. The optimisation process from point O to D is elaborated by the following generalised example. In the example the objective is to minimise the strain energy. The structure is in a state of equilibrium and the loads are assumed design independent.

The optimisation process sketched in figure 3.3 runs as follows:

1. The optimisation process is initialised with a gradient-based optimiser from some arbitrary location O using fibre angles and thicknesses as design variables.

2. From the initial location, the optimisation algorithm will typically converge to a solution which is a local minimum, illustrated by point A. The lay-up here is denoted as a *sub-optimal* lay-up.

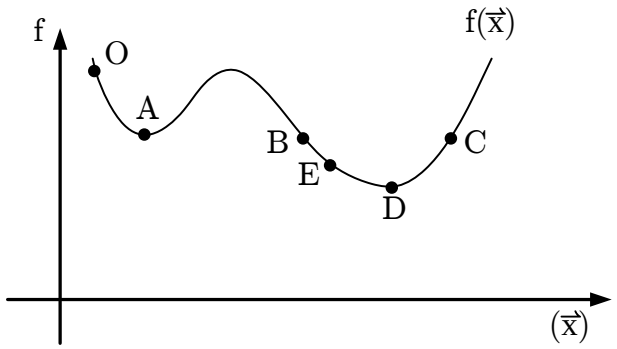

Figure 3.3: *Two-Step optimisation approach. Design variables are ply-orientations and thicknesses*

3. From point A an *identification process* is initialised where the purpose is to determine a new location somewhere between points B and C. This identification process is elaborated in section 3.6.1.

4. Assuming the identification was successful and some location E has been determined, the gradient based optimisation algorithm is re-initialised at this location. This leads to the determination of point D which again may be a local minimum.

5. Located at point D the identification process is repeated. If no new lay-ups can be determined it is assumed that the global minimum of the objective function has been determined and the optimisation is terminated.

3.6.1 The Identification Process

The identification process first proposed by [Foldager, 1999] utilises the lamination parameters to determine a new location in the design space, illustrated in figure 3.3 as point E. In order to clarify how this is made possible the expression for the strain energy's dependency upon the lamination parameters is re-examined:

$$U = \frac{1}{2} \sum_{e=1}^{n_{elem}} \left(\vec{d}_e \left(\vec{\xi^n} \right)^T \underline{k}_e \left(\vec{\xi} \right) \vec{d}_e \left(\vec{\xi^n} \right) \right) \tag{3.15}$$

As can be seen from the expression the lamination parameters define the stiffness of a given element, and in turn the level of strain energy. Because point B and C share the same level of strain energy, they must also share the same structural stiffness due to the loads being design independent. As a consequence the three points A,B, and C may also share the same set of lamination parameters. The idea presented by [Foldager, 1999] is to identify other physical lay-ups which produce the same set of lamination parameters as the lay-up associated with point A. Such lay-ups will produce the same level of strain energy and hence represent a new location in the design space from which the optimisation can be re-initiated.

The identification process presented by [Foldager, 1999] is formulated as an optimisation problem where the objective is to minimise a suitable function — the so-called *identification function*. This identification function utilises the physical parameters of the laminate i.e. ply orientations and thicknesses thus avoiding the problems regarding feasibility. The purpose of the identification function is thus to compare and grade the lamination parameters from the new lay-up to the lamination parameters of the old lay-up i.e. the lay-up associated with the local minimum. If a new lay-up is

determined the identification process is terminated and the new lay-up is applied in the further optimisation of the structure.

However, the identification function presented by [Foldager, 1999] also searched for of lay-ups in between points B and C, meaning that the identification function accepted lamination parameters which could be very different compared to those from point A. By accepting different lamination parameters the identified lay-up will also produce a new stiffness. However, because the displacements and the loads were kept fixed during the identification, the new lay-up would not be able to produce the level of strain energy and thus violate the structures state of equilibrium. Further analysis of the presented identification function revealed other problems. For a detailed analysis of the function the reader is referred to [Kann and Sørensen, 2010] (available at the in appendix C enclosed CD). A brief presentation of the main problems are given here though:

Singularities: The function presented by [Foldager, 1999] included singularities for lamination parameters having values of both 0 and 1, which obviously affects the performance of the procedure. Furthermore it is a problem of fundamental character that an optimisation algorithm cannot predict a basic case such as all fibres aligned in the direction of the first axis of the SCS, which e.g. would be the optimum of a structure in pure tension (that is, pure tension in the direction of the first axis of the SCS). This was documented in [Kann and Sørensen, 2010].

Variation of sensitivities: The identification function developed by [Foldager, 1999] incorporated the assumption that the sensitivities of the strain energy density w.r.t. the lamination parameters would remain constant through the identification process no matter the step size and direction. This is obviously not correct, and it was shown by the authors that the sensitivities associated with the new accepted lamination parameters would often have changed size compared to the initial sensitivities determined at location A in figure 3.3 [Kann and Sørensen, 2010].

Method of minimisation: The identification function presented by [Foldager, 1999] was minimised using a gradient based optimiser. However, the identification function itself has later on been proven to be highly non-convex. Thus the minimisation of the identification function was prone to get stuck in a local minimum, meaning that the results were not necessarily optimal. The combination of the non-convexity of the identification function together with the variation of the sensitivities did that nothing qualified could be said about the results of an identification. What "saved" the method (in the sense that good results were also obtained) was an "iterative scheme" were the algorithm was restarted several times with random starting points. Also only lay-ups which produced similar or lower levels of strain energy would be accepted by the algorithm. Thus the identification process was in fact nothing but a guessing routine. This was also documented in [Kann and Sørensen, 2010].

The preceding ideas of the method developed by [Foldager, 1999], which bypassed the problems of feasibility, were quite ingenious. However, as a consequence of the unsatisfactory results associated with the above mentioned problems, a new identification function was previously developed by the authors which is presented in the following. This identification function likewise has to be optimised and utilises ply-orientations and thicknesses as design variables, hence avoiding the problem of feasibility. Also, because of the new formulation the need for the "iterative scheme", where only lay-ups which produced equal or lower levels of strain energy would be accepted, is eliminated. However, the task of finding a set of design variables with the exact same lamination parameters can be a laborious task. This can be eased a little by expanding the interval of accepted lamination parameters. The formulation of such an expansion is elaborated in the following section.

3.6.2 Expansion of Lamination Parameters

Expanding the interval of sought lamination parameters enables an acceptance of lay-ups with lamination parameters that are different from those being subjected to identification. However, by changing the lamination parameters the stiffness of the structure is also changed, and unless the displacements are recalculated the state of equilibrium is violated. Following the mindset from variational methods a small variation of the stiffness while keeping the displacements fixed still gives a good approximation of equilibrium though, and thus eliminates the time consuming process of redetermining the displacements. Such a variation can be achieved through a local linearisation of the objective function i.e. the strain energy with respect to the lamination parameters. The level of variation is thus controlled by the step size i.e. confidence interval of the linearisation. If the linearisation is restricted to be in the direction which minimises the value of the objective function, the identified lay-ups would either give a value equal to or lower than the original level of the objective function. The procedure is illustrated in figure 3.4.

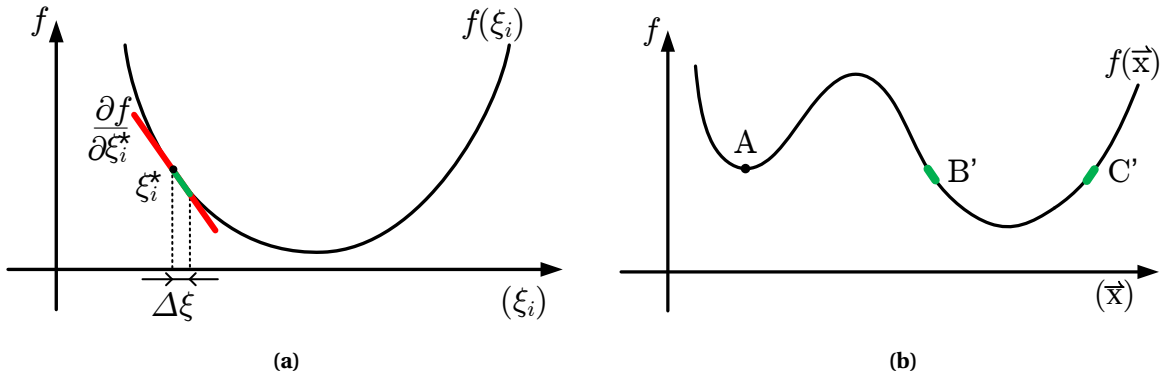

Figure 3.4: *Strain energy in (a) lamination parameter space, (b) design variable space.*

As can be seen in figure 3.4a the linearisation around the original lamination parameter, ξ_i^*, is directed such that the step size, $\Delta\xi$, lowers the value of the objective function. The effect of the expansion is, in the design space described by the design variables, an expansion of points B and C into the two intervals B' and C', respectively, as illustrated in figure 3.4b.

Expanding the lamination parameters may thus allow for other feasible sets of design variables to appear in the identification. However, this may not always be the case as the expansion also can produce an infeasible set of lamination parameters. This effect is illustrated in figure 3.5 where the expanded region of the lamination parameters is illustrated by the green curve enclosing the hatched area. As illustrated the expansion has revealed a new set of feasible lamination parameters, indicated by the green dot, which can be determined through the identification process. However, the expansion has also revealed a new set of infeasible lamination parameters from which no physical lay-up can be identified, indicated by the black dot.

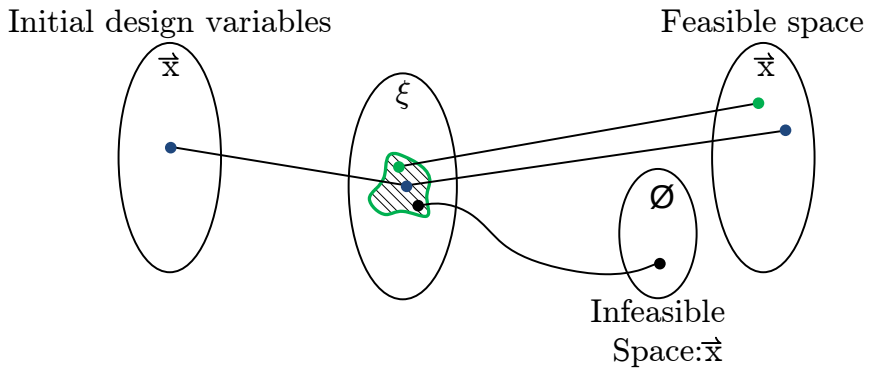

Figure 3.5: *Matching of design variables through expanded lamination parameters.*

It is thus not certain that a new lay-up can be identified by expanding the lamination parameters. It is also possible that the expansion of one parameter may guide the design variable in one direction, where the expansion of another parameter may guide the same design variable in the opposite direction. In such a scenario the expansion has no positive effect. This is illustrated in figure 3.6 where two lamination parameters are shown as functions of one design variable. An expansion of ξ_1^j allows for a larger value of the initial design variable, whereas an expansion of ξ_2^j allows for a smaller value of the initial design variable.

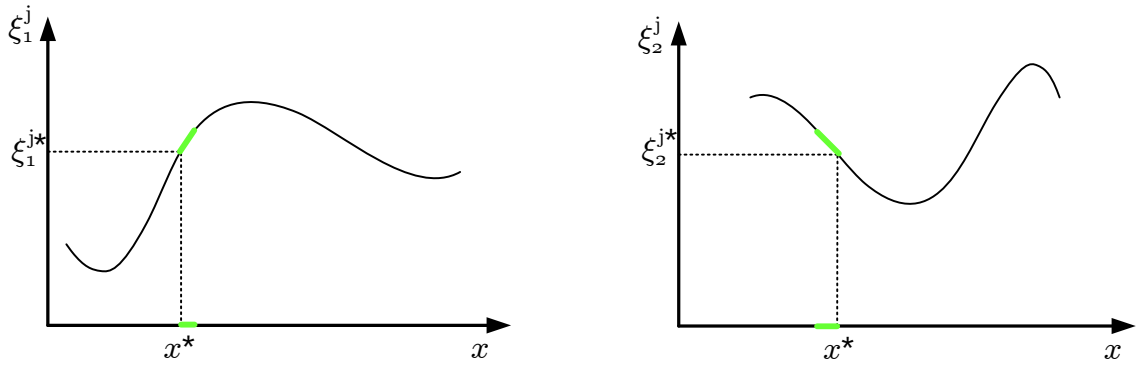

(a) **(b)**

Figure 3.6: *Two lamination parameters as a function of one design variable. In (a) an expansion of ξ_1^j allows for a larger value of the initial design variable. In (b) an expansion of ξ_2^j allows for a smaller value of the initial design variable. The green lines represent the expanded regions.*

As can be seen in the figure the two expansions of the lamination parameters do not result in them sharing a common interval described by the design variable, but rather a common point. This means that the expansion in fact does not open up for any new identifiable design variables and as such the expansion has no effect.

It can, however, be expected that the positive effect of the expansion may increase as the number of design variables is increased. If the two lamination parameters from figure 3.6 did share a common interval it would be confined in the form of a line, which would contain new lay-ups that could be identified. However, if two design variables were used to define the two lamination parameters the shared interval could be extended from a line to a surface which would increase the possibility for identifying a new lay-up. If three design variables were used a shared cubic space could appear and so

forth. Adding more and more design variables should then further increase the possibility of creating common multi-dimensional spaces containing more and more different feasible lay-ups which can be identified.

The above principle of expanding the lamination parameters was verified in the previous work presented by the authors [Kann and Sørensen, 2010]. The verification was performed by observing that some of the identified lay-ups had in fact a lower value, and none had a higher value of the objective function, thus showing that the effect of the expansion was transferred from the lamination parameters to the design variables.

3.6.3 Identification Formulation

When applying a linearisation of the objective function as a means of expanding the values of the lamination parameters, a suitable trust region or step size has to be established. If a fixed step size is applied this value may become too large as the global minimum gradually is approached, resulting in a linearisation which opens up for the possibility of identifying a new lay-up which has a higher value of the objective function. This is illustrated is figure 3.7.

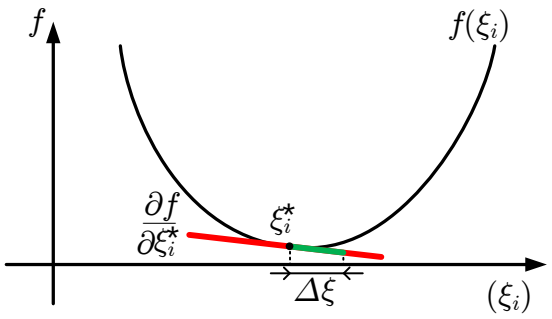

Figure 3.7: *Illustration of the problem with a fixed step-size formulation i.e.* $\Delta\xi = constant$.

The above mentioned ambiguity can be removed by incorporating the sensitivities in the determination of the step size:

$$\vec{d} = \frac{\frac{\partial f}{\partial \vec{\xi}^*}}{\sqrt{1 + \left|\left| \frac{\partial f}{\partial \vec{\xi}^*} \right|\right|^2}} \tag{3.16}$$

where:

$\left|\left| \frac{\partial f}{\partial \vec{\xi}^*} \right|\right|$ Euclidean norm of all $\frac{\partial f}{\partial \xi_i^*}$ assembled in a vector.

$\vec{\xi}^*$ The initial set of lamination parameters assembled in a vector.

Thus as the global minimum of the objective function is being reached the step size gradually goes to zero, and if it is far away from a minimum, i.e $\left|\left| \frac{\partial f}{\partial \vec{\xi}^*} \right|\right| >> 1$, the vector is normalised to unity and the maximum step size becomes $\Delta\xi$. Thus the expanded region is uniquely defined for each lamination parameter as:

$$\Delta\xi_i = -d_i \Delta\xi \tag{3.17}$$

where: $\Delta\xi_i$ Individual allowable variation of each lamination parameter.

$\Delta\xi$ Fixed step size.

The objective function is, as in the previous work [Kann and Sørensen, 2010], chosen to include sensitivities of the strain energy density w.r.t. the lamination parameters. For other objective functions, e.g. maximising the minimum buckling load, the sensitivities may be of a different numeric magnitude. Thus the determination of $\Delta\xi$ should be done on the basis of numerical examples. Applying the above formulations the identification function is defined as:

$$I = \sum_{i=1}^{n_{LP}} \begin{cases} \begin{cases} \left(\xi_i^* - \xi_i(\vec{x})\right) & \left| \quad \xi_i(\vec{x}) < \xi_i^* \right. \\ 0 & \left| \quad \xi_i^* \le \xi_i(\vec{x}) < \left(\Delta\xi_i + \xi_i^*\right) \right. \\ \left(\xi_i(\vec{x}) - \left(\Delta\xi_i + \xi_i^*\right)\right) & \left| \quad \xi_i(\vec{x}) \ge \left(\Delta\xi_i + \xi_i^*\right) \right. \end{cases} & d_i \le 0 \\ \begin{cases} \left(\left(\Delta\xi_i + \xi_i^*\right) - \xi_i(\vec{x})\right) & \left| \quad \xi_i(\vec{x}) \le \left(\Delta\xi_i + \xi_i^*\right) \right. \\ 0 & \left| \quad \left(\Delta\xi_i + \xi_i^*\right) < \xi_i(\vec{x}) \le \xi_i^* \right. \\ \left(\xi_i(\vec{x}) - \xi_i^*\right) & \left| \quad \xi_i(\vec{x}) > \xi_i^* \right. \end{cases} & d_i > 0 \end{cases} \tag{3.18}$$

where: $\xi_i(\vec{x})$ Lamination parameter described by new design variables.

ξ_i^* Initial lamination parameter.

d_i Normalised sensitivity of strain energy density.

n_{LP} Number of lamination parameters.

which can be understood as a mathematical realisation of the expanded interval of accepted lamination parameters accounted for in the previous section. A plot of the function[1] is seen in figure 3.8.

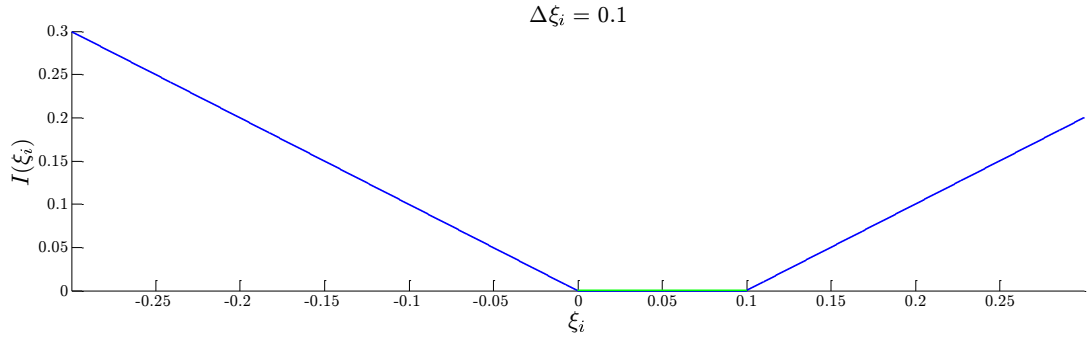

Figure 3.8: *Plot of the identification function.* $\xi_i^* = 0$, $d_i < 0$ *and* $\Delta\xi_i = 0.1$.

As can be seen from the formulation new lay-ups which have lamination parameters within their expanded regions produce an identification function value of zero. If the lay-up has a lamination parameter outside the expanded region, the function value increases linearly the further away the new parameter is from the extended region. Whether the expanded region is to the left or the right of the current parameter is determined by the sign of the gradient for that specific parameter e.g. if $d_i < 0$ the interval is to the right and vice versa.

The value of the lamination parameter being sought identified in the plotted example is $\xi_i^* = 0$ and the sign of the sensitivity is set to $d_i < 0$. As can be seen in the figure the step size implemented in equation (3.18) gives an interval of accepted lamination parameters (indicated by the flat green line) rather than just a single point.

[1] Note that the interval has been truncated to [-0.3; 0.3] for illustrative purposes.

3.6.4 Successful Identification — Dependency on the Number of Layers

A successful identification of a new laminate lay-up through a set of lamination parameters is only possible if other matching lay-ups actually exist. The relationship between design variables and lamination parameters has to be what, for the remainder of this thesis, is referred to as a *several-to-one* relationship. That is, there has to be more than one set of design variables sharing the same set of lamination parameters. If this is not the case and the relationship is *one-to-one* an identification is not possible. It is thus essential to ensure that a several-to-one relationship exists between the design variables and the lamination parameters. The dominating factor for this problem is the number of design variables used to define the laminate, i.e. the number of plies and hence the number of ply thicknesses and orientations. If the number of design variables is too small the relationship is one-to-one, and all sets of lamination parameters giving the same level of strain energy are each connected to each of their unique set of design variables. At a certain level the number of design variables is great enough to create a several-to-one relationship. This claim shall be underpinned by a small investigation of the identification process applied on a two-dimensional example.

The two-layer uniform laminated plate is investigated. The lay-up is $(\theta_1@t, \theta_2@t)$ with fixed thicknesses, and the loads are uniform over the plate. The design space is truncated to $[0;\pi[$ on both axes in order to prohibit permutations of $\pm\pi$. Figure 3.9 shows the design space with values of the strain energy density on the third axis.

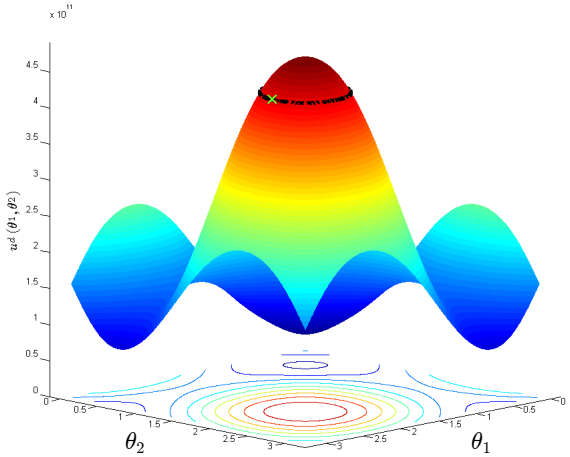

Figure 3.9: *The design space of the two-layer laminate with values of the strain energy density. Reproduced from [Kann and Sørensen, 2010].*

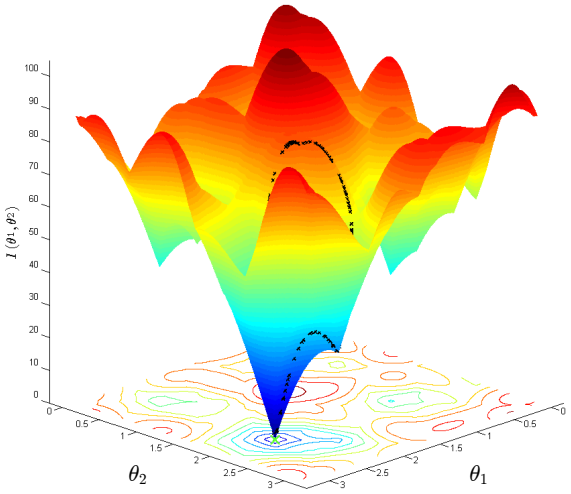

Figure 3.10: *The design space of the two-layer laminate with values of the identification function. Reproduced from [Kann and Sørensen, 2010].*

In the design space an initial point is chosen at $\vec{\theta}^* = [2.53, 2.1]^T$. The point is illustrated with a green cross. The black crosses represent points with equal strain energy density. These points are thus points that possibly could be identified in an identification process provided that they give similar lamination parameters (that is, they should lie within the "expanded region"). The identification process is now set up with the green cross as initial location. Figure 3.10 shows the same design space but now with values of the identification function on the third axis. What is seen is that there is only one single location where the identification function is zero, namely the initial location. This tells that even though there are several points that share the same level of the strain energy, there are not a single set of design variables with similar lamination parameters. Hence no new sets of design variables can be identified. For verification of this point, the lamination parameters of all the black crosses in figure 3.9 have been determined, and it has in fact been verified that they all give different lamination parameters. Obviously, a numerical analysis like this is dependent on the resolution. For

the small analysis conducted here, the design space has been divided into 500 × 500 sub-locations which is believed to be sufficient.

In previous studies the lower bound for the number of design variables was determined through numerical experiments to be 11, when identifying through a total of 12 lamination parameters [Kann and Sørensen, 2010]. In the same study it was shown that increasing the number of design variables likewise increased the rate of success for the identification process. It was thus not a problem to identify a new lay-up when the laminate was described by e.g. 50 design variables.

As earlier mentioned, the expansion of the interval of accepted lamination parameters has in earlier studies by the authors been proven to have a positive effect. However, it was also observed that the expansion only had little influence on the number of identified lay-ups for high numbers (as e.g. 50) of design variables. This is believed to be the consequence of the increased several-to-one connection between the lamination parameters and the design variables, meaning that the expanded interval was in fact not necessary. Obviously the values of the identification function obtained with and without the expansion differed, but with such high numbers of design variables the number of identified lay-ups were similar.

3.6.5 Optimisation of Identification Function

As mentioned above the identification function is designed such that a new lay-up is determined by minimising the function. If a function value of zero is obtained then the new lay-up is within the accepted interval of the lamination parameters. However, because the lamination parameters are described by harmonic functions the design space of the identification function becomes discrete. This is sketched in figure 3.11 where one lamination parameter is sketched as a function of one ply-orientation — the example is in fact artificially constructed as a simple sine function. Though the plot actually does not represent a lamination parameter the periodic characteristics are similar, and thus the points made are valid for lamination parameters as well. Hence the plot will just be referred to as if it was actually representing a lamination parameter.

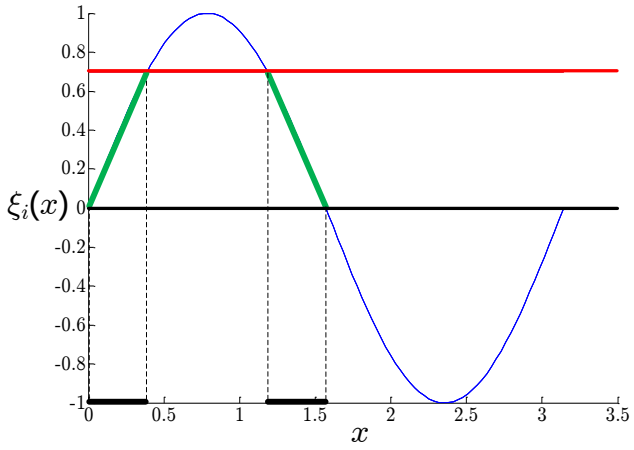

Figure 3.11: *Illustration of one lamination parameter described by a harmonic function, blue curve. Black line: Initial value $\xi_i^* = 0$. Red line: Upper bound of expansion. Green Lines: Expanded intervals. Thick black lines: Allowed intervals of the design variable.*

The blue harmonic curve represents the value of the lamination parameter as a function of the angular orientation of the ply. The black line represents the initial value of the lamination parameter, ξ_i^*, which in this example is zero. The red line represents the upper bound of the lamination parameter as a consequence of the expansion, this has been greatly exaggerated for illustrative purposes. The

green lines in between the initial value and the upper bound thus represent the expanded intervals of the lamination parameter. The thick black lines on the abscissa correspond to the values which the design variable x can assign.
As can be seen these intervals are scattered along the design space which becomes a problem when optimising the identification function using conventional gradient based algorithms. These algorithms are prone to get stuck in a local minimum and both of the shown intervals represent their own optimum solution. Thus a successful identification is highly dependent upon the initial guess of the new lay-up. It is thus essential to perform an initial search of the design space, and thus determine a suitable location to initialise the optimisation algorithm from.

This determination of a suitable location can be done in many ways. What is needed is essentially nothing but a good guess. However, to produce a good guess without evaluating the global objective function can be quite difficult. The identification function formulated in section 3.6.3 has the property that it is very computationally lightweight, and as such the cost of evaluating this function many times is, to a large extent, affordable. Hence, one possible method could be to simply make a large number of random guesses and hope for it to give good results. In order to do something a little more structured (but still based on random guesses) a genetic algorithm has been developed, which incorporates a standard gradient based optimiser to perform local optimisation on the best performing candidate lay-ups. For a complete description of how the implemented algorithm operates the reader is referred to appendix A which is taken from the authors previous work [Kann and Sørensen, 2010]. The combination of a genetic algorithm and the local optimisation on candidate lay-ups does theoretically not guarantee a solution. However, it has proven itself very useful not only by the authors but also by [Huang and Haftka, 2005] who used a similar approach for optimisation of fibre orientation distribution near a hole in composite laminates. The technique has also been suggested in a more general context to improve the performance of genetic algorithms [North et al., 1996]. The current implementation of the genetic algorithm applies the method of feasible directions to perform the local candidate optimisation described in appendix A.1.7. This algorithm is a constrained gradient based optimiser and is included in MUST as a part of the DOT optimisation library originally developed by Vanderplaats Research & Development inc. The only constraints supported in the current implementation of the genetic algorithm are the bounds on the design variables.

Another aspect of choosing a genetic algorithm is that with this, it is possible to include manufacturing constraints as well as discrete domains of definition for the design variables directly into the identification process. These aspects reach beyond the scope of this thesis and are thus not studied. However, large parts of the necessary code is actually implemented.

3.7 Optimisation Process

With the addition of the genetic algorithm applied during the identification of a new laminate design, the optimisation process can be illustrated by the flowchart in figure 3.12.
As can be seen in the figure the optimisation begins with an initial design of the laminate, which is subjected to conventional gradient based optimisation. This will most likely lead to the determination of a suboptimal lay-up, from which the lamination parameters are determined and utilised for the identification process. When a new lay-up has been determined the process is repeated until no other lay-up can be identified.

Because there is a periodic tendency when optimising with ply orientations, the identification function may lead to what is believed to be a new lay-up, which in fact may be the original lay-up or a lay-up simply turned π. The gradient based optimiser will then again initialise the identification of a new lay-up, which may again determine the same lay-up and thus creating an infinite loop. In order to avoid this scenario the optimisation process is terminated if ten successive identifications have been performed, where the gradient based optimiser has been unsuccessful in continuing to reduce the

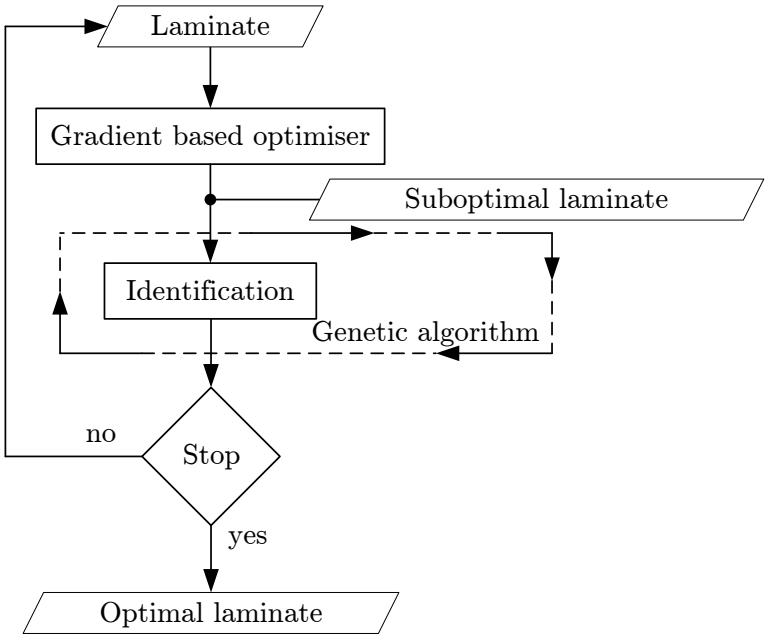

Figure 3.12: *Overview of the optimisation process given as a flowchart.*

value of the objective function in all ten attempts. The reason for the number ten shall be elaborated in chapter 5. Smarter methods could possibly be used if history of the previous designs were in fact implemented in the identification process, e.g. a simple improvement could be to prohibit designs that had already been tried. However, that kind of history is not a part of the current implementation.

3.8 Summary

This chapter has introduced the concept of optimisation with reference to the standard model. Focus was put on maximising the stiffness, for which reason analytical expressions have been derived in order to determine the sensitivities of the design variables w.r.t the element stiffness efficiently. The idea of patch formulations has also been introduced.

Next, feasibility and convexity of the lamination parameters introduced in section 2.4.3 were elaborated on with the purpose of utilising these in an optimisation algorithm. The method developed by [Foldager, 1999] were found to have significant flaws, though the preliminary ideas were quite ingenious. Thus the overall idea of a two-step approach was adopted, but with a new identification function and method for minimising this. The new formulation was based on a local linearisation of the strain energy w.r.t. the lamination parameters.

Previous results by the authors have shown that in order to do a successful identification of a new lay-up, the relationship between the number of design variables per set of lamination parameter must be *several-to-one*. Such a relationship can be accomplished by ensuring a sufficient amount of layers in the laminate, which in the previous work was found to be at least 11 when utilising 12 lamination parameters in the identification process.

Chapter

4

Implementation of Optimisation Algorithm

The algorithm described in the previous chapter and sketched with a flowchart in figure 3.12 has been implemented in the finite element analysis tool MUST developed at Aalborg University at the Department of Mechanical and Manufacturing Engineering. In the following the implementation of the algorithm is presented together with the different options and their effects.

4.1 Integration Type

The method has been implemented such that it requires the element stiffness matrix to be determined using explicit thickness integration as presented in section 2.3.2. The support for explicit thickness integration and approximate explicit thickness integration was implemented by [Hvejsel and Hansen, 2007]. The current implementation, which is build on top of the explicit thickness integration, supports both of these methods.

4.2 Number of Applied Lamination Parameters

It is possible to specify the number of applied lamination parameters in the identification function to either 12, 20, or 28. The specified number is substituted into identification function (3.18), where n_{LP} is set to the specified number. If this have not been specified the algorithm determines the number of applied lamination parameters on the basis of the chosen integration type. If the full explicit thickness integration has been selected then $n_{LP} = 28$. For the approximate thickness integration the magnitude of Δ_V influences whether 20 or 12 lamination parameters are sought identified. If $\Delta_V = 0$ then, as previously mentioned, the shell may be regarded as a plate, hence the stiffness is only dependent upon the first 12 lamination parameters. However, instead of evaluating the value of Δ_V the ratio $\frac{\Delta_V}{\Delta_A}$ has been chosen in order to obtain a normalised value for the comparison. Thus if $\frac{\Delta_V}{\Delta_A} \leq 10^{-3}$ the element subjected to identification is treated as a plate. Remark that the stiffness is, nonetheless, still determined using all 20 parameters during the conventional gradient-based optimisation. Because of this, the inaccuracy associated with this reduction is considered to be negligible for such a low value of the ratio $\frac{\Delta_V}{\Delta_A}$.

4.2.1 Step Size

In the work previously presented by the authors [Kann and Sørensen, 2010] the fixed step size applied for the expansion of the lamination parameters was set to $\Delta\xi = 0.01$ on the basis of results from numerical experiments. However, as mentioned in section 3.6.3 the determination of $\Delta\xi$ may be problem dependent, thus a value of 0.01 may prove to be inadequate in the current implementation. Thus in chapter 5 a series of numerical experiments is performed with different step sizes, so as to test whether the previous step size is adequate.

4.3 Patches

The identification process has been implemented such that it supports the use of patches in the finite element model. The implementation has been setup to handle a patch as if it was a single element, i.e. if no patches are present each element is managed as it if was a patch. As a consequence of the patch formulation all the elements in the patch must have the same lay-up and material properties in order for the identification process to produce valid results. In the following subsections a description of how the algorithm manages the presence of a patch is presented.

4.3.1 Choice of Number of Applied Lamination Parameters

As previously mentioned the chosen type of integration influences how many lamination parameters are sought identified during the identification process. For the approximate method this could result in either 20 or 12 lamination parameters depending upon the size of the ratio $\frac{\Delta_V}{\Delta_A}$.

When a new lay-up of a patch is sought identified the patch has to be analysed in order to determine if it should be identified as a plate or a shell. However, because each element can have its own distinct value of $\frac{\Delta_V}{\Delta_A}$ the decision can only be done when all the elements in the patch has been analysed. A simple way of deciding if a patch should be identified with 20 or 12 lamination parameters could be to determining the average ratio for the patch, however, this could lead to a non-conservative approximation of the patch e.g. if half the elements could be modelled as a plate and the rest as a shell, then the averaging could lead to the patch being identified as a plate which can be regarded as an non-conservative simplification of the structure. Thus in order to avoid this scenario the ratio for the patch, $\frac{\Delta_{V_p}}{\Delta_{A_p}}$, is defined as the sum of all the elements ratios:

$$\frac{\Delta_{V_p}}{\Delta_{A_p}} = \sum_{e=1}^{n_{elemP}} \frac{\Delta_{V_e}}{\Delta_{A_e}} \tag{4.1}$$

where:

Δ_{V_p}	Variation of Jacobian square root for a patch.
Δ_{A_p}	Average of Jacobian square root for a patch.
n_{elemP}	Number of elements in a patch.
Δ_{V_e}	Variation of Jacobian square root for element no. e.
Δ_{A_e}	Average of Jacobian square root for element no. e.

This implementation is believed to be conservative in the determination of whether a patch can be sought identified as a plate or as a shell.

4.3.2 Lamination Parameters

Because all the elements in a patch are assumed to have the same lay-up and material properties the patch lamination parameters are simply copied from the first element in the patch, which are then

supplied to the identification function. It is thus essential that a patch only contains elements with the same lay-up and material properties, as otherwise the identification process will change the patch lay-up based on invalid results.

4.3.3 Sensitivities

As mentioned in section 3.6.3 the sensitivities used in the identification function are of the strain energy density w.r.t. the lamination parameters. The sensitivities of the strain energy density for a patch are determined as the sum of all the element sensitivities of the strain energy divided by the patch volume:

$$\frac{\partial U_d}{\partial\left(\xi_i^j\right)_p} = \frac{1}{V_p}\left(\sum_{e=1}^{n_{elem^P}} \frac{\partial U}{\partial\left(\xi_i^j\right)_e}\right) \tag{4.2}$$

where:

U_d	Strain energy density.
$\frac{\partial U_d}{\partial\left(\xi_i^j\right)_p}$	Patch sensitivity of strain energy density w.r.t lamination parameter ξ_j^i.
V_p	Patch volume.
$\frac{\partial U}{\partial\left(\xi_i^j\right)_e}$	Sensitivity of strain energy w.r.t lamination parameter ξ_j^i for element no. e.

Because all the sensitivities of the strain energy are summed and afterwards divided by the patch volume it is possible for the patch to contain different sized elements.

4.4 Pseudo Code for Identification Routine

When the gradient based optimiser has converged the identification subroutine is called from inside the main optimisation loop. In table 4.1 the pseudo code for this subroutine is presented in order to give a brief overview of how the identification routine operates.

# 1	Loop for design variables:
# 2	| Loop for associated elements:
# 3	| | If element already has been processed: Go to # 2
# 4	| | If first element in patch: Extract lamination parameters and bounds for all design variables
# 5	| | Determine for element: $\frac{\partial U}{\partial \xi_i^j}$, Volume, Δ_V,Δ_A
# 6	| | Mark element as processed
# 7	| | If last element associated with design variable:
# 8	| | | Determine patch sensitivities $\frac{\partial U_d}{\partial\left(\xi_i^j\right)_p}$
# 9	| | | Determine if patch is a plate or a shell
# 10	| | | Perform identification of new lay-up
# 11	| | | If new lay-up determined: Replace old design variables with new design variables
# 12	| | End if
# 13	| End loop for elements
# 14	End loop for design variables:

Table 4.1: *Pseudo code for identification process.*

4.4.1 Added MUST Files

The implementation of the identification process in MUST has naturally resulted in parts of the original code being rewritten. However, a number of new files has also been added. These are listed here with a brief description of the contents.

- `FEShellLamPar.f90`
  - This module contains routines for shell elements with explicit thickness integration, all applying lamination parameters.
- `Genetic.f90`
  - These modules contain routines for doing optimisation applying a genetic algorithm.
- `IdFunc.f90`
  - This module contains the identification function.
- `LamParOpt.f90`
  - This module contains the main loop of the identification process as well as other subroutines related to this.
- `Mrgrnk.f90`
  - This module is downloaded from [Olagnon]. It includes routines for ranking an array.
- `Refsor.f90`
  - This module is downloaded from [Olagnon]. It includes routines for sorting an array.

4.4.2 Added Input Commands

The implementation has furthermore resulted in a series of new input commands to MUST needed to run the optimisation procedure. The commands are listed below together with a description of what the specific command does.

- `lamparoptimisation`
  - Enable identification
- `lamparoptimisation idtype Y`
  - Enable identification with Y number of lamination parameters applied in the identification function. Y can be assigned the following values: 12,20, or 28. If any other value is assigned, the number of applied lamination parameters is determined on the basis of the selected thickness integration scheme.
- `lamparoptimisation storagemode maxid X`
  - Enables identification where data is written to the disk for each identification. This will slow down the process. `maxid X` specifies how many identifications that are expected to be performed. If the number `X` is exceeded the last performed identification will be stored as number `X` and thus erase the previous data. The following data is written to the disk:
    - Initial lamination parameters for first element in a patch.

        * Sensitivities of the patch strain energy density w.r.t. the lamination parameters.
        * Main iteration number corresponding to when the identification was performed.
        * Identification number.
        * Element number for last element in patch.
        * Design variables for each main iteration.
        * Objective function value for each main iteration.

- `developmentmode showmenewlampars`
    - When enabled, the lamination parameters after an identification are re-determined and written to the disk. Remark: Should only be enabled if `storagemode` is enabled.

These commands are simply added to the traditional MUST input file.

Chapter

5

Numerical Examples

In this chapter the described two-step method of optimising composite structures using lamination parameters is tested on several numerical examples. However, first a few characteristics that are common to all the conducted experiments are presented.

All numerical experiments are, as a first overview, evaluated by observing an iteration history plot of the strain energy. An Arbitrary example of such a plot is shown in figure 5.1. The plot shows the level of the average strain energy for all iterations of the main optimisation loop. Performed identification processes are marked with a red cross. Thus what in general is looked for in the plots is places where the gradient-based optimisation runs until a certain level of strain energy where after an identification process is conducted, resulting in a new set of design variables wherefrom the gradient-based optimiser can lower the strain energy significantly. This phenomenon is seen around iteration no. 151 in the figure.

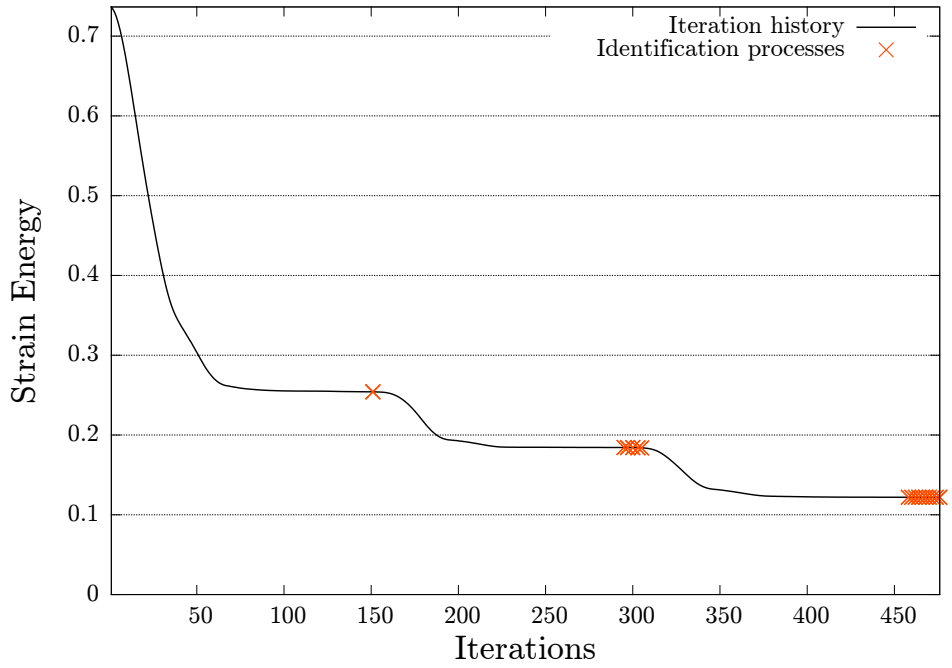

Figure 5.1: *Example of iteration history plot of the strain energy.*

As described in section 3.7 the main optimisation is stopped if ten successive identifications are

observed. This is what is seen in iteration no. 476 in the plot. As seen around iteration no. 300 there is a good reason why the number of identification processes before a complete stop is as high as ten — namely that sometimes it takes a couple of identification processes before the gradient-based optimiser can succeed. Thus the number ten has arisen as a simple estimated sensible trade-off between being time-efficient and not stopping the process too early.

The value of the strain energy seen on the y-axis is in general scaled by some number inside MUST. Thus the absolute value on the axis is of no interest — the values can only be used relatively to each other. For all experiments only the fibre orientations are applied as design variables and the bounds are set to $\vec{x} \in [-90.9°; 90.9°]$.

The experiments have all been performed with the 9-node shell elements available in the MUST element library.

All numerical experiments are conducted with the gradient-based optimiser chosen as a *Method of Moveable Asymptotes* (MMA) with adaptive move-limits. The MMA is applied with standard MUST options, meaning that the performance should be solid for optimisation of fibre orientations in composite laminates. A detail worth noticing is that the MMA move-limits are not reset when an identification process has been conducted. The reason for this is that experiments have shown that a reset at this point might result in a too large step size for the MMA resulting in an increased level of strain energy. The consequence of the move-limits not being reset is that the move-limits are a bit too tight right after an identification process. Thus the level of the strain energy does not drop as quickly as actually should be possible. This is seen in an iteration plot as a rather flat curve following an identification process where after the level of strain energy in a few iterations starts to decrease more quickly. In figure 5.1 this phenomenon is seen right after the identification process in iteration 151.

As for the genetic algorithm used in the identification process, the used options are shown in table 5.1. Further info regarding the genetic algorithm can be found in appendix A.

Quantity	**Set to**	**More info found in appendix**
Number of individuals in the population	500	A.1.1
Tolerance	10^{-3}	—
Maximum number of generations	400	—
Number of optimum individuals to select	5	A.1.9
Percentage of the population selected for mating	90	A.1.3
Number of variables selected for mutation	10	A.1.6
Percentage of the total population selected for mutation	10	A.1.6

Table 5.1: *Options used for the genetic algorithm.*

Most experiments are conducted using the material properties for graphite-epoxy (AS/3501). These can be seen in table 5.2. The properties of the table are used in all examples where nothing else is noted.

Quantity	E_1	E_2	E_3	G_{12}	ν_{12}	ν_{23}	ν_{13}
Set to	$138MPa$	$9Mpa$	$9Mpa$	$7MPa$	0.3	0.3	0.3

Table 5.2: *Material properties for Graphite-Epoxy (AS/3501).*

Next some examples of how the optimisation procedure performs are presented.

5.1 Cantilever Beam Subjected to Uniformly Distributed Load

The first numerical experiment conducted is a standard test within minimum compliance fibre angle optimisation of composite structures, namely a cantilever beam subjected to a uniformly distributed load. The beam is thus in a state of in-plane loading. The scenario is sketched in figure 5.2. The beam has a thickness h, and the ratio between the other two dimensions is $a/b = 3/1 = 3$.

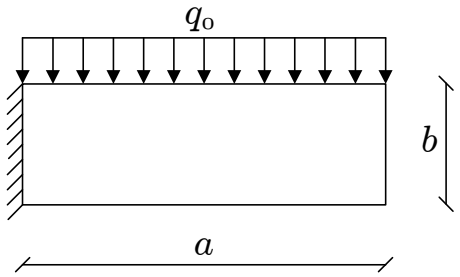

Figure 5.2: *Cantilever beam subjected to uniform distributed load.* $a = 3m$, $b = 1m$, $q_0 = 8\frac{kN}{m}$.

The classical example has only one layer over the entire plate. However, as earlier mentioned previous studies have shown that a minimum of 11 layers should be used in order to be able to identify new sets of design variables. Hence 20 layers are used, in order to be sure that the number of layers is sufficient. However, with the current loading all layers should give the same orientation, and hence the results can still be compared to results of the classical problem.

The example is known to show local minimums if the fibre orientations are gradient-based optimised from a vertical orientation of all elements. Hence the example is initiated in this configuration, first of all to determine a suitable value for $\Delta\xi$ as mentioned in section 4.2.1. Three examples are conducted with $\Delta\xi$ assigned values of 0.01, 0.05, and 0.1, respectively. For these experiments the beam has been divided into 192 elements which are assembled in 48 patches. The results of the three runs are shown in figures 5.3, 5.4, and 5.5. All optimisations are run with approximate explicit thickness integration.

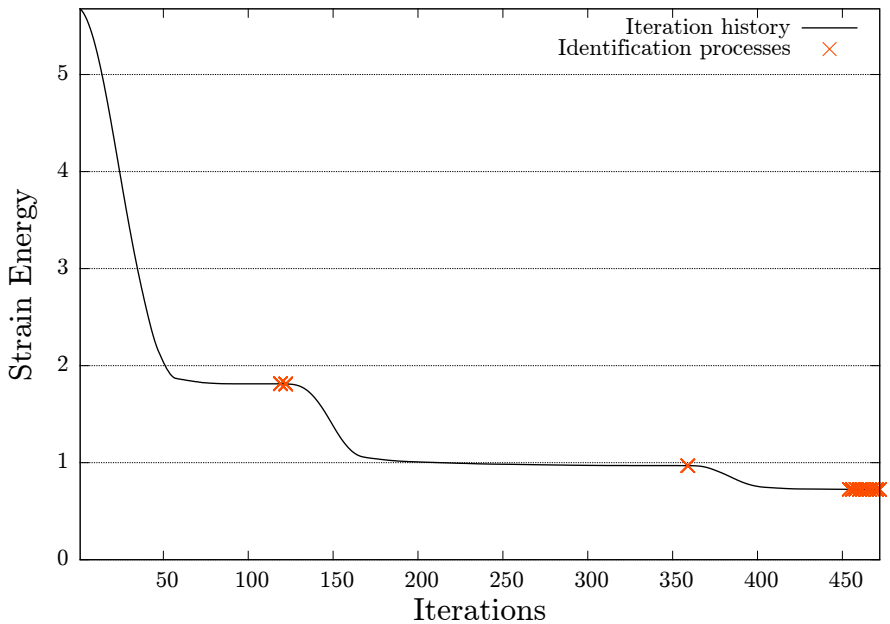

Figure 5.3: *Optimisation of cantilever beam with* $\Delta\xi = 0.01$. *Final level of strain energy: 0.72.*

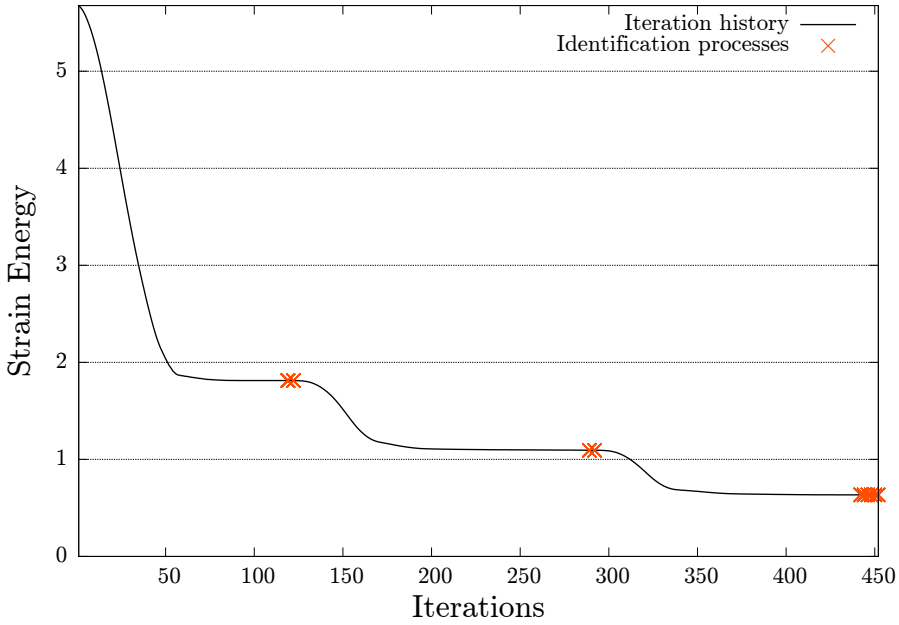

Figure 5.4: *Optimisation of cantilever beam with* $\Delta\xi = 0.05$. *Final level of strain energy: 0.63.*

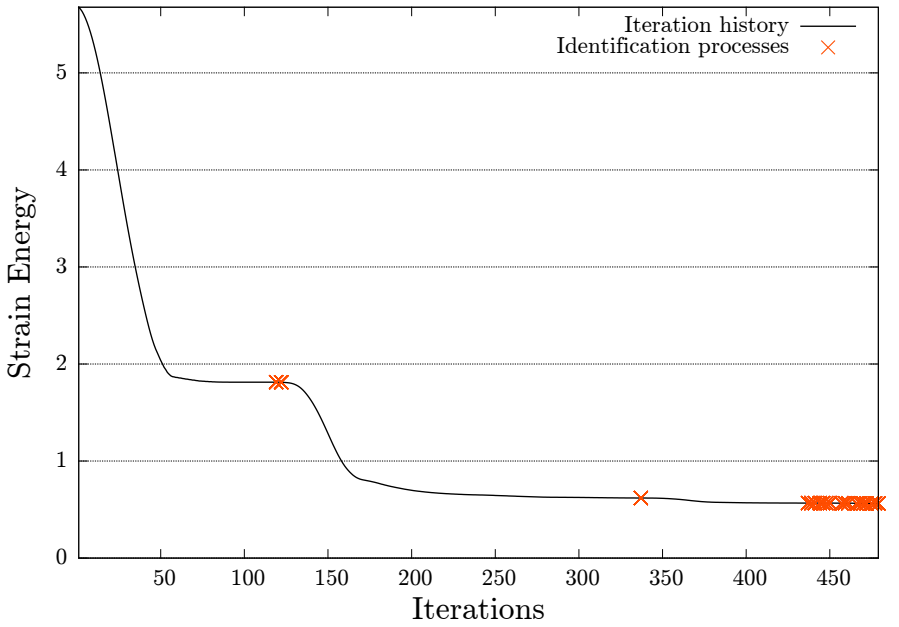

Figure 5.5: *Optimisation of cantilever beam with* $\Delta\xi = 0.1$. *Final level of strain energy: 0.56.*

With each optimisation process having 960 design variables which vary for several hundred iterations it is not really possible to list all design variables in a clear and sensible way. In order to illustrate the results, the final values of the design variables from the three optimisations are shown as lines in each element of the geometry indicating the fibre orientations. In order to show all 20 layers, these are plotted on top of each other. The final design variables of the three optimisations are shown in figures 5.6, 5.7, and 5.8, respectively.

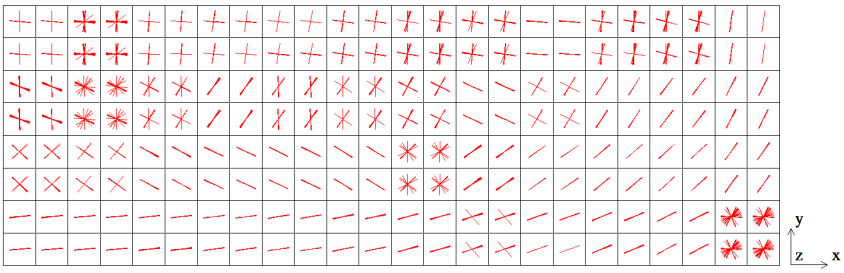

Figure 5.6: *Final design variables for optimisation with* $\Delta\xi = 0.01$ *illustrated as lines within all elements. In order to show all layers these are plotted on top of each other.*

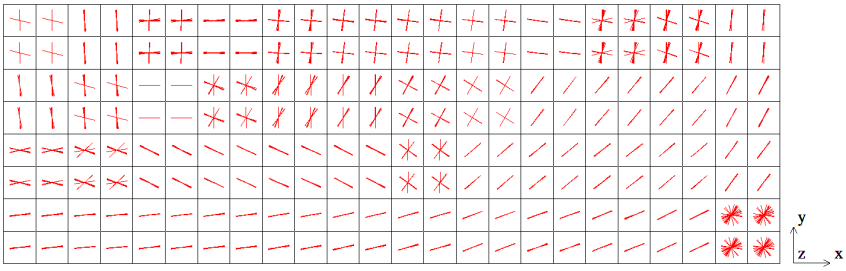

Figure 5.7: *Final design variables for optimisation with* $\Delta\xi = 0.05$ *illustrated as lines within all elements. In order to show all layers these are plotted on top of each other.*

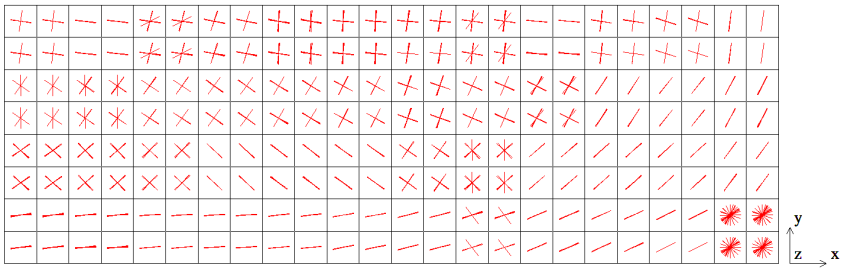

Figure 5.8: *Final design variables for optimisation with* $\Delta\xi = 0.1$ *illustrated as lines within all elements. In order to show all layers these are plotted on top of each other.*

What is seen in the figures is both some elements with a very clear preferred orientation for all layers, but also some elements where the tendency is not as clear. This is typically due to the optimisation routine not being able to capture the last effects, but it can also be due to the most optimal material at that position actually being e.g. an isotropic material. All in all, the picture given by the three figures is very much alike, and as such it is hard to bring out any significant differences of the three plots.

Each optimisation has in fact been run twice. The results, in terms of strain energy level, are shown in table 5.3. It should be noted that in the identification processes performed, all patches are assumed to be plates cf. the criterion in section 4.1. This is obviously in correspondence with what would be expected and thus just confirms that the criterion at least seems to work for geometries that are in fact plates.

	$\Delta\xi = 0.01$		$\Delta\xi = 0.05$		$\Delta\xi = 0.1$	
	U	FRAFLM	U	FRAFLM	U	FRAFLM
First run	0.77	18%	1.11	12%	0.56	22%
Second run	0.72	19%	0.63	21%	0.56	22%

Table 5.3: *Final level of strain energy for the three performed optimisations. FRAFLM = further reduction after first local minimum (when compared to the initial value of the strain energy).*

As seen in the figures and the results the three optimisations end up at approximately the same level of strain energy. The small differences found between the plots can just as well be due to coincidences as it can be due to the difference in $\Delta\xi$. Thus, as the conservative approach is to keep the value as low as possible and it seems to work with $\Delta\xi = 0.01$ this value is chosen for further studies.

For the chosen value of $\Delta\xi$ the results are studied a bit further. As clearly seen in the plot (in figure 5.3) the identification process does in fact in some cases facilitate further optimisation w.r.t. the strain energy, where as in other cases there is no effect. In order to study these tendencies, the change of design variables in the identification processes have been examined and categorised into three subgroups, namely variables that within a tolerance of 3° not have changed, variables that within the same tolerance have changed 180°, and variables that have changed to other values. The categories are referred to as *constant*, *bound switches*, and *new values*, respectively. The number of variables in each of these groups for the current results are shown in table 5.4.

Iteration no.	Identification no.	Constants	Bound switches	New values
119	1	924	36	0
122	2	880	76	4
359	3	919	23	18
454	4	941	0	19
456	5	940	0	20
458	6	938	0	22
460	7	932	0	28
462	8	932	0	28
464	9	923	0	37
466	10	912	0	48
468	11	922	0	38
470	12	920	0	40

Table 5.4: *The identification processes of the iteration history plot in figure 5.3. The last identification process is not presented in the table, as no new design variables are obtained for this identification process.*

As seen in the table both instances with bound switches and new values do in fact occur. The table shows a tendency that changes from one bound to the other (that is, a change of 180° in a design variable) often occur in the identification processes that actually result in further reduction of the strain energy. As also seen, new values do actually occur in most identification processes. Many of these changes lie within 3°–5° but there is also a significant amount that change to completely new values. However, as clearly seen in the last ten identification processes (note that the last identification process not is presented in the plot), this does not necessarily mean a further reduction in strain energy.

Next the same example is studied with mesh refinement in order to see if the tendencies are the same.

5.1.1 Mesh Refinement

Each element from the previous geometries are now divided into four smaller elements, thus resulting in 768 elements. However, as the patches are kept as before no new design variables arise. The result, in terms of a iteration history plot is shown in figure 5.9.

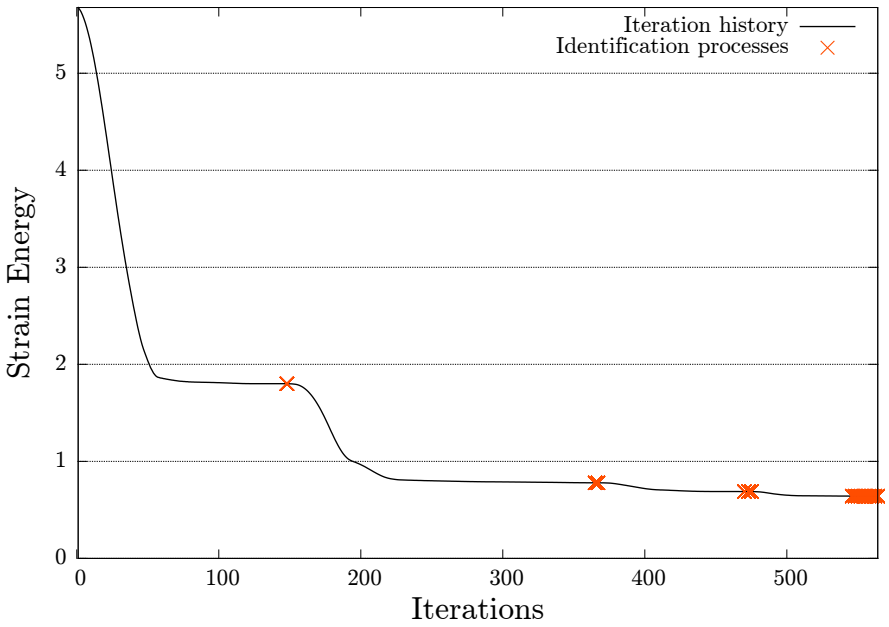

Figure 5.9: *Iteration history of cantilever beam with mesh refinement. Final level of strain energy: 0.64.*

The iteration history plot shows a progress of the optimisation which is very much like the previously seen progresses. The final level of strain energy is 0.64 with a further reduction after first local minimum of 20%.

The behaviour of the design variables in the identification processes is shown in table 5.5. As can be seen, the tendency is very much the same. At the identification processes that actually lead to further reduction of the strain energy there is a significant amount of bound switches. The number of new values on the other hand seems rather constant for most of the identification processes.

The final design variables are shown as a "through the thickness"-plot in figure 5.10a. The same example has also been studied by [Stegmann and Lund, 2005] using *Discrete Material Optimisation* (DMO). In their example 12 candidate material orientations were applied:±15°,±30°,±45°, ±60°, ±75°, 90°, 0°. For comparison, the result obtained by [Stegmann and Lund, 2005] is shown in figure 5.10b. What is seen from the figures is an overall tendency towards the same. At the large tensile areas the alignments there is a quite clear common alignment in both results. Furthermore both methods agree that the big middle-part of the beam must be aligned at ±45° in order to carry shear in the best possible way. However, there is a slight disagreement of the two methods in the top of the beam. Here the DMO-method aligns the fibres in the x-direction, whereas the method for optimisation with lamination parameters, where 20 individually orientated layers are allowed, tends to align some of the layers with the y-direction. This is believed to a consequence of the loads being applied directly on top of these patches. This seems to be a general tendency of all optimisations done with several layers.

As a last experiment with the cantilever beam, the optimisation is conducted still with mesh refinement but without patches.

Iteration no.	Identification no.	Constants	Bound switches	New values
148	1	911	48	1
365	2	935	5	20
367	3	932	7	21
470	4	929	12	19
473	5	941	0	19
475	6	931	13	16
546	7	941	0	19
548	8	943	0	17
550	9	940	0	20
552	10	938	0	22
554	11	938	0	22
556	12	933	0	27
558	13	931	0	29
560	14	929	0	31
562	15	934	0	26

Table 5.5: *Identification processes of cantilever beam with mesh refinement, i.e. 768 elements. The identification processes belong to the iteration history plot in figure 5.9.*

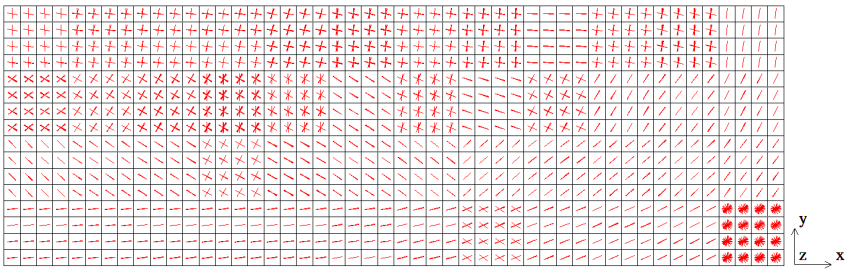

(a)

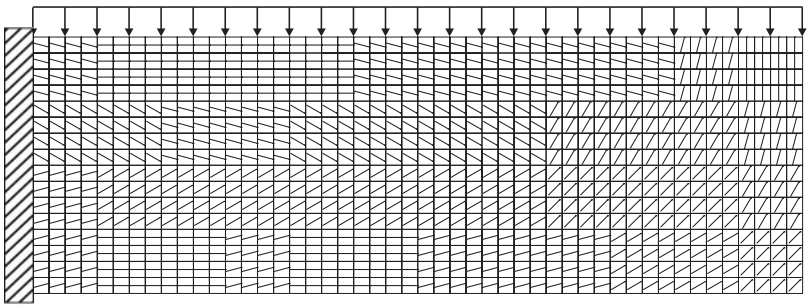

(b)

Figure 5.10: *Final design variables of the optimised cantilever beam with mesh refinement from optimisation with (a) lamination parameters and (b) DMO (reproduced from [Stegmann and Lund, 2005]).*

5.1.2 Example without patches

By removing the patch-configuration of the elements, the number of design variables is raised to 15360 making the optimisation much heavier in terms of computational requirements. The iteration history for the optimisation is shown in figure 5.11. The optimisation results in a strain energy level of 0.57 with a further reduction after first local minimum of 13%.

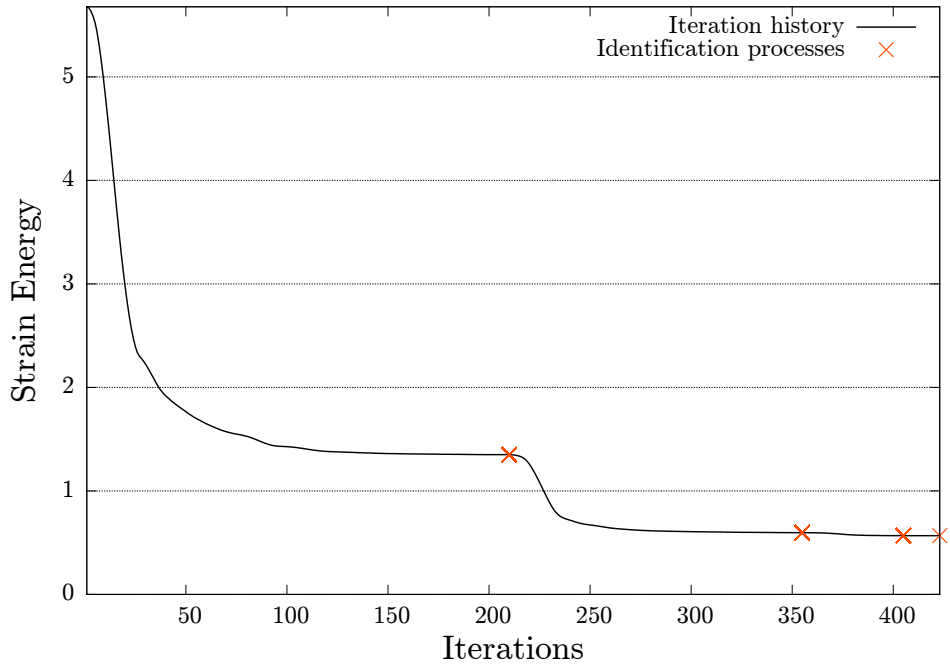

Figure 5.11: *Iteration history of cantilever beam with mesh refinement and no patches. Final level of strain energy: 0.57.*

In short words, the more design variables do not give any significant reductions in the strain energy. The main difference in the optimisation progress is that the first local minimum has a lower level of strain energy than previously seen.

Again, the final design variables through the thickness are shown in figure 5.12a. Furthermore results for the same scenario have been obtained by [Stegmann and Lund, 2005] using DMO with the same candidate material orientations as in the previous example. These results are shown in figure 5.12b. Also [Setoodeh et al., 2006] have obtained the results seen in figure 5.12c using an approach where the optimisation is performed directly on the lamination parameters as design variables (which is only possible because the feasibility constraints have been determined for the in-plane loading scenario). In the article by [Setoodeh et al., 2006] it is shown that the design space is convex for the given formulation. Because of the convexity the solution obtained by [Setoodeh et al., 2006] is the global minimum solution.

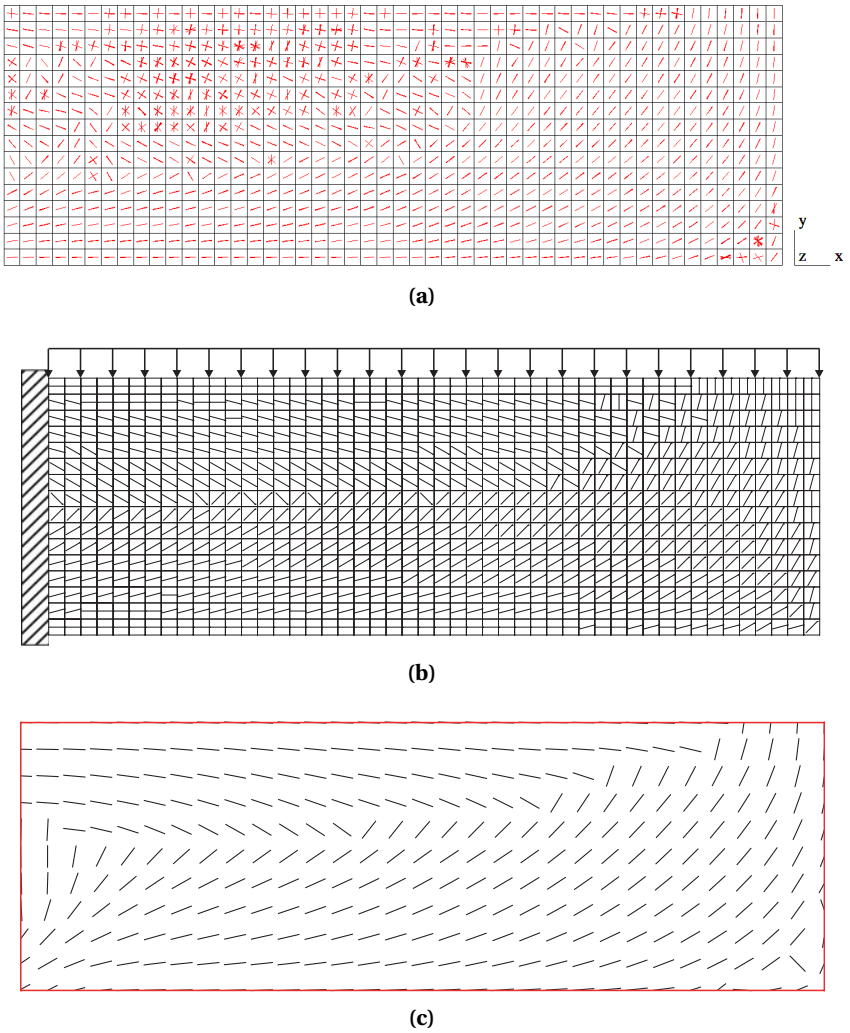

(a)

(b)

(c)

Figure 5.12: *Final design variables of the optimised cantilever beam with mesh refinement from optimisation with (a) lamination parameters, (b) DMO (reproduced from [Stegmann and Lund, 2005]), and (c) lamination parameters directly (reproduced from [Setoodeh et al., 2006]).*

The figures show a clear tendency towards the same orientations along the edges of the structure. However, it is also clear that the presented optimisation method with lamination parameter identification does not catch the effects of all elements in the middle of the structure. The behaviour of the design variables in the identification processes are shown in table 5.6.

Iteration no.	Identification no.	Constants	Bound switches	New values
210	1	14270	1090	0
355	2	15275	55	30
405	3	15327	21	12

Table 5.6: *Identification processes of cantilever beam with mesh refinement and no patches. The identification processes belong to the iteration history plot in figure 5.11.*

The main conclusion of this last optimisation must be that when optimising with single elements instead of patches, there is an even more significant need for post-processing the optimised design.

Next, experiments with other geometries and load conditions are conducted in order to study other aspects of the new method.

5.2 Plate Subjected to Uniform Pressure

In the following example a clamped plate subjected to an out-of-plane load in the form of a uniformly distributed pressure is optimised. As a consequence of the plate geometry the thickness integration is performed applying the approximate formulation, hence 12 lamination parameters are applied during the identification process. The plate and boundary conditions are illustrated in figure 5.13.

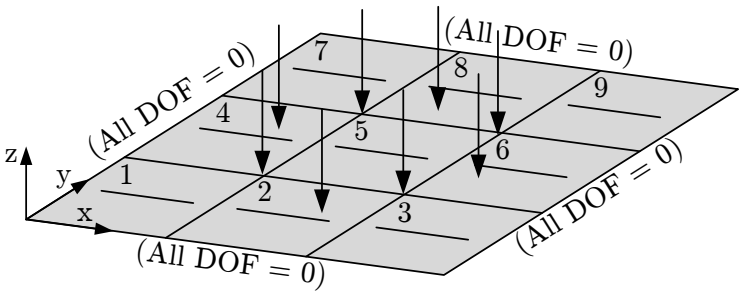

Figure 5.13: *Clamped plate subjected to uniformly distributed pressure. Shown with nine patches and initial fibre directions for all layers. The dimensions of the plate are* $1m \cdot 1m$ *and the load is* $1kN/m^2$.

The plate has 30 layers and is meshed with 12 × 12 equal sized elements. The number of design variables is 4320 if all elements are treated individually. The optimised lay-up is compared with solutions obtained using other parameterisations and design variables. At first, however, the plate is optimised with nine patches covering the plate where each patch contains 4 × 4 equal sized elements. The number of design variables is then reduced to 270. The iteration history for the patch formulation is shown in figure 5.14.

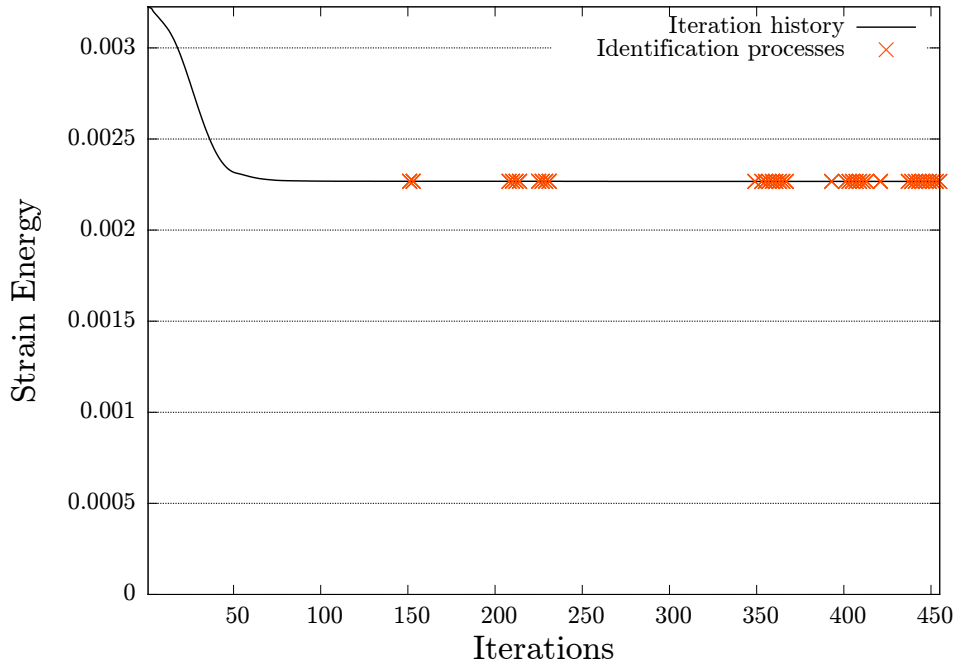

Figure 5.14: *Iteration history for clamped plate subjected to uniformly distributed pressure. Modelled with nine patches, 144 elements, and a total of 270 design variables. Total number of iterations: 455. Final objective value:* $2.26 \cdot 10^{-3}$.

As can be seen from the iteration history, the identification process did not result in the gradient based optimiser producing a significant reduction of the strain energy, indicating that the first identification occurred close to the global optimum. The first identification occurred at iteration no. 151 where the value of the objective function was $2.27 \cdot 10^{-3}$. The optimisation ended at iteration no. 455 due to 10 successive identification where the gradient based optimiser was unable to further reduce the objective function after each identification. The final value of the objective function was $2.27 \cdot 10^{-3}$, i.e. the same as before the first identification. A total of 37 identifications were performed during the optimisation. Figures 5.15 and 5.16 show the through-the-thickness lay-ups before the first identification and at the end of the identification, respectively.

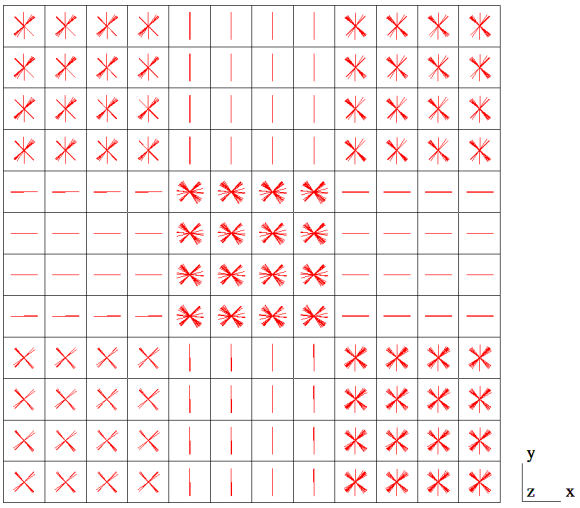

Figure 5.15: *Lay-up at first identification viewed through the thickness of patch model.*

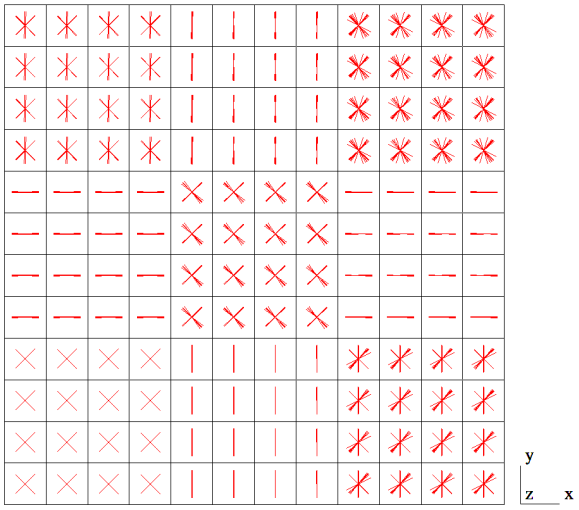

Figure 5.16: *Final optimised lay-up viewed through the thickness of patch model.*

As the figures show the two designs have not changed significantly, which is also indicated by the very low decrease of the objective function. Also the two designs show clear tendencies towards a solution which simply consists of ±45°, 0°, and 90° ply-orientations. This corresponds to what may be expected when applying the shown patch subdivision of the plate. However, the final design still has some plies which are not correctly aligned. These are mainly confined to the middle of the plate i.e. layers 13-18. This may be a consequence of the bending moments being of a lower magnitude around these layers, thus the sensitivities for these plies likewise becomes of negligible magnitude resulting in the optimisation reaching what is interpreted as a minimum. In table 5.7 a brief overview of the design changes due to the individual identifications is shown.

Iteration no.	Identification no.	Constants	Bound switches	New values
151	1	217	31	22
153	2	223	29	18
229	9	234	36	0
231	10	210	36	24
451	36	234	34	2
453	37	241	26	3

Table 5.7: *Sample from identification history associated with figure 5.14. New values of design variables determined as a change by more than* 3°.

The first identification resulted in 31 design variables changing their values of either the lower bound to the upper bound, or vice versa. Also 22 new design variables were determined, where a new design

variable is defined as a change in value by more than 3°. The new lay-up was, however, also located in another minimum, since the MMA algorithm only iterated one time before calling the identification again in iteration no. 153. The second identification did result in a new lay-up from which the MMA algorithm could continue from, even though the identification determined fewer new lay-ups and fewer bound switches. This illustrates the complex nature of both the design space and the process of identification.

5.2.1 Example without patches

Next, the patches are removed so each element can be subjected to identification. The initial design is kept as shown in figure 5.13. The result is compared with solutions obtained by applying the DMO method from [Stegmann and Lund, 2005] and the method from [Setoodeh et al., 2006] who optimised directly with lamination parameters. The latter is only possible due to the fact that the feasible domain is known for the four out-of-plane lamination parameters, i.e. ξ_i^B [Fukunaga and Sekine, 1992]. As in the cantilever beam example in section 5.1.2 the solution by [Setoodeh et al., 2006] represents the global minimum solution. The iteration, and identification history for the optimisation applying the identification approach is shown in figure 5.17 and table 5.8, respectively.

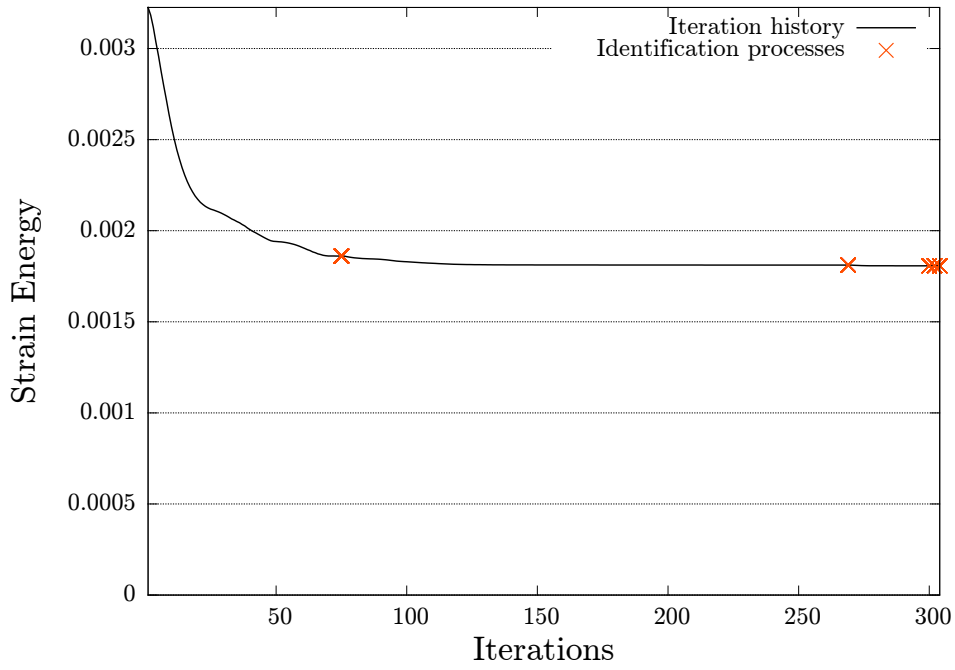

Figure 5.17: *Iteration history for a clamped plate subjected to uniformly distributed pressure. Modelled with 144 elements, and a total of 4320 design variables. Total number of iterations: 304. Initial and final objective value:* $3.23 \cdot 10^{-3}$ *and* $1.81 \cdot 10^{-3}$.

Iteration no.	Identification no.	Constants	Bound switches	New values
75	1	4121	199	0
269	2	3863	39	418
300	3	4038	0	282
302	4	3970	0	350

Table 5.8: *Identification history associated with figure 5.17.*

The first identification occurred at iteration no. 75 and with an value of the objective function of $1.86 \cdot 10^{-3}$. As can be seen from table 5.8 the identification was unsuccessful in determining any new values for the design variables, however, 199 of the design variables was apparently at either their upper or lower bound, where the identification resulted in the values being swapped to the other bound value. The second minimum was determined at iteration no. 269 where the value of the objective function was $1.81 \cdot 10^{-3}$. The bound swaps from the first identification thus resulted in the MMA algorithm being able to reduce the objective function almost 3% before reaching another minimum. The remaining identifications were successful in determining new values for the design variables, however, the reduction in the strain energy from iteration no. 269 to the final at 304 was less than 0.5%, which can be regarded as negligible compared to the extra computations required to perform identification on all the elements in the model. The optimisation was terminated because the genetic algorithm was unable to determine any new lay-ups. Thus the global minimum was assumed to be determined. The final lay-up through the thickness is shown in figure 5.18.

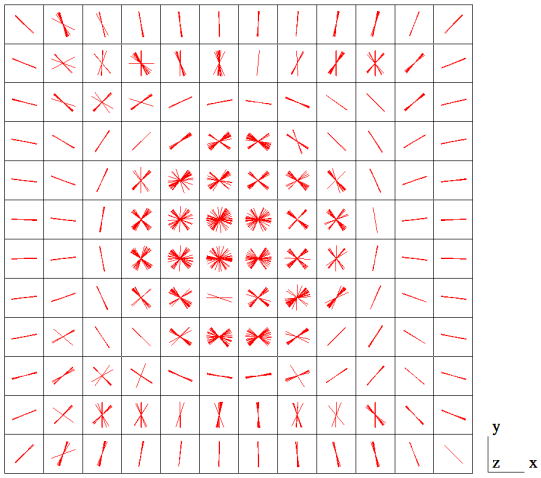

Figure 5.18: *Final optimised lay-up viewed through the plate thickness.*

The final lay-up obtained by the DMO method is shown in figure 5.19. The optimisation with DMO was performed with 12 candidate materials: ±15°,±30°,±45°, ±60°, ±75°, 90°, 0°. The lay-up determined by [Setoodeh et al., 2006] is reproduced in figure 5.20.

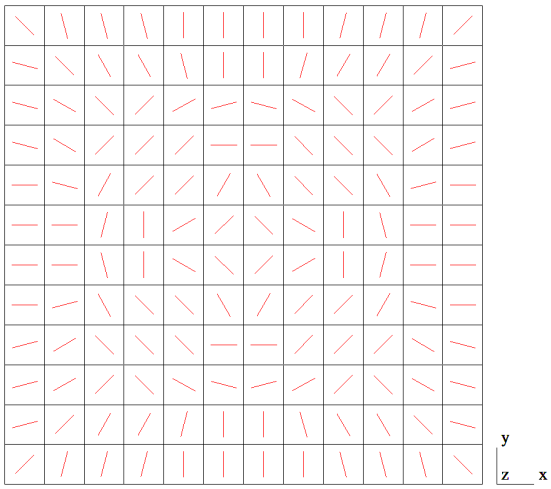

Figure 5.19: *Lay-up obtained applying DMO with 12 candidate materials:* ±15°,±30°,±45°, ±60°, ±75°, 90°, 0°. *Initial and final objective value:* $3.11 \cdot 10^{-3}$ *and* $1.78 \cdot 10^{-3}$.

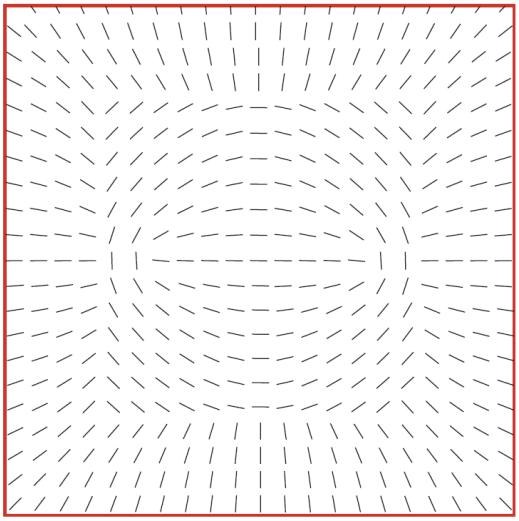

Figure 5.20: *Global optimum lay-up archived applying lamination parameters as design variables. Modelled with* 21×21 *nodes. Reproduced from [Setoodeh et al., 2006]*

As can be seen from figures 5.19 and 5.20 the optimum determined applying the DMO method is very close to the global minimum solution determined by [Setoodeh et al., 2006]. Because of this coherence the two results are considered to be valid for comparison. Comparing these results with the optimised lay-up shown in figure 5.18 some clear tendencies are recognised around the edges of the plate where the bending moments have a great influence. However, closing in towards the centre of the plate the lay-up becomes more inconsistent with the other results. The application of the identification process did thus not produce the exact global minimum solution, however, the final value of the objective function is only 1.67% higher than the final result obtained by the DMO method. This small deviation may be regarded as negligible.

5.3 Pinched Hemisphere

In this section the influence of how many lamination parameters that are applied in the identification process is analysed. In order to do so a curved geometry is required so that more than 12 lamination parameters are needed for determining the stiffness. The pinched hemisphere, from section 2.5.1, is applied for the experiments. In this example the pinched hemisphere is loaded in a mixed membrane and bending situation. Two scenarios are investigated in the experiments.

1. If an successful identification with 12 lamination parameters results in a discontinuity/"jump" in the value of the objective function, it may be due to a poor representation of the stiffness with only 12 lamination parameters. The structure is thus too "shell like" and additional lamination parameters may be required in order to identify a new lay-up with the correct stiffness.

2. In the previous experiments it was shown that with 12 lamination parameters the essential several-to-one relationship needed for identifying a new lay-up can be found. Here the lower limit to the number of layers have been estimated to be 11 layers [Kann and Sørensen, 2010]. However, this lower limit is not known for more than 12 lamination parameters. It is thus investigated whether it is possible to identify new lay-ups on the basis of more than 12 lamination parameters, that is either 20 or 28.

In order to test the influence of the structures curvature vs. number of applied lamination parameters, the experiments are divided into two separate categories where the radius-of-curvature to thickness ratio, $\frac{R}{h}$, is the dividing parameter. The first experiments are conducted with $\frac{R}{h} = 25$, which may be regarded as a thin curved structure. Next the ratio is changed to $\frac{R}{h} = 10$, which may be regarded as a limit value for applying degenerated shell elements in describing the kinematics of the structure cf. section 2.5.1. For the sake of consistency, all the examples have been conducted with the approximative explicit thickness integration scheme, even though this scheme is less accurate for radius to thickness ratios $\frac{R}{h} \leq 10$. As a consequence of the selected integration scheme the experiments are only shown for 12 and 20 lamination parameters, hence no experiments are shown for 28 lamination parameters.

The pinched hemisphere is modelled with a radius, $R = 0.5m$ and all the experiments have been modelled with 20 layers but with different ply-thicknesses. It is realised that the individual ply-thicknesses become unrealistically thin by maintaining a radius of 0.5m, however, with the purpose of the experiments in mind this ambiguity can be regarded as insignificant. Because of the symmetry only one quarter of the sphere is modelled. The model has likewise been subdivided into 20 patches, where each patch contains 4×4 elements. The model applied is shown with the associated boundary conditions in figure 5.21.

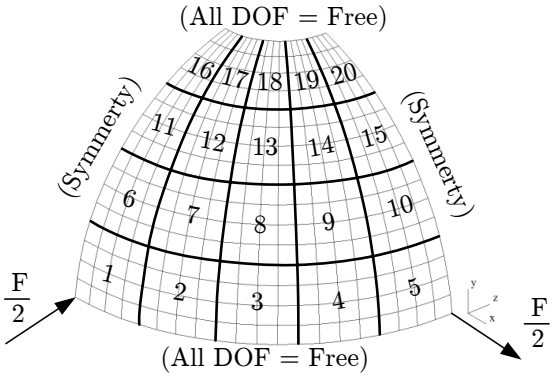

Figure 5.21: *Pinched hemisphere shown with boundary conditions and 20 patches with* 4×4 *elements in each. Radius = 0.5m, F = 2000N.*

The optimisations are performed with ply-orientations as design variables which, due to the patch formulation, sums to a total number of 400 design variables.

5.3.1 Pinched Hemisphere $R/h = 25$

In this subsection the pinched hemisphere is modelled such that it has a curvature-to-thickness ratio of 25. First the results from one optimisation is presented where $n_{LP} = 12$, and followed by another presentation where $n_{LP} = 20$.

5.3.1.1 Lamination Parameters: 12

In the following experiment 12 lamination parameters have been applied during the identification of a new lay-up. The iteration and identification history are shown in figure 5.22 and table 5.9, respectively.

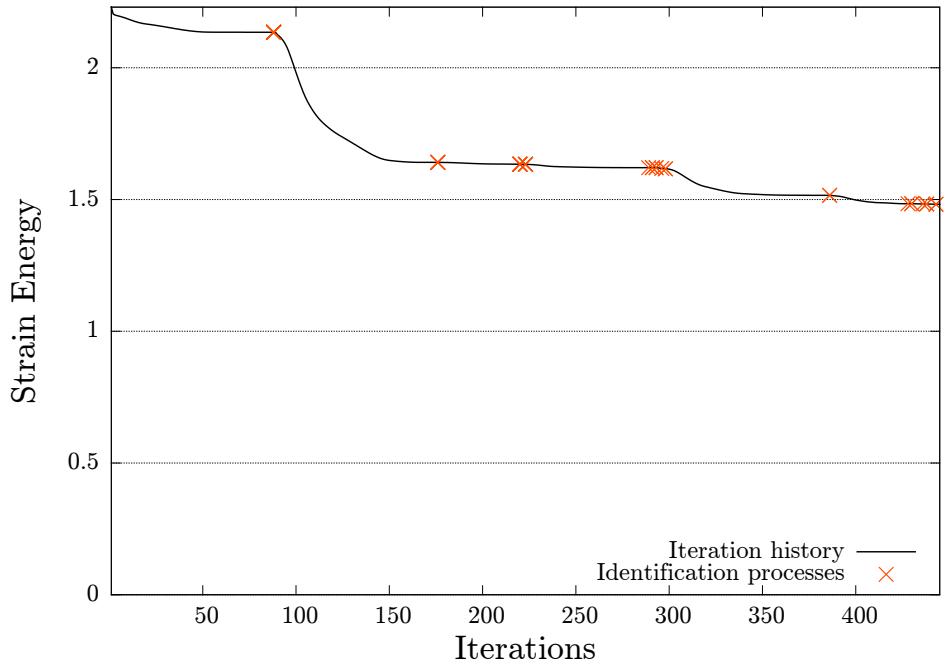

Figure 5.22: *Iteration history for pinched hemisphere.* $\frac{R}{h} = 25$, $n_{LP} = 12$. *Initial and final objective value: 2.230176 and 1.481842.*

Iteration no.	Identification no.	Constants	Bound switches	New values
88	1	359	41	0
176	2	386	9	5
220	3	398	2	0
223	4	385	15	0
289	5	400	0	0
291	6	400	0	0
293	7	393	7	0
296	8	400	0	0
298	9	387	13	0
386	10	380	5	15
428	11	400	0	0
430	12	385	0	15
436	13	400	0	0
438	14	389	8	3

Table 5.9: *Identification history associated with figure 5.22.* $\frac{R}{h} = 25$, $n_{LP} = 12$.

The first local minimum occurred at iteration 88 with a value of 2.134790. The application of the identification thus resulted in a further reduction after the first local minimum of 31%. The most substantial reduction occurred after the first identification, and as can be seen from table 5.9 the first identification resulted in 41 bound switches and 0 new values were determined. As can be seen from the figure no "jumps" occurred after any of the identifications, indicating that 12 lamination parameters might be enough for identifying new lay-ups for structures with a $\frac{R}{h}$ value of 25.

5.3.1.2 Lamination Parameters: 20

In the following 20 lamination parameters have been applied during the identification process. The iteration and identification history is shown in figure 5.23 and table 5.10, respectively.

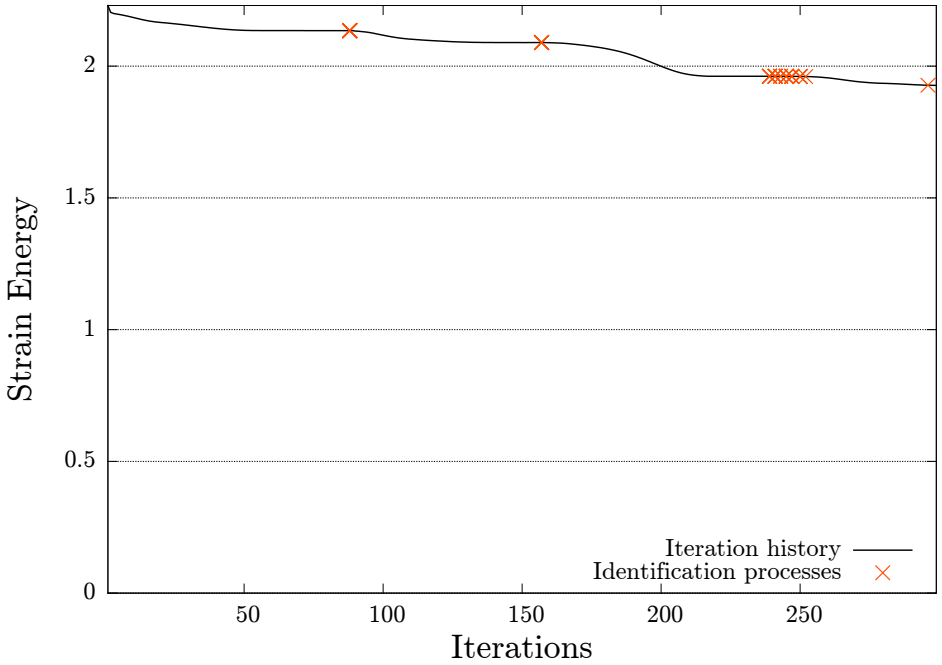

Figure 5.23: *Iteration history for pinched hemisphere.* $\frac{R}{h} = 25$. $n_{LP} = 20$. *Initial and final objective value: 2.230176 and 1.927029*

Iteration no.	Identification no.	Constants	Bound switches	New values
88	1	380	20	0
157	2	389	11	0
239	3	398	2	0
241	4	397	3	0
243	5	400	0	0
245	6	394	5	1
247	7	396	4	0
250	8	400	0	0
252	9	400	0	0

Table 5.10: *Identification history associated with figure 5.23.* $\frac{R}{h} = 25$, $n_{LP} = 20$.

From the table it is seen that only one identification resulted in a design variable being assigned a new value. The absolute difference between the new and old value was 3.1° i.e. just above the tolerance. It may be argued whether this is a new value or simply a slight adjustment of the old value due to the linearisation/ expansion of the lamination parameters. Combined with the fact that the final value of the objective function is 30% higher than for the previous example, it may be reasoned that the identification was unsuccessful when performed with 20 lamination parameters. The example has furthermore been optimised two additional times where similar tendencies were observed.

5.3.2 Pinched Hemisphere $R/h = 10$

In the following the curvature-to-thickness ratio for the pinched hemisphere is changed to 10, thus approaching what may be regarded as the limit for where the applied shell theory can produce accurate results. First an experiment where 12 lamination parameters are utilised for the identification is shown, followed by another experiment with 20 lamination parameters.

5.3.2.1 Lamination Parameters: 12

In this subsection 12 lamination parameters have been applied during the identification of new layups. The iteration and identification history is shown in figure 5.24 and table 5.11, respectively.

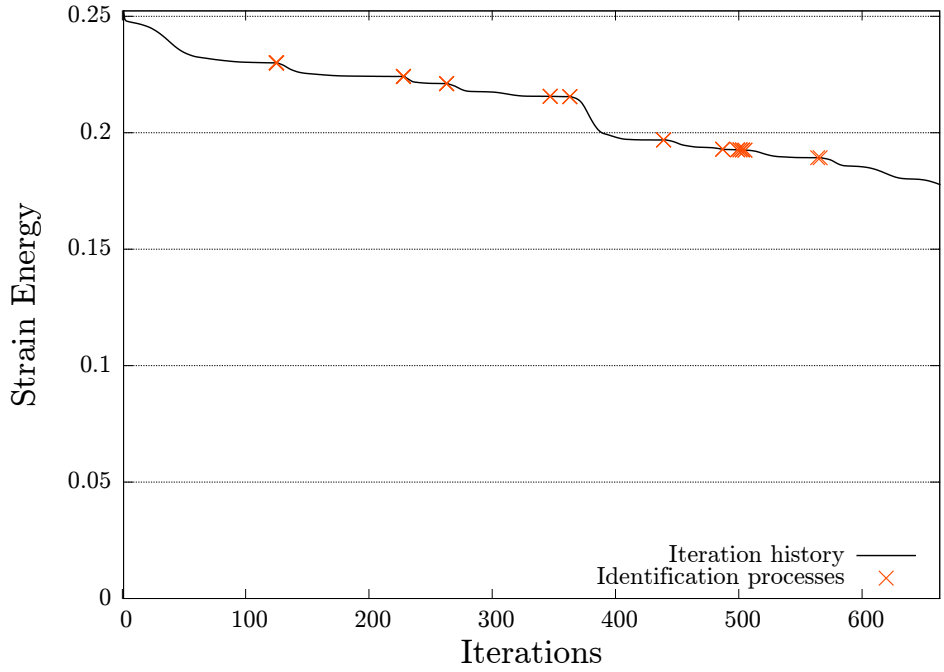

Figure 5.24: *Iteration history for a pinched hemisphere.* $\frac{R}{h} = 10$. $n_{LP} = 12$. *Initial and final objective value: 0.252320 and 0.177776.*

Iteration no.	Identification no.	Constants	Bound switches	New values
125	1	370	29	1
228	2	378	22	0
263	3	380	8	12
347	4	382	0	18
363	5	376	9	15
439	6	384	0	16
487	7	384	0	16
499	8	397	3	0
501	9	381	0	19
503	10	381	0	19
505	11	365	0	35
564	12	387	0	13

Table 5.11: *Identification history associated with figure 5.24.* $\frac{R}{h} = 10$. $n_{LP} = 12$.

The first identification occurred at iteration no. 125 with a value of the objective function of 0.2299871. Thus a further reduction of the objective function after the first identification of 23% was achieved. The optimisation was terminated because the genetic algorithm was unable to identify any new lay-up. Studying the iteration history in the figure it can be concluded that no "jumps" have occurred after any of the identifications. The identified lay-ups were thus able to represent the correct stiffness, even though only 12 lamination parameters were applied during the identification. As with the previous examples the first identification mainly resulted in design variables located at either their lower or upper bound having their value interchanged. The design variables which were assigned new values in the remaining identifications had their values changed by an absolute value somewhat randomly within the interval $]3° - 177°[$. It can thus be concluded that 12 lamination parameters seem adequate for identifying a new lay-up for what can be regarded as very curved structures.

Because all the data concerned with the identifications have been stored for the experiments, it is possible to determine whether the identified lay-ups would have been accepted by the identification process if 20 lamination parameters had been applied instead of 12. Consider identification no.11, where 35 design variables were assigned new values. This identification resulted in patches no. 5 and 6 being assigned new lay-ups. In table 5.12 the function values for the two identifications are presented, both for the applied 12 lamination parameters and for the case were all 20 lamination parameters have been evaluated in the identification function, i.e. corresponding to $n_{LP} = 20$.

Patch no.	I, $n_{LP} = 12$	I, $n_{LP} = 20$
5	0	0.7396
6	0.0003	0.2832

Table 5.12: *Function values for identification no.11 for both $n_{LP} = 12$ and $n_{LP} = 20$.*

As expected the function values for 12 lamination parameters are below the tolerance of 10^{-3}. However, if all 20 lamination parameters are evaluated, the two lay-ups fail to pass the tolerance level. Investigating other identifications, both from this example but also from the example where $\frac{R}{h} = 25$, shows that fewer lay-ups are accepted if 20 lamination parameters are applied, which indicates that, as expected, applying 12 lamination parameters is less restrictive than applying 20. It further shows that it is indeed possible to identify a new lay-up when applying 20 lamination parameters. However, it is not known if these identified lay-ups were the "driving force" in the further reduction of the objective function in the associated experiments, or if they were associated with changes which may be regarded as trivial, i.e. as was encountered in the previous example in subsection 5.3.1.2. In the following subsection the phenomenon is further investigated with 20 lamination parameters applied during the identification.

5.3.2.2 Lamination Parameters: 20

In the following experiment 20 lamination parameters have been applied during the identification of a new lay-up for the pinched hemisphere. The iteration and identification history is shown in figure 5.25 and table 5.13, respectively.

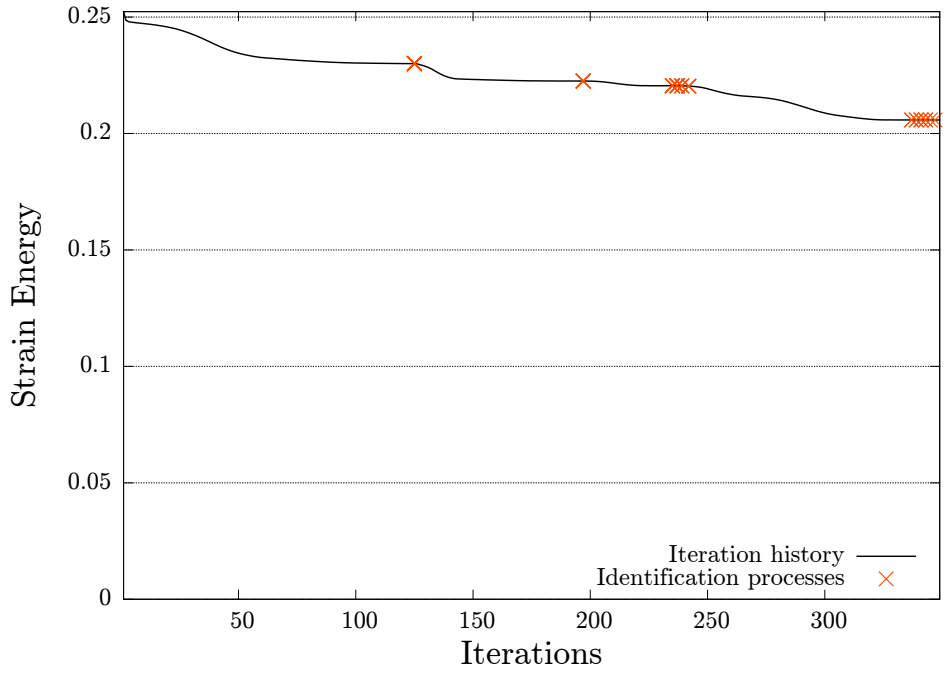

Figure 5.25: *Iteration history for pinched hemisphere.* $\frac{R}{h} = 10$, $n_{LP} = 20$. *Initial and final objective value: 0.252320 and 0.205777*

Iteration no.	Identification no.	Constants	Bound switches	New values
125	1	378	22	0
197	2	394	6	0
235	3	398	2	0
237	4	391	8	1
239	5	390	8	2
242	6	396	4	0
337	7	400	0	0
339	8	399	0	1
341	9	399	1	0
343	10	400	0	0
345	11	398	2	0

Table 5.13: *Identification history associated with figure 5.25.* $\frac{R}{h} = 10$, $n_{LP} = 20$

As can be seen from figure 5.25 the final result is almost 16% above the optimised result from the example where only 12 lamination parameters were applied during the identification, indicating that the identification may have failed. During the optimisation a total of 4 design variables had their values changed to new values. As with the previous example, where 20 lamination parameters were utilised during the identification, the new values have again just been changed enough so they are above the tolerance of 3°. Their absolute changes in value are shown in table 5.14.

Identification no.	**Absolute change (Original)**	
4	3.1° (20°)	
5	176.1° (89.5°)	176.4° (−86.2°)
8	3.5° (23.6°)	

Table 5.14: *Absolute changes in design variables.*

As can be seen from the table, the design variables have not changed significantly compared to their previous values. The changes for identifications 4 and 8 may have been a result of the linearisation of the lamination parameters. The two in identification no. 5 have been turned 180° and slightly changed, perhaps again due to the linearisation and local optimisation. It may then again be argued whether the identification process have been successful in determining any new lay-ups, or that it simply has fine-tuned their previous values. Nevertheless, the experiment again verifies that identifying with 20 lamination parameters is more restrictive compared to applying 12.

5.3.3 Summary

In the analysis of the pinched hemisphere four numerical experiments have been presented. The results have shown that identifying new lay-ups on the basis of just 12 lamination parameters is possible even for a low curvature-to-thickness ratio e.g. $\frac{R}{h} = 10$. None of the identifications with 12 lamination parameters resulted in an increase of the objective function, indicating that the new lay-ups produced a similar stiffness to the previous lay-ups. By applying the identification process a further reduction of the objective function was made possible, where the largest reduction after the first identification was 31% for the example with $\frac{R}{h} = 25$.

The two experiments where 20 lamination parameters were utilised in the identification process both performed worse than their equivalent experiments with 12 lamination parameters. Generally it was observed that fewer design variables were assigned new values, and those that were could be questioned whether the new value was "different enough" to be categorised as new, or simply a consequence of the expanded lamination parameters. It was further shown that lay-ups identified with 12 lamination parameters, wouldn't have been accepted if 20 lamination parameters had been applied. This again indicates that identifying with 20 lamination parameters is more restrictive than identifying with 12 lamination parameters.

As described in section 3.6.4 the number of design variables influences whether a several-to-one relationship can be established between the lamination parameters and the design variables. The poor performance observed when applying 20 lamination parameters may be a consequence of too few design variables in comparison with the number of applied lamination parameters. Hence the experiments have been conducted again where the pinched hemisphere was modelled with 40 layers, i.e. doubling the number of design variables. The experiments showed similar tendencies i.e. few new design variables were determined when applying 20 lamination parameters and the reductions in strain energy after the first identification were lower than when applying 12 lamination parameters. Experiments where the step size $\Delta\xi$ was increased to 0.05 were also conducted for the 40 layered model, however, the same tendencies were observed as previously.

On the basis of these experiments it is not recommended to apply 20 lamination parameters in the identification process, especially when compared to identifying with 12, which has shown to produce good results for both plates and thick shell structures.

5.4 Generic Main Spar

In the previous sections various benchmark examples have demonstrated that the presented optimisation method performs as intended. Several of the examples exhibited local minimum solutions during the optimisation which were bypassed with success by applying the identification process. In this section an example with more industrial relevance is presented in the form of a main spar from a wind turbine blade.

As with other industries that operate in a competitive market parameters such as quality vs. price and price vs. demand are always analysed and compared by the manufacturers and their competitors. When it comes to the wind turbine industry, quality can be associated with performance, as their consumers will be interested in buying a product which can deliver the most power contra the cost of the product. The performance of a wind turbine is controlled by a vast quantity of parameters e.g. aerodynamic design, gearbox, electronic controllers, and so on. When it comes to structural design the weight of the turbine blades are of interest. By lowering the weight of the blades less of the energy in the moving wind will be required to lift the blade and thus more energy will be transferred to the drive shaft. In this example the blade is built from two aerodynamic shell profiles which are fused together around a centre beam, also referred to as the main spar. The main spar is the primary load-carrying structure of the wind turbine blade. The assembly is sketched in figure 5.26.

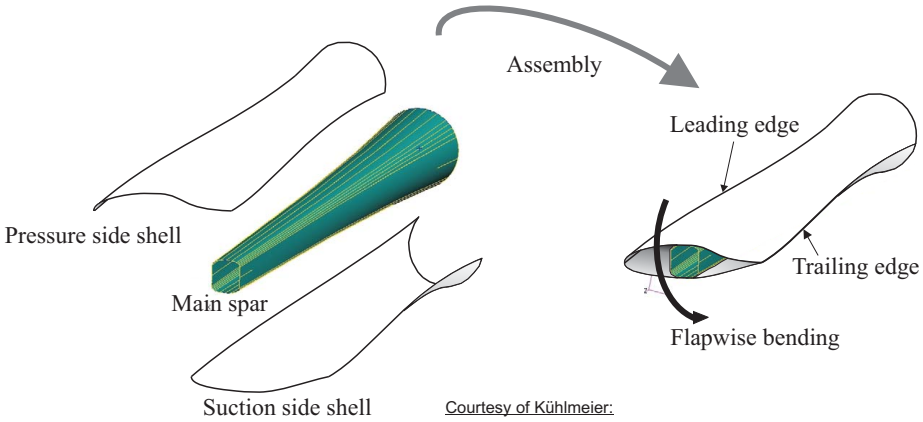

Figure 5.26: *Cut-through of windturbine blade, showing outer aerodynamic profile and the main spar. (courtesy of Lennart Kühlmeier, Vestas Wind Systems A/S)*

Because the aerodynamic profile is determined on the basis of aerodynamic performance, not much weight can be saved from a structural point of view, as the geometry in a sense is predetermined and the structure does not carry much of the load. Hence focus is turned on the main spar which carries the main load. As the blade is primarily loaded in flapwise bending much weight can be saved by building the shear dominated wedges/side panels of the main spar as a sandwich structure. Here the outer layers can be made from fibre composite materials and the inner part from a light weight material e.g. foam or wood. The top and bottom sides of the main spar are primarily subjected to compression or tension, respectively. Hence these parts can with advantage be built from fibre composite material as well. However, as the presented method in this thesis requires the material through the thickness to be the same, the sandwich design cannot be realised. Nevertheless, the example can still be utilised to see how the method performs on real life structures. Thus the light weight material in the side panels has been disregarded in this example. Originally the main spar was 25m long, however, in this example the tip of the blade has been removed resulting in the model having a total length of 14m. The model is divided into three parts named the tip, mid, and root section. These are shown for the meshed model in figure 5.27.

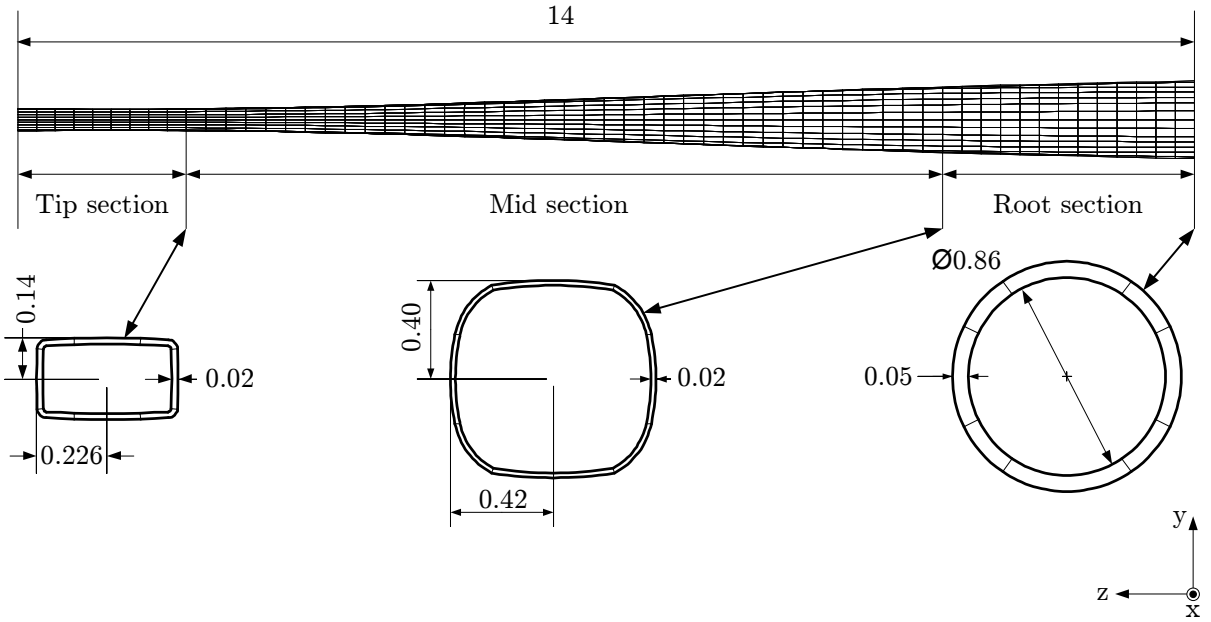

Figure 5.27: *Meshed model of generic main spar with section names. All dimensions are in metres.*

The model is constructed from three different materials. Two directional materials consisting of unidirectional, and biaxial glass fibre reinforced polymers (GFRP). The third material is divinycell H130/HC130 which is an isotropic polymer. The materials and their properties are shown in table 5.15.

Quantity	E_1	E_2	E_3	G_{12}	G_{23}	G_{13}	ν_{12}	ν_{23}	ν_{13}
Mat 1, UD (GFRP)	$45GPa$	$10GPa$	$10GPa$	$5GPa$	$4GPa$	$5GPa$	0.3	0.005	0.3
Mat 2, BI (GFRP)	$24GPa$	$24GPa$	$10GPa$	$4.5GPa$	$4.5GPa$	$4.5GPa$	0.11	0.3	0.0053
Mat 3,H130/HC130	$160MPa$	-	-	-	-	-	0.45	-	-

Table 5.15: *Material properties for generic main spar model.*

The lay-up and applied material for the tip and root sections are shown in table 5.16 and 5.17, respectively.

Layer no.	**Material no.**	**Orientation (MCS)**
1,10	2	+45°
2-9	1	0°

Table 5.16: *Lay-up for tip section of model.*

Layer no.	**Material no.**	**Orientation (MCS)**
1-10	3	–

Table 5.17: *Lay-up for root section of model.*

The optimisation of the main spar is focused on the middle section which has been subdivided into 16 patches, where each patch has 20 layers of unidirectional glass fibre reinforced polymer (material no. 1). The design variables are the fibre orientations for each patch, resulting in the model having 320 design variables. The model with associated boundary conditions and patch layout is shown in figure 5.28.

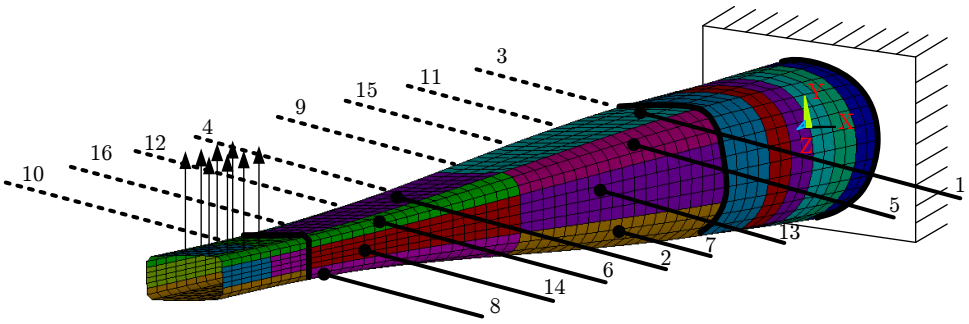

Figure 5.28: *Finite element model of generic main spar. Shown with patch numbers, distributed load, and clamped boundary condition.*

The structure is divided into 1680 elements. The load at the tip of the main spar is defined as a force of $164,729N$ uniformly distributed over an area of $0.2667m^2$.

The optimisation has been initialised with the fibre orientations following the "hoop" direction of the structure, i.e. fibres in patch no. 1 are aligned with the x-axis (SCS) whereas the fibres in patch no. 13 are aligned with the y-axis and so forth. Considering the loading condition this may be regarded as a poor design. As a consequence of the result obtained in section 5.3 the identification process has been set to identify new lay-ups on the basis of 12 lamination parameters. The iteration history is shown in figure 5.29 and the changes in each identification is shown in table 5.18.

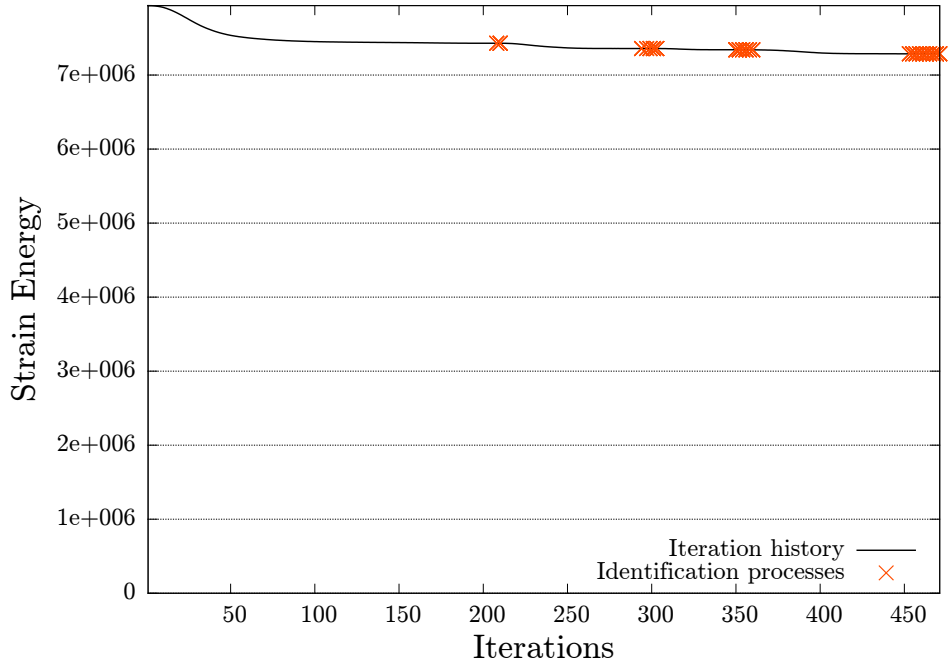

Figure 5.29: *Iteration history for generic main spar. Initial vale:* $7.94 \cdot 10^6$. *Final value:* $7.29 \cdot 10^6$.

Iteration no.	Identification no.	Constants	Bound switches	New values
208	1	312	1	7
210	2	289	11	20
294	3	318	2	0
297	4	317	0	3
299	5	313	1	6
301	6	306	0	14
303	7	289	3	28
350	8	300	1	19
352	9	296	2	22
354	10	302	2	16
356	11	311	1	8
358	12	310	0	10
360	13	307	8	5
453	14	319	0	1
455	15	308	0	12
457	16	314	1	5
459	17	300	2	18
461	18	307	2	11
463	19	297	2	21
465	20	309	4	7
467	21	310	3	7
469	22	292	4	24

Table 5.18: *Identification history for generic main spar. Associated with figure 5.29.*

The value of the objective function at the first identification was $7.43 \cdot 10^6$ resulting in a further reduction until the final value of 1.9% which may be regarded as negligible. In table 5.18 it is seen that the identification process resulted in several new design variables being determined during the optimisation. However, the results indicate that the model is relatively simple to optimise. This may be due to the coarse patch design combined with the simple loading condition. This is further investigated in the following where the optimised design variables are presented and commented.

The presentation is performed in a qualitative manner rather than a quantitative, as the purpose of the example is simply to illustrate that the presented optimisation method can be applied on large real life structures. Hence no in-depth analysis is made with regards to the optimised lay-up. However, the final lay-up shows that it consists of what may have been expected given the geometry, loads, and boundary conditions.

In figure 5.30 the design variables for the side panels, i.e. patches 13,15,14, and 16, are shown for all the layers in each of the respective patches. Layer no. 1 is the inside layer whereas layer no. 20 is the outside layer.

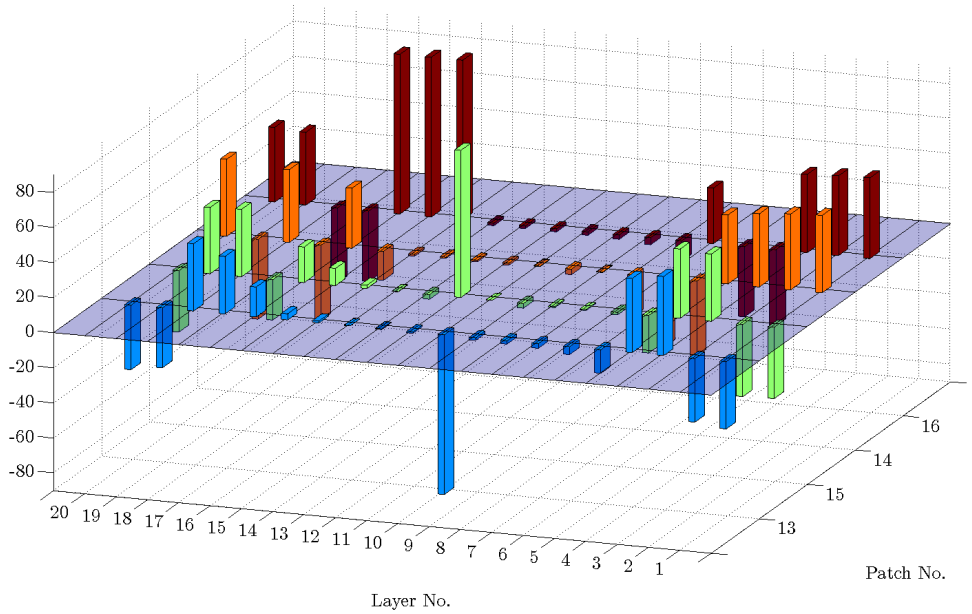

Figure 5.30: *Final design variables for the four side panels, i.e patches: 13, 15, 14, 16. Each patch no. has been assigned a unique colour. The third axis shows the fibre orientation (MCS) in the given layer for the specific patch.*

As can be seen from the figure the outer layers have been orientated so as to comprehend the in-plane shearing, whereas the centre layers have been aligned with the length direction of the main spar. This is believed to be a consequence of the patches being relatively "tall" when measured from the centre line to the top and bottom of the panels. Had the patches been divided into smaller areas a more uniform distribution of fibre orientations through the laminate thickness could have been achieved. I.e. the centre would absorb the shearing forces whereas the upper and lower parts would be more aligned with the length direction of the main spar.

In figure 5.31 the design variables for the corners are shown i.e. patches 5,11,6,12,7,9,8, and 10.

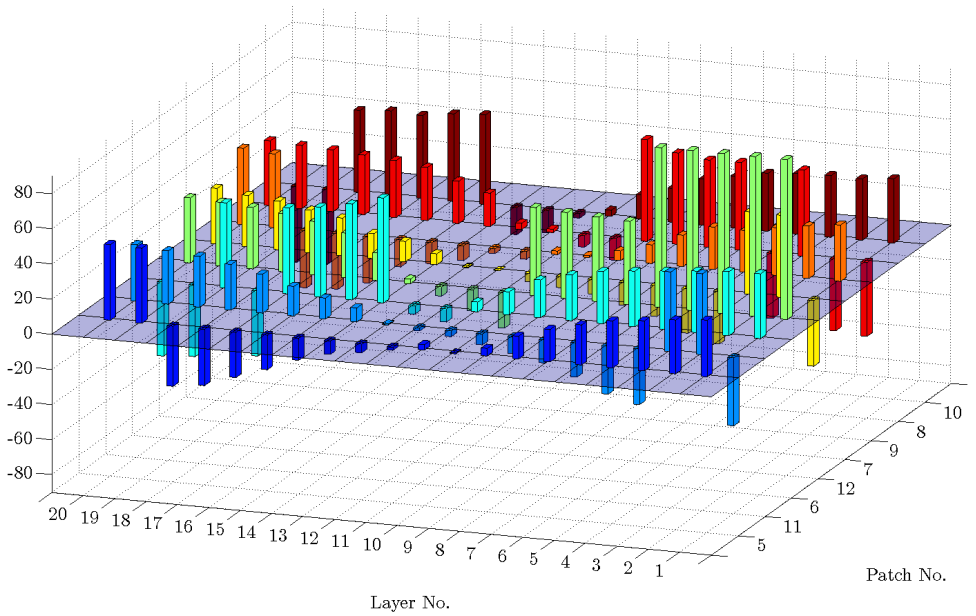

Figure 5.31: *Final design variables for the eight corner patches, i.e patches: 5, 11, 6, 12, 7, 9, 8, 10. Each patch no. has been assigned a unique colour. The third axis shows the fibre orientation (MCS) in the given layer for the specific patch.*

The remaining patches are for the top and bottom panels, i.e. patches 1,3,2, and 4. As can be seen from figure 5.32 some of the patches have layers which are not aligned according to what could be expected. For example patch no. 2 was expected to have all its fibres aligned with the z-axis as it is loaded mainly in compressive bending. However, the fibres in layers no. 10 and 11 still have their original alignment. Further analysis shows that these variables have mainly been influenced during the identification process where their values have been changed repeatedly to either the upper or lower bound. The misalignment is believed to be a consequence of the patch being loaded primarily in bending, hence the influence of the centre layers upon the bending stiffness becomes negligible when compared to the outer layers. This tendency is also present in the other patches shown in the figure.

Based on the above presentation of the design variables the minimum determined by the optimisation process is not the exact global minimum. However, it is believed to be close to it. One of the more conspicuous observations is the misalignment of the centre layers, which is believed to be a consequence of the structure being loaded in bending. Performing the optimisation again, now where the initial fibre orientations are aligned with the z-axis (SCS), should thus reveal if the hypothesis is correct. The results for the top and bottom panels are shown in figure 5.33.
As can be seen from the figure the new initial alignment have resulted in the before mentioned layers obtaining their expected orientation, hence supporting the above hypothesis. Recalling that the final value of the objective function was $7.29 \cdot 10^6$ with the previous initial configuration, whereas the final value for this optimisation was $7.26 \cdot 10^6$ shows the relative small influence of these misaligned centre layers. It is worth noticing that the second optimisation converged in 59 iterations instead of the 471 iterations needed for the original initial configuration. This indicates that many of the design variables had been initialised close to their optimum values.

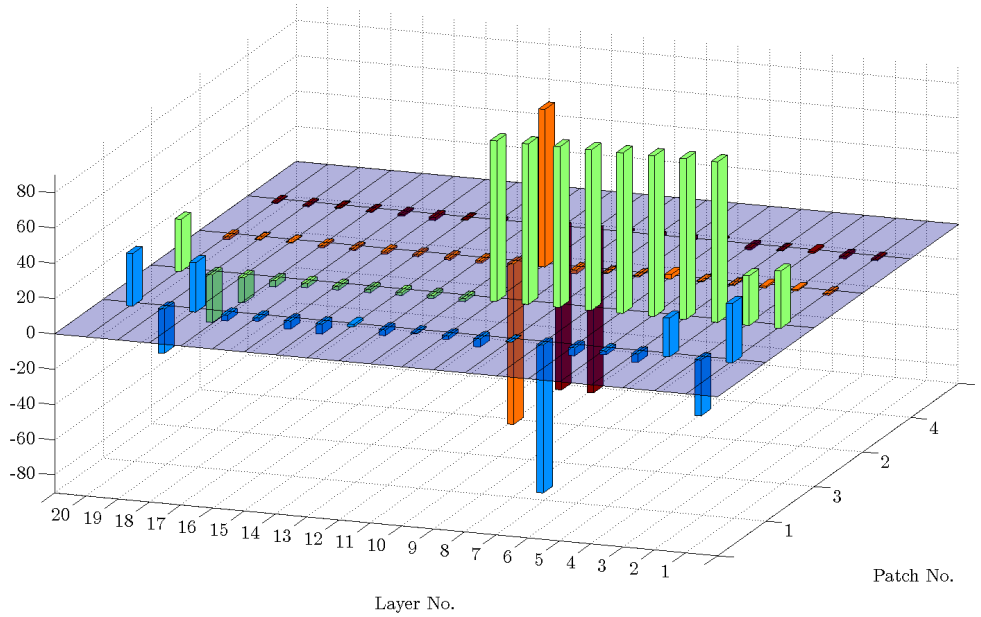

Figure 5.32: *Final design variables for the four top and bottom patches i.e: 1, 3, 2, 4. Each patch no. has been assigned a unique colour. The third axis shows the fibre orientation (MCS) in the given layer for the specific patch.*

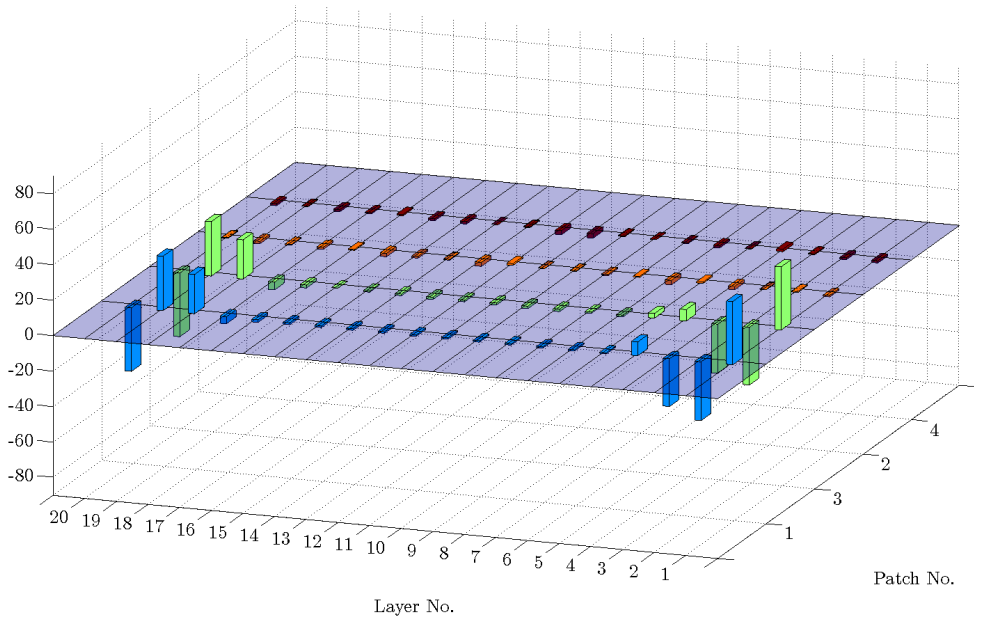

Figure 5.33: *Optimised top and bottom patches, i.e patches: 1, 3, 2, 4. Initially aligned with the z-axis (SCS). Each patch no. has been assigned a unique colour. The third axis shows the fibre orientation (MCS) in the given layer for the specific patch.*

For comparative reasons the main spar has also been optimised applying the DMO method. Here twelve candidate materials were applied: 0°, ±15°, ±30°, ±45°, ±60°, ±75°, 90°. The lay-ups produced by this method were similar to those presented in the above. The final value of the objective function was $7.63 \cdot 10^6$ which is in good coherence as the lay-ups were similar.

5.4.1 Summary

In the above it has been shown that the presented method for optimising composite structures can be applied on real life structures. However, the application of the identification process only resulted in a further reduction after the first identification of 1.9%. The results indicated that the given patch subdivision may have been too coarse, resulting in the problem being sufficiently optimised without the application of the identification process. The effect of the coarse patch design was also observed for the lay-ups associated with the side panels i.e. patches 13, 15, 14, and 16. Here it was argued that the optimised lay-up could have been refined if additional patches had been applied in these regions.

It was also shown that if a given laminate has layers which are aligned "incorrectly" and the identification can determine another lay-up, either by changing the design variable to something new or by switching the bounds, this new lay-up may still prove to be improper for further optimisation. This was observed for patches where the main state of stress was normal stresses due to bending. Here the middle layers in the laminate had little influence on the overall bending stiffness, resulting in the sensitivities being of too low a magnitude for the gradient based optimiser to "catch" the specific design variable and adjust it to the "correct" alignment. The misalignment was removed by utilising a different initial set of values for the design variables which resulted in a relatively low reduction of the strain energy. The reduction indicated that the misaligned lay-ups had the expected minor influence upon the stiffness.

Even though the optimisation resulted in a reasonable lay-up this can hardly be applied without first post-processing the design. E.g. The layers which had been aligned with the length direction were not exactly aligned, many of them were off by $\pm 2-5°$, which is unpractical from a manufacturing point of view. This can also be argued for other alignments which are offset from what can be regarded as "standard" orientations. In order for such problems to be eliminated manufacturing constraints w.r.t fibre-continuity and -alignment should be implemented in the optimisation and identification process.

Chapter

6

Discussions & Conclusions

In this chapter discussions and conclusions are made on basis of the preceding chapters. First different aspects and results from the thesis will be discussed in a great overview. Afterwards some conclusions will be drawn.

This thesis has been concerned with the development and implementation of a new method for performing optimising of laminated composite structures. The method has been implemented into the finite element analysis and optimisation tool MUST, which is developed and maintained by the Department of Mechanical & Manufacturing Engineering at Aalborg University.

The new method is based on preliminary ideas of another method originally presented by [Foldager, 1999]. The method by [Foldager, 1999] used a *two-step approach* in attempt to overcome the non-convex nature of the design space associated with optimisation of composite structures w.r.t the fibre orientations. However, the method proved to be flawed and was rejected. The idea of a two-step approach were quite ingenious though. Thus the preliminary ideas of [Foldager, 1999] were adopted by the authors of this thesis in an attempt to develop a new and more robust method which was presented in [Kann and Sørensen, 2010]. The method utilises characteristics of the so-called *lamination parameters* to overcome the non-convex nature of the design space associated with performing fibre angle optimisation of composite laminates. The method was, as well as the method by [Foldager, 1999], developed for application on laminated plates described by CLT or FSDT. The work in this thesis has been concerned with expanding the previously presented method so as it could be used on shell structures in a finite element application. In order to do so the essential lamination parameters had to be extracted from the finite element equations describing the shell stiffness. This required the application of explicit thickness integration of the constitutive properties of the shells. This extraction of the lamination parameters was first shown by [Hvejsel and Hansen, 2007]. With the shell lamination parameters at hand the new method was formulated for the application on shell structures, as have been illustrated throughout this thesis.

In order to test the performance of the newly developed method a number of numerical experiments were conducted. In general, the conducted experiments can be divided into two groups, namely experiments of "academic" character, which are well known examples that are tested with the new method in order to benchmark its performance against some frame of reference, and experiments of "industrial/practical" character, which are experiments with no frame of reference that are conducted in order to test the performance in a more real-life context.

Several "academic" benchmark experiments have been conducted and it was shown that the presented two-step method indeed is capable of bypassing the local minimum solutions often determined when performing stiffness optimisation on laminated composite structures. The final results from the experiments were compared with both solutions published by other authors and solutions obtained by use of the method of *Discrete Material Optimisation*, which has been presented by

[Stegmann and Lund, 2005]. The obtained results proved to be in good coherence with these other solutions.

Identification of new lay-ups on the basis of 12 lamination parameters have shown to be very efficient for plates, as well as for both thin and thick curved shells. Experiments have also been performed where 20 lamination parameters were used for identifying new lay-ups for curved shells. This formulation did, however, prove to be so restrictive with regards to determining new lay-ups that it is not recommended — especially in the light of the results obtained with 12 lamination parameters. However, it is clear that if a new lay-up for a curved structure is found by applying only 12 lamination parameters some information is also lost. This means that the identified lay-up will in fact be more "different" from the original lay-up than a lay-up identified with 20 lamination parameters would. It could be argued though that if optimisation is used in the design of a structure, then the exact development of the specific design is in some ways a little out of the designers hands anyway, and as such it might seem as a peculiar principle to keep the lamination parameters on such a tight leash. On the other hand, applying to few lamination parameters enables the risk that the stiffness change unexpected. However, the results of this thesis indicates that the last 8 of the 20 lamination parameters tend to "follow" the first 12 lamination parameters, thus reducing the risk.

Generally it has been observed that many of the numerical experiments exhibited the first local minimum due to the gradient based optimiser being "stuck" on the bounds of the design space. In these situations the identification process often resulted in the affected design variables having their value interchanged to the opposite bound value. This substitution of bounds often proved to be enough for the gradient based optimiser to continue minimising the objective function. The switching of the bounds was of course only possible because the bounds in the experiments were mirrored with respect to the same value i.e. $[-x^\circ; x^\circ]$. In general, it also seems that the first identification processes characterised by many bound switches are also followed by a rather large decrease in strain energy over the succeeding iterations. Thus it must be considered to be a significant function of the identification process. In fact, it might make good sense to structure this part of the identification process a little more. If such a decrease in the objective function can be obtained by simply switching a number of bounds, then it might be worth to do some kind of structured switching of bounds prior to the identification process. A "poor mans approach" to such an improvement could be to do an expansion of the design space and thus make it contain the same physical lay-ups several times. E.g. instead of using $[-90^\circ, 90^\circ]$ as bounds, $[-360^\circ, 360^\circ]$ could be used. It is worth noticing though that lay-ups with new values also are seen to reduce the objective function several places. A structures switching of bounds should not replace the identification process, but simply be run prior to it.

The results also showed that even though a successful identification of a new lay-up could be performed, it might not result in the gradient based optimiser being able to reduce the objective function further. This could happen if the identified lay-up also was located in a minimum, or if the global minimum had been reached. For the latter scenario, it might seem contradictory that other lay-ups can be identified if the global minimum has been determined. However, because of the periodic nature of the design space the global optimum solution may be located in several locations rotated by 180°. These "redundant" identified lay-ups can thus be regarded as trivial. However, other lay-ups can also be identified if the optimisation has converged to a, strictly speaking, non-optimum solution. This can e.g. become a problem for structures loaded in pure-bending. Here the middle layers have little to none influence on the bending stiffness, and thus they may be aligned somewhat randomly even if the optimisation has converged to what can be interpreted as a minimum within the current tolerance. The identification process can thus repeatedly determine new orientations for these layers, without the gradient based optimiser being able to adjust the fibre direction to the correct alignment. In order to overcome this ambiguity of repeatedly determining trivial solutions, the identification process has been set to terminate if ten successive identified lay-ups haven't resulted in any further reduction of the objective function. This procedure could be improved significantly if history of the previous design were available in the implementation. Eliminating previously tried

designs, and periodic repetitions of it, from the possible outputs could make the routine somewhat smarter. However, the effect of such an implementation is unknown since this data history is not enabled at current time.

In general the final designs determined by the optimisation algorithm are not directly applicable from a manufacturing point of view. This is mainly due to numerical issues. The problem arises at the areas where the fibres are in fact aligned properly in one direction. Even though the fibres here all seem orientated at a common angle, they do, with the current tolerances, vary with 0°–2°. A similar problem is observed for the case for the middle layers of a laminate in pure-bending. Here the middle layers give so little contribution (due to the z'-coordinate being close to 0) to the bending stiffness that the optimisation algorithm is simply not able to catch the numerical differences. The result is that the fibre orientations in such areas are somewhat randomly aligned, even though examining the equations indicates that there is a preferred orientation. These problems strongly substantiate the need for post-processing. With the current method, post-processing can simply not be avoided. However, it is possible to imagine that some of the post-processing could be done automatically if an algorithm were developed for it. However, it should also be noted that many of these issues would be solved if the identification process could succeed with only a few layers.

The method has also been tested on what may be referred to as a real life structure. The chosen structure was a generic main spar which is the primary load carrying structure in some designs of wind turbine blades. The load scenario applied in the example was bending by a traverse pressure load at the tip of the main spar. Thus emulating the flap-wise bending occurring in the blade as a consequence of the wind load. The optimisation resulted in a design which seems reasonable for the given patch breakdown and load scenario. However, the application of the identification process only resulted in a further improvement of 1.9% which is regarded as negligible. This low improvement is believed to be a consequence of the patch breakdown being too coarse in combination with a relatively simple load scenario. Hence, the initial optimisation performed by a gradient based algorithm was able to determine a design close to the global minimum. Nevertheless, the example showed that the method can be applied on real life structures.

6.1 Conclusions

The conclusion of the thesis is that a method for doing maximum stiffness optimisation of composite shell structures have been developed an implemented with success. The results have shown that local minima can be bypassed by use of the implemented identification process. This identification process can be performed with either 12, 20, or 28 lamination parameters, thus giving full support for shell structures. However, the results show that using 20 or 28 lamination parameters is very restrictive and hence no new lay-ups are identified. Using just 12 lamination parameters on the other hand, is seen to give good results both for plates and for curved shells, both provided that the structure is made with at least 11 layers. Worth mentioning is though that the effect of the (first) identification process, to a large extent, is that design variables are switched from one bound to the other. Thus the optimisation process could profitably be performed with an expanded design space. Also the need for post-processing is apparent in all results obtained. However, the final conclusion shall be that the method can in fact be applied to real-life structures, provided that the material is the same throughout the thickness of the laminate.

Chapter

7

Future Perspectives

In this short chapter some suggestions for further work within the area of this thesis are given.

In the numerical experiments it was noticed that many of the design variables were caught on the bounds of the design space. This was observed by the fact that many of the initial identifications resulted in design variables located on a bound having their value changed to the opposite boundary value. After which the gradient based optimiser was able to reduce the objective function a substantial amount. The applied bounds were obviously too tight as most of the experiments got stuck on either of the bounds. Thus an expansion of the bounds seem to be appropriate e.g. to $[-360°;360°]$. Thus reducing the possibility of the optimiser getting stuck in a local minimum due to the bounds. Alternatively a loop through the design variables could be initiated, when the gradient based optimiser has converged, to check if any of them are at the bounds and the ones that are may have their values switched to the opposite bound. After this the optimiser can be reengaged to see if further reduction of the objective function has been made possible. If this is not possible the identification process can be initiated. This procedure is of course only applicable for design variables which represent the fibre orientations.

The current implementation of the method employs a scheme where if ten successive failed identification processes have occurred, the optimisation process will be terminated. This has been implemented in order to avoid the scenario where the optimisation algorithm gets stuck in an infinite loop of successful, but trivial, identified lay-ups. Instead a more systematic solution to the problem could be applied. If an identification resulted in a lay-up which proved not to be different enough for the gradient based optimiser to reduce the objective function any further, this lay-up could be stored and utilised for comparison in the next identification. Thus if this lay-up should appear again in the next identification it may be disregarded and removed from the current population in the genetic algorithm. Hence if two successive identified lay-ups were unable to reduce the objective function any further, the third identification would have two lay-ups to compare the new lay-up against. This procedure could possibly reduce the amount of computational time required for determining if the optimisation process has converged to a near global minimum solution.

As previously noted throughout the thesis it is only possible to identify new lay-ups if the essential several-to-one relationship can be established between the lamination parameters and the design variables. This requires a minimum of 11 layers in an element when applying ply-orientations as design variables [Kann and Sørensen, 2010]. However, this requirement may be reduced if thicknesses are added as design variables. The current implementation does not support thicknesses as design variables. It is, however, believed to be possible to add thickness support in the genetic algorithm, both in the form of continues and discrete sets of allowable thicknesses. Most of the functionalities have already been implemented. What is still needed is bookkeeping as the design variables have to be separated into two groups, i.e. fibre orientations and ply-thicknesses, in order to apply discrete

values for the thicknesses.

One of the characteristics with lamination parameters is that there always is a constant number of parameters, no matter how many layers the laminate consists of. This property can be exploited to add or remove layers from a laminate during the identification process. The identification algorithm is simply supplied the lamination parameters as usual, however, by supplying a modified set of bounds which represent the new lay-up, the identification algorithm can determine a lay-up, with the specified number of plies, which match the supplied lamination parameters. The optimisation process can thus continue to reduce the objective function with the new lay-up.

The genetic algorithm which has been developed and implemented in MUST does currently only support constraints in the form of upper and lower bounds on the design variables. However, if thicknesses are to be included in future versions of the identification algorithm it would be desirable to have support for different types of constraints e.g. equality and inequality constraints. The simplest way of adding these constraints is to convert the constrained problem into an unconstrained problem by penalising the objective function. However, more sophisticated methods have also been developed specifically for genetic algorithms. Here the reader is referred to i.e. [Nanakorn and Meesomklin, 2001]. Note that the local gradient based optimisation in the current implementation is performed by use of a *Methods of Feasible Directions* algorithm, which supports both equality and inequality constraints.

Another form of relevant constraints that could be implemented in future versions are failure criteria. Furthermore the method has only been applied for minimising the compliance of a laminate. The application of other objective functions such as maximising the lowest buckling load are just as essential when dealing with thin composite structures such as laminated plates and shells. Here it is worth noting that maximisation of the minimum buckling load according to [Svanberg, 1984] also displays convexity when formulated with lamination parameters as design variables, and thus the performance of such a formulation can be be expected to be somewhat similar.

References

Jasbir S. Arora. *Introduction to Optimum Design*. Elsevier Academic Press, 2 edition, 2004. ISBN 0120641550.

M.W. Bloomfield, C.G. Diaconu, and P.M. Weaver. On feasible regions of lamination parameters for lay-up optimization of laminated composites. *Proceedings of the Royal Society of London, Series A (Mathematical, Physical and Engineering Sciences)*, 465(2104):1123–1143, April 8 2009. ISSN 1364-5021.

Robert D. Cook, David S. Malkus, Michael E. Plesha, and Robert J. Witt. *Concepts and Applications of Finite Element Analysis*. John Wiley & Sons, INC, 111 River Street, Hoboken, NJ 07030, 4 edition, 2002. ISBN 9780471356059.

Jacob Peled Foldager. *Design of Composite Structures*. PhD thesis, Institute of Mechanical Engineering, Aalborg University, July 1999. ISSN 0905-2305.

Hisao Fukunaga and Hideki Sekine. Stiffness design method of symmetric laminates using lamination parameters. *AIAA*, 30(11):2791–2793, 1992. doi: 10.2514/3.11304.

J. L. Grenestedt and P. Gudmundson. Lay-up optimisation of composite material structures. In P. Pedersen, editor, *Optimal Design with Advanced Materials*, volume The Frithiof Niordson, pages 311–336. IUTAM, Elsevier, 1993. ISBN 0444898697.

V. B. Hammer, M. P. Bendsøe, R. Lipton, and P. Pedersen. Parametrization in laminate design for optimal compliance. *International Journal of Solids and Structures*, 34(4):415–434, 1997. ISSN 0020-7683. doi: DOI:10.1016/S0020-7683(96)00023-6. URL http://www.sciencedirect.com/science/article/B6VJS-3T5X39J-K/2/ded7d85a09927726281ecef8b2e2c05c.

J. Huang and R.T. Haftka. Optimization of fiber orientations near a hole for increased load-carrying capacity of composite laminates. *Structural and Multidisciplinary Optimization*, 30:335–341, 2005. ISSN 1615-147X. URL http://dx.doi.org/10.1007/s00158-005-0519-z. 10.1007/s00158-005-0519-z.

Christian Gram Hvejsel and Henrik Fredslund Hansen. Efficent finite element formulation for analysis and optimization of laminated composite shell structures. Master's thesis, Department of Mechanical Engineering, Aalborg University, June 2007.

Robert M. Jones. *Mechanics of Composite Materials*. Taylor & Francis Group, 2 edition, 1999. ISBN 1-56032-712-X.

Jesper Kann and René Sørensen. Optimisation of composite structures by use of a lamination parameters approach. 9th semesters report, Aalborg University Department of Mechanical & Manufacturing Engineering, Pontoppidanstræde 105 Aalborg Ø, December 2010.

W. P. Prema Kumar and R. Palaninathan. Finite element analysis of laminated shells with exact through-thickness integration. *Computers & Structures*, 63(1):173 – 184, 1997. ISSN 0045-7949. doi: DOI:10.1016/S0045-7949(96)00297-0. URL http://www.sciencedirect.com/science/article/B6V28-3SMSMYB-H/2/faa7ee555109613e5fd66ee59868e8b9.

W. P. Prema Kumar and R. Palaninathan. Explicit through-thickness integration schemes for geometric nonlinear analysis of laminated composite shells. *Finite Elements in Analysis and Design*, 32(4):235 – 256, 1999. ISSN 0168-874X. doi: DOI:10.1016/S0168-874X(99)00006-2. URL http://www.sciencedirect.com/science/article/B6V36-3X23HR4-3/2/6ef069e6748899072ffd417f6492e2e9.

Steffen Laustsen and Jakob Vestergaard. Design study of a wind turbine blade. Master's thesis, Institute of Mechanical and Manufacturing Engineering, Aalborg University, Denmark, Fibigerstræde 16, DK-9220 Aalborg East, Denmark, June 2010.

R. Lipton. On optimal reinforcement of plates and choice of design parameters. *Control and Cybernetics*, 23(3):481–493, 1994. ISSN 0324-8569.

Mitsunori Miki. Material design of composite laminates with required in-plane elastic properties. In *Progress in Science and Engineering of Composites*, pages 1725–1731. ICCM-IV, 1982.

Pruettha Nanakorn and Konlakarn Meesomklin. An adaptive penalty function in genetic algorithms for structural design optimization. *Computers & Structures*, 79(29-30):2527 – 2539, 2001. ISSN 0045-7949. doi: DOI:10.1016/S0045-7949(01)00137-7. URL http://www.sciencedirect.com/science/article/pii/S0045794901001377.

Christopher Houck North, Jeffery A. Joines, Michael G. Kay, Christopher R. Houck, and Christopher R. Houck. A genetic algorithm for function optimization: A Matlab implementation. Technical report, 1996. URL http://citeseerx.ist.psu.edu/viewdoc/summary?doi=10.1.1.22.4413.

Michel Olagnon. Orderpack 2.0 – unconditional, unique, and partial ranking, sorting, and permutation downloadable fortran 90 source code. Downloaded at March 1st 2011. URL http://www.fortran-2000.com/rank/.

Hartmut Pohlheim. Evolutionary algorithms. December 6th 2010. URL http://www.geatbx.com/docu/algindex.html.

Shahriar Setoodeh, Mostafa M. Abdalla, and Zafer Gürdal. Design of variable-stiffness laminates using lamination parameters. *Composites Part B: Engineering*, 37(4-5):301 – 309, 2006. ISSN 1359-8368. doi: DOI:10.1016/j.compositesb.2005.12.001. URL http://www.sciencedirect.com/science/article/B6TWK-4JBGKM2-1/2/8d04f6a0cfb99a3ff3167b9c9fa31795.

Jan Stegmann and Erik Lund. Notes on structural analysis of composite structures. Institue of Mechanical Engineering, Aalborg University, Pontoppidanstraede 101, DK-9220 Aalborg East, Denmark, November 2002. 2nd Edition.

Jan Stegmann and Erik Lund. Discrete material optimisation of general composite shell structures. *International Journal for Numerical Methods in Engineering*, 62(14):2009–2027, February 9th 2005.

S. Sumathi, T. Hamsapriya, and P. Surekha. *Evolutionary Intelligence*. Springer-Verlag Berlin Heidelberg, 2008. ISBN 978-3-540-75158-8.

Krister Svanberg. On local and global minima in structural optimisation. *New directions in optimum structural design*, page 327Ű341, 1984.

Stephen W. Tsai and Nicholas J. Pagano. *Invariant Properties of Composite Materials, in Composite Materials Workshop*, pages 233–253. Tehnomic Pub. Co., 1968.

Olgired Cecil Zienkiewicz and R.L Taylor. *The Finite Element Method*, volume 1. McGraw-Hill Book Company, 4 edition, 1989. ISBN 0-07-084174-8. Basic formulation and linear problems.

Nomenclature

Latin Letters

$\underline{B}$	The strain-displacement matrix.
C	Compliance.
C_{ijkl}	The constitutive tensor.
d_i	Normalised sensitivity of strain energy density.
$\vec{d}_e$	Element displacement vector.
$\vec{D}$	Global displacement vector.
$\underline{G}$	Matrix containing shape function derivatives with respect to global coordinates.
h	The thickness of the shell.
h_a	The thickness of the shell in node a.
h_l	The thickness of the l'th layer.
$\vec{i}, \vec{j}, \vec{k}$	Global Cartesian base vectors.
$\underline{J}$	The Jacobian matrix.
$\underline{k}_e$	Element stiffness matrix.
$\underline{K}$	Global stiffness matrix.
n_{elem}	Number of elements.
n_{elemP}	Number of elements in a patch.
n_{LP}	Number of lamination parameters.
n_{shell}	The number of nodes in a shell element.
n_{solid}	Number of nodes in a solid element.
N_a^{2D}	Interpolation function for node a — is a function of the natural (r,s)-coordinates.
N_a^{3D}	Interpolation function for node a — is a function of the natural (r,s,t)-coordinates.
$N_{a,p}$	The partial derivative of N_a w.r.t. the variable p.
Q_{ij}	The components of the constitutive tensor, which traditionally is denoted as $\underline{Q}$ instead of $\underline{C}$ when dealing with laminaes.
r,s,t	Natural curvilinear coordinates.
$\vec{R}$	Global force vector.
$\underline{T}_{MG}$	Transformation matrix from MCS to global coordinate system.
$u_{,p}, v_{,p}, w_{,p}$	The partial derivative of the displacements w.r.t. the variable p.
$\vec{u}$	Global Cartesian displacements.
$\vec{u}_a$	Global Cartesian displacements of node a.
U	Strain energy.
U_d	Strain energy density.
V_p	Patch volume.
W	Work done by external loads.
$\vec{v}_3$	The thickness direction unit vector.
$\Delta\vec{v}_3^a$	Relative displacements of the node director in node a.
var_j	$= \frac{1}{j}(z'^j_k - z'^j_{k-1})$.
$x_1, x_2, ..., x_n$	Design variables.
$\vec{x}$	Design variable vector. Note the ambiguity with the next line as well.

$\vec{x}$	Global Cartesian coordinates of arbitrary point. Note the ambiguity with the previous line as well.
$\vec{x}_0$	Point on the reference surface.
$\vec{x}_a$	Global Cartesian coordinates of the nodes on the reference surface of a shell element.
$\vec{x}_a^{3D}$	Global Cartesian coordinates of node a in the solid element.

Greek Letters

γ	$= \frac{2\Delta_V}{h\Delta_A}$.
Δ_{A_e}	Average of Jacobian square root for element no. e.
Δ_{A_p}	Average of Jacobian square root for a patch.
Δ_{V_e}	Variation of Jacobian square root for element no. e.
Δ_{V_p}	Variation of Jacobian square root for a patch.
ε_{kl}	The strain tensor.
$\vec{\theta}$	Fibre orientations assembled in a vector.
$\vec{\theta}^*$	Initial/suboptimal angles assembled in a vector.
$\Delta\xi$	Fixed step size.
$\Delta\xi_i$	Individual allowable variation of each lamination parameter.
ξ_i^*	Initial lamination parameter.
$\vec{\xi}^*$	The initial set of lamination parameters assembled in a vector.
σ_{ij}	The stress tensor.

Other Symbols

$\underline{\partial}$	Differential operator matrix.

Appendix

A

Genetic Algorithm

This appendix is taken from the authors pervious work and only serves to give the reader an opportunity to fully understand how the genetic algorithm operates. The algorithm was originally coded in Matlab but has now been translated into Fortan code and implemented in MUST.

A.1 Description of the Algorithm

The section (and the implemented algorithm) is based on [Sumathi et al., 2008] and [Pohlheim, 2010].

Genetic algorithms are based on an idea to replicate natural evolution. The overall thought is to let a *population* of solutions to the problem evolve by *breeding* for a number of *generations* and thereby determine the solution to the problem. Which solutions to "breed" from is selected by a measure of *fitness*. Thus such algorithms are popularly said based on the principle of "survival of the fittest".

Components of Genetic Algorithms
Due to the descent from biology, genetics algorithms employ a number of new terms which are not normally used in the field of mechanics. The most important of these terms are explained in short here:

Individuals:	An individual is to be understood as a possible solution to the problem.
Population:	A population is a collection of all the current individuals.
Fitness function:	A fitness function is a function which in some way measures how good each solution is for the current problem. The fitness function can be understood as a kind of objective function for the genetic algorithm.

Parent selection: Parent selection is the process where it is decided which of the individuals from the current population that should be used for breeding. The individuals used for breeding are referred to as *parents*.

Recombination: Recombination is the process of combining variables from the parents to obtain new solutions. The process is also referred to as breeding.

Mutation: Mutation is a process incorporated in order to avoid "inbreeding" of the population.

The latter four of these terms will furthermore be elaborated on in the following overview of the implemented algorithm.

Brief Overview of Algorithm

A flowchart of the implemented algorithm is shown in figure A.1. In the following each of the boxes/-subroutines are explained in greater detail.

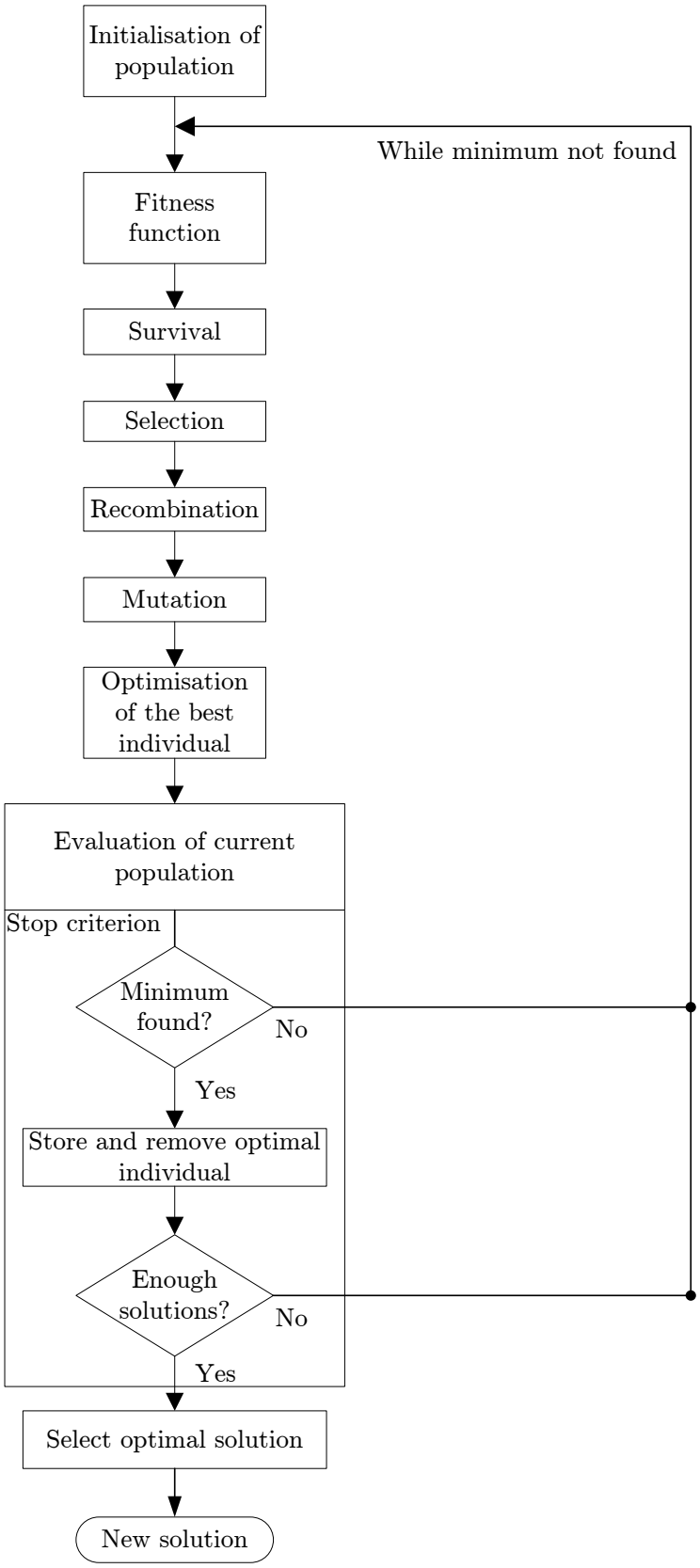

Figure A.1: *Flowchart of the implemented genetic algorithm. Each box represents a subroutine. The rhombus represents an if-statement.*

A.1.1 Initialisation of Population

Before starting the optimisation routine an initial population must be constructed. On beforehand it is determined how many individuals the population should consist of. The number of individuals in a population is referred to as N_{ind}. The population is simply created by creating N_{ind} individuals, where each individuals design variables are generated as random numbers within the bounds of the variables.

A.1.2 Fitness Function

The fitness function is a way to quantify how optimal each solution is. The objective is to rank the different individuals of the population depending on their optimality for the problem. Different ranking methods with both linear and nonlinear variants are available. However, what is used in this report is simply the identification function. However, genetic algorithms are meant to *maximise* rather than minimise, so the values have to be changed. This is simply done as:

$$fitness(\vec{\theta}) = I_{max} - I\left(\vec{\theta}\right) \tag{A.1}$$

where: I_{max} The maximum value of I found in the population.

A.1.3 Survival

In the survival-routine a predefined percentage of the best individuals of the population is selected for survival, also called elite survivors. This principal is applied so as to ensure that the best solutions are not lost due to either breeding or mutation in the next generation. Both uniform and nonuniform methods can be applied. What is used in this report is a uniform method. The uniform method passes a fixed percentage of elite survivors from the current generation to the next. The percentage is based on the percentage of parents which are to be selected for breeding. Thus if 90% of the population is selected for breeding, then the remaining 10% is selected for survival. However, no matter the specified percentage it is always ensured that the best individual survives for the next generation.

A.1.4 Selection

The selection routine determines which individuals of the current population that should be used for breeding. Different selection methods are available. In this project a method called *stochastic universal sampling method* (SUS method) is used.

The SUS method is illustrated in figure A.2. All individuals of the population are mapped to a continuous line segment where each individuals part of the line is equal in size to its fitness value relative to the sum of all fitness values. If the number of individuals to be selected is N_{sel}, then a line with N_{sel} pointers is generated. The individual, which each pointer points at, is selected for breeding. The pointer line is generated in two steps, first the location of pointer 1 is determined as a random number between 0 and $\frac{\sum_{i=1}^{N_{ind}} fitness_i}{N_{sel}}$. Secondly the remaining $N_{sel} - 1$ pointers are distributed evenly with a distance of $\frac{\sum_{i=1}^{N_{ind}} fitness_i}{N_{sel}}$ in between them.

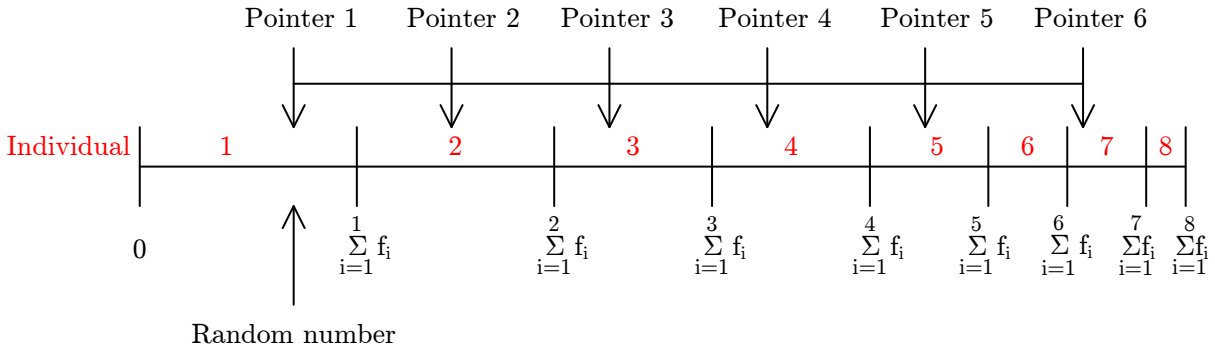

Figure A.2: *Illustration of how the stochastic universal sampling method works. Example where 6 individuals are selected. The selected individuals are 1, 2, 3, 4, 5, and 7.*

The SUS method roughly ensures that an individual with e.g. a 20% fitness value has a 20% chance of getting selected. The SUS method thus favours individuals with larger fitness values when compared to other selection methods such as the *roulette method*.

A.1.5 Recombination

Recombination, also called breeding, is the process of generating new solutions based upon other solutions. In this report a method called *arithmetic* is applied, however, other methods are also available. In connection with the methods name, the act of recombination is done as a simple linear combination of the two parents selected for breeding. The new solution, or child thus consists of a percentage of each parent, where the percentage is selected as a random number between 0 and 1 for each design variable. As two parents always have to give two new individuals the two linear combinations are made as:

$$\theta_i^{child_1} = r_i \theta_i^{parent_1} + (1 - r_i)\theta_i^{parent_2} \tag{A.2a}$$

$$\theta_i^{child_2} = (1 - r_i)\theta_i^{parent_1} + r_i \theta_i^{parent_2} \tag{A.2b}$$

where:

$\theta_i^{child_j}$	Design variable number i of child number j.
$\theta_i^{parent_j}$	Design variable number i of parent number j.
r_i	Random number.

A.1.6 Mutation

In order to avoid "inbreeding" (which also is known to give unfortunate consequences in genetic algorithms) some of the new childrens design variables are changed randomly in a mutation-process. On beforehand it is selected how large a percentage of the population that should undergo a mutation process and how many design variables each of these should have changed. The developed mutation algorithm works in three steps. First the individuals for mutation are selected randomly between the new children. Next, the design variables which are to be mutated is selected randomly, and at last the design variables are changed by a random number within the bounds of the selected variable. In this report a uniform mutation process is implemented, meaning that the percentage of mutation is constant through out the optimisation. Other methods have also been made available.

When all breeding and mutation are completed the elite survivors selected in the survival-routine are put into the population as well to give a new complete population.

A.1.7 Optimisation of the Best Individual

According to [North et al., 1996] local improvement of individuals can greatly improve the performance of a genetic algorithm. Thus a selection of the best individuals in the population is selected for conventional gradient-based optimisation, whereafter they are released back into the population. If the number of selected individuals is too high, the population may converge rapidly towards a local minimum before a thorough search of the design space has been made. Thus an upper bound of five individuals has been implemented.

A.1.8 Evaluation of Current Population

At last before the loop is started over the new population is evaluated w.r.t. stopping criteria. For the algorithm three criteria have been incorporated:

Stop if:

1. Current generation ≥ Maximum allowable number of generations.
2. (Mean value)-(Min value) ≤ ϵ.
3. (Min value) ≤ ϵ.

Here the mean value is the mean of the current population, min value is the minimum value, and ϵ is a small number. Criterion nr. 1 ensures that the algorithm does not continue indefinitely, whereas nr. 2 ensures that the algorithm stops if the population has converged to a suboptimal solution. If the third criterion is archived the specific solution is stored and removed from the current population. The motivation for this is that the population may contain better solutions than the current optimum solution. Here a better solution is defined as a solution which contains angles that differ from the angles the gradient based optimisation terminated with. If enough solutions have been extracted from the population, or if one of the other stop criteria is active, the best solution is selected.

A.1.9 Select Optimal Individual

If only one optimum solution has been extracted from the population, this solution is returned as the new solution and thus ending the identification process. If, however, more solutions have been extracted the best solution must be identified. Each solution is compared to the initial/suboptimal angles from which the gradient-based optimiser ended. The comparison between the solutions is determined as:

$$q_j = \left|\left|\cos\left(2\vec{\theta}^*\right) - \cos\left(2\vec{\theta}_j\right)\right|\right| \tag{A.3}$$

where:

q_j	Norm difference for extracted solution nr. j.
$\vec{\theta}_j$	Extracted solution nr. j. assembled in a vector
$\vec{\theta}^*$	Initial/suboptimal angles assembled in a vector.

Because fiber orientations of i.e $\theta = \pi$ gives the same stiffness in a lamina as $\theta = 0$, the factor of two is introduced in the comparison. Thus ensuring that two equivalent angles produce the same cosine value. When all extracted solutions have been compared to the suboptimal solution, the solution which produced the largest difference is selected as the new solution, and thus terminating the identification process.

Appendix

B

Stiffness Sensitivities w.r.t Lamination Parameters

In this appendix the analytic element stiffness sensitivities with respect to the lamination parameters are derived for each parameter.

B.1 Sensitivity for Element Stiffness Matrix

In section 3.2.2 a general expression for the sensitivity of an element stiffness matrix with respect to the lamination parameters were derived. This expression is repeated here for conveniens:

$$\begin{aligned}\frac{\partial \underline{k}_e}{\partial \xi_i^j} = \int_{-1}^{1}\int_{-1}^{1}\Bigg(& \underline{B}_1^T \frac{\partial \underline{E}_1}{\partial \xi_i^j}\underline{B}_1 + \underline{B}_1^T \frac{\partial \underline{E}_2}{\partial \xi_i^j}\underline{B}_2 + \underline{B}_1^T \frac{\partial \underline{E}_3}{\partial \xi_i^j}\underline{B}_3 \\ & + \underline{B}_2^T \frac{\partial \underline{E}_2}{\partial \xi_i^j}\underline{B}_1 + \underline{B}_2^T \frac{\partial \underline{E}_3}{\partial \xi_i^j}\underline{B}_2 + \underline{B}_2^T \frac{\partial \underline{E}_4}{\partial \xi_i^j}\underline{B}_3 \\ & + \underline{B}_3^T \frac{\partial \underline{E}_3}{\partial \xi_i^j}\underline{B}_1 + \underline{B}_3^T \frac{\partial \underline{E}_4}{\partial \xi_i^j}\underline{B}_2 + \underline{B}_3^T \frac{\partial \underline{E}_5}{\partial \xi_i^j}\underline{B}_3 \Bigg) \tfrac{2}{h}\Delta_A^2 \, dr\,ds \end{aligned} \tag{B.1}$$

where $i = 1,2,3,4$ and $j = A,B,D,E,F,G,H$.

Because the lamination parameters have different dependencies with respect to the thickness integrated constitutive properties, the above expression is reduced for each set of lamination parameters. The dependencies are as follows:

$$\underline{E}_1 = \underline{E}_1\left(\xi_i^A, \xi_i^B, \xi_i^D\right) \tag{B.2a}$$
$$\underline{E}_2 = \underline{E}_2\left(\xi_i^B, \xi_i^D, \xi_i^E\right) \tag{B.2b}$$
$$\underline{E}_3 = \underline{E}_3\left(\xi_i^D, \xi_i^E, \xi_i^F\right) \tag{B.2c}$$
$$\underline{E}_4 = \underline{E}_4\left(\xi_i^E, \xi_i^F, \xi_i^G\right) \tag{B.2d}$$
$$\underline{E}_5 = \underline{E}_5\left(\xi_i^F, \xi_i^G, \xi_i^H\right) \tag{B.2e}$$

In the following subsections expression (B.1) is shown for each lamination parameter. These were first shown by [Hvejsel and Hansen, 2007] and has been verified both analytically and numerically by the authors.

B.1.1 Sensitivity w.r.t Lamination Parameters ξ_i^A

$$\frac{\partial \underline{k}_e}{\partial \xi_i^A} = \int_{-1}^{1}\int_{-1}^{1} \left(\underline{B}_1^T \frac{\partial \underline{E}_1}{\partial \xi_i^A} \underline{B}_1 \right) \tfrac{2}{h} \Delta_A^2 \, dr\,ds \tag{B.3}$$

where

$$\frac{\partial \underline{E}_1}{\partial \xi_1^A} = \underline{T}_{MG}^T \underline{U} h \{0 \quad 1 \quad 0 \quad 0 \quad 0\}^T \underline{T}_{MG} \tag{B.4a}$$

$$\frac{\partial \underline{E}_1}{\partial \xi_2^A} = \underline{T}_{MG}^T \underline{U} h \{0 \quad 0 \quad 1 \quad 0 \quad 0\}^T \underline{T}_{MG} \tag{B.4b}$$

$$\frac{\partial \underline{E}_1}{\partial \xi_3^A} = \underline{T}_{MG}^T \underline{U} h \{0 \quad 0 \quad 0 \quad 1 \quad 0\}^T \underline{T}_{MG} \tag{B.4c}$$

$$\frac{\partial \underline{E}_1}{\partial \xi_4^A} = \underline{T}_{MG}^T \underline{U} h \{0 \quad 0 \quad 0 \quad 0 \quad 1\}^T \underline{T}_{MG} \tag{B.4d}$$

B.1.2 Sensitivity w.r.t Lamination Parameters ξ_i^B

$$\frac{\partial \underline{k}_e}{\partial \xi_i^B} = \int_{-1}^{1}\int_{-1}^{1} \left(\underline{B}_1^T \frac{\partial \underline{E}_1}{\partial \xi_i^B} \underline{B}_1 + \underline{B}_1^T \frac{\partial \underline{E}_2}{\partial \xi_i^B} \underline{B}_2 + \underline{B}_2^T \frac{\partial \underline{E}_2}{\partial \xi_i^B} \underline{B}_1 \right) \tfrac{2}{h} \Delta_A^2 \, dr\,ds \tag{B.5}$$

where

$$\frac{\partial \underline{E}_1}{\partial \xi_1^B} = \underline{T}_{MG}^T \underline{U} 2\gamma \tfrac{h^2}{4} \{0 \quad 1 \quad 0 \quad 0 \quad 0\}^T \underline{T}_{MG} \tag{B.6a}$$

$$\frac{\partial \underline{E}_1}{\partial \xi_2^B} = \underline{T}_{MG}^T \underline{U} 2\gamma \tfrac{h^2}{4} \{0 \quad 0 \quad 1 \quad 0 \quad 0\}^T \underline{T}_{MG} \tag{B.6b}$$

$$\frac{\partial \underline{E}_1}{\partial \xi_3^B} = \underline{T}_{MG}^T \underline{U} 2\gamma \tfrac{h^2}{4} \{0 \quad 0 \quad 0 \quad 1 \quad 0\}^T \underline{T}_{MG} \tag{B.6c}$$

$$\frac{\partial \underline{E}_1}{\partial \xi_4^B} = \underline{T}_{MG}^T \underline{U} 2\gamma \tfrac{h^2}{4} \{0 \quad 0 \quad 0 \quad 0 \quad 1\}^T \underline{T}_{MG} \tag{B.6d}$$

$$\frac{\partial \underline{E}_2}{\partial \xi_1^B} = \underline{T}_{MG}^T \underline{U} \tfrac{h^2}{4} \{0 \quad 1 \quad 0 \quad 0 \quad 0\}^T \underline{T}_{MG} \tag{B.6e}$$

$$\frac{\partial \underline{E}_2}{\partial \xi_2^B} = \underline{T}_{MG}^T \underline{U} \tfrac{h^2}{4} \{0 \quad 0 \quad 1 \quad 0 \quad 0\}^T \underline{T}_{MG} \tag{B.6f}$$

$$\frac{\partial \underline{E}_2}{\partial \xi_3^B} = \underline{T}_{MG}^T \underline{U} \tfrac{h^2}{4} \{0 \quad 0 \quad 0 \quad 1 \quad 0\}^T \underline{T}_{MG} \tag{B.6g}$$

$$\frac{\partial \underline{E}_2}{\partial \xi_4^B} = \underline{T}_{MG}^T \underline{U} \tfrac{h^2}{4} \{0 \quad 0 \quad 0 \quad 0 \quad 1\}^T \underline{T}_{MG} \tag{B.6h}$$

B.1.3 Sensitivity w.r.t Lamination Parameters ξ_i^D

$$\frac{\partial \underline{k}_e}{\partial \xi_i^D} = \int_{-1}^{1}\int_{-1}^{1}\Bigg(\underline{B}_1^T \frac{\partial \underline{E}_1}{\partial \xi_i^D}\underline{B}_1 + \underline{B}_1^T \frac{\partial \underline{E}_2}{\partial \xi_i^D}\underline{B}_2 + \underline{B}_1^T \frac{\partial \underline{E}_3}{\partial \xi_i^D}\underline{B}_3 + \underline{B}_2^T \frac{\partial \underline{E}_2}{\partial \xi_i^D}\underline{B}_1 + \underline{B}_2^T \frac{\partial \underline{E}_3}{\partial \xi_i^D}\underline{B}_2 + \underline{B}_3^T \frac{\partial \underline{E}_3}{\partial \xi_i^D}\underline{B}_1\Bigg)\frac{2}{h}\Delta_A^2 drds \tag{B.7}$$

where

$$\frac{\partial \underline{E}_1}{\partial \xi_1^D} = \underline{T}_{MG}^T \underline{U}\gamma^2 \frac{h^3}{12}\{0 \quad 1 \quad 0 \quad 0 \quad 0\}^T \underline{T}_{MG} \tag{B.8a}$$

$$\frac{\partial \underline{E}_1}{\partial \xi_2^D} = \underline{T}_{MG}^T \underline{U}\gamma^2 \frac{h^3}{12}\{0 \quad 0 \quad 1 \quad 0 \quad 0\}^T \underline{T}_{MG} \tag{B.8b}$$

$$\frac{\partial \underline{E}_1}{\partial \xi_3^D} = \underline{T}_{MG}^T \underline{U}\gamma^2 \frac{h^3}{12}\{0 \quad 0 \quad 0 \quad 1 \quad 0\}^T \underline{T}_{MG} \tag{B.8c}$$

$$\frac{\partial \underline{E}_1}{\partial \xi_4^D} = \underline{T}_{MG}^T \underline{U}\gamma^2 \frac{h^3}{12}\{0 \quad 0 \quad 0 \quad 0 \quad 1\}^T \underline{T}_{MG} \tag{B.8d}$$

$$\frac{\partial \underline{E}_2}{\partial \xi_1^D} = \underline{T}_{MG}^T \underline{U}2\gamma \frac{h^3}{12}\{0 \quad 1 \quad 0 \quad 0 \quad 0\}^T \underline{T}_{MG} \tag{B.8e}$$

$$\frac{\partial \underline{E}_2}{\partial \xi_2^D} = \underline{T}_{MG}^T \underline{U}2\gamma \frac{h^3}{12}\{0 \quad 0 \quad 1 \quad 0 \quad 0\}^T \underline{T}_{MG} \tag{B.8f}$$

$$\frac{\partial \underline{E}_2}{\partial \xi_3^D} = \underline{T}_{MG}^T \underline{U}2\gamma \frac{h^3}{12}\{0 \quad 0 \quad 0 \quad 1 \quad 0\}^T \underline{T}_{MG} \tag{B.8g}$$

$$\frac{\partial \underline{E}_2}{\partial \xi_4^D} = \underline{T}_{MG}^T \underline{U}2\gamma \frac{h^3}{12}\{0 \quad 0 \quad 0 \quad 0 \quad 1\}^T \underline{T}_{MG} \tag{B.8h}$$

$$\frac{\partial \underline{E}_3}{\partial \xi_1^D} = \underline{T}_{MG}^T \underline{U}\frac{h^3}{12}\{0 \quad 1 \quad 0 \quad 0 \quad 0\}^T \underline{T}_{MG} \tag{B.8i}$$

$$\frac{\partial \underline{E}_3}{\partial \xi_2^D} = \underline{T}_{MG}^T \underline{U}\frac{h^3}{12}\{0 \quad 0 \quad 1 \quad 0 \quad 0\}^T \underline{T}_{MG} \tag{B.8j}$$

$$\frac{\partial \underline{E}_3}{\partial \xi_3^D} = \underline{T}_{MG}^T \underline{U}\frac{h^3}{12}\{0 \quad 0 \quad 0 \quad 1 \quad 0\}^T \underline{T}_{MG} \tag{B.8k}$$

$$\frac{\partial \underline{E}_3}{\partial \xi_4^D} = \underline{T}_{MG}^T \underline{U}\frac{h^3}{12}\{0 \quad 0 \quad 0 \quad 0 \quad 1\}^T \underline{T}_{MG} \tag{B.8l}$$

B.1.4 Sensitivity w.r.t Lamination Parameters ξ_i^E

$$\frac{\partial \underline{k}_e}{\partial \xi_i^E} = \int_{-1}^{1}\int_{-1}^{1} \Bigg(\underline{B}_1^T \frac{\partial \underline{E}_2}{\partial \xi_i^E} \underline{B}_2 + \underline{B}_1^T \frac{\partial \underline{E}_3}{\partial \xi_i^E} \underline{B}_3 + \underline{B}_2^T \frac{\partial \underline{E}_2}{\partial \xi_i^E} \underline{B}_1 + \underline{B}_2^T \frac{\partial \underline{E}_3}{\partial \xi_i^E} \underline{B}_2 + \underline{B}_2^T \frac{\partial \underline{E}_4}{\partial \xi_i^E} \underline{B}_3 + \underline{B}_3^T \frac{\partial \underline{E}_3}{\partial \xi_i^E} \underline{B}_1 + \underline{B}_3^T \frac{\partial \underline{E}_4}{\partial \xi_i^E} \underline{B}_2 \Bigg) \tfrac{2}{h} \Delta_A^2 \, dr\,ds \tag{B.9}$$

where

$$\frac{\partial \underline{E}_2}{\partial \xi_1^E} = \underline{T}_{MG}^T \underline{U} \gamma^2 \tfrac{h^4}{32} \{0 \quad 1 \quad 0 \quad 0 \quad 0\}^T \underline{T}_{MG} \tag{B.10a}$$

$$\frac{\partial \underline{E}_2}{\partial \xi_2^E} = \underline{T}_{MG}^T \underline{U} \gamma^2 \tfrac{h^4}{32} \{0 \quad 0 \quad 1 \quad 0 \quad 0\}^T \underline{T}_{MG} \tag{B.10b}$$

$$\frac{\partial \underline{E}_2}{\partial \xi_3^E} = \underline{T}_{MG}^T \underline{U} \gamma^2 \tfrac{h^4}{32} \{0 \quad 0 \quad 0 \quad 1 \quad 0\}^T \underline{T}_{MG} \tag{B.10c}$$

$$\frac{\partial \underline{E}_2}{\partial \xi_4^E} = \underline{T}_{MG}^T \underline{U} \gamma^2 \tfrac{h^4}{32} \{0 \quad 0 \quad 0 \quad 0 \quad 1\}^T \underline{T}_{MG} \tag{B.10d}$$

$$\frac{\partial \underline{E}_3}{\partial \xi_1^E} = \underline{T}_{MG}^T \underline{U} 2\gamma \tfrac{h^4}{32} \{0 \quad 1 \quad 0 \quad 0 \quad 0\}^T \underline{T}_{MG} \tag{B.10e}$$

$$\frac{\partial \underline{E}_3}{\partial \xi_2^E} = \underline{T}_{MG}^T \underline{U} 2\gamma \tfrac{h^4}{32} \{0 \quad 0 \quad 1 \quad 0 \quad 0\}^T \underline{T}_{MG} \tag{B.10f}$$

$$\frac{\partial \underline{E}_3}{\partial \xi_3^E} = \underline{T}_{MG}^T \underline{U} 2\gamma \tfrac{h^4}{32} \{0 \quad 0 \quad 0 \quad 1 \quad 0\}^T \underline{T}_{MG} \tag{B.10g}$$

$$\frac{\partial \underline{E}_3}{\partial \xi_4^E} = \underline{T}_{MG}^T \underline{U} 2\gamma \tfrac{h^4}{32} \{0 \quad 0 \quad 0 \quad 0 \quad 1\}^T \underline{T}_{MG} \tag{B.10h}$$

$$\frac{\partial \underline{E}_4}{\partial \xi_1^E} = \underline{T}_{MG}^T \underline{U} \tfrac{h^4}{32} \{0 \quad 1 \quad 0 \quad 0 \quad 0\}^T \underline{T}_{MG} \tag{B.10i}$$

$$\frac{\partial \underline{E}_4}{\partial \xi_2^E} = \underline{T}_{MG}^T \underline{U} \tfrac{h^4}{32} \{0 \quad 0 \quad 1 \quad 0 \quad 0\}^T \underline{T}_{MG} \tag{B.10j}$$

$$\frac{\partial \underline{E}_4}{\partial \xi_3^E} = \underline{T}_{MG}^T \underline{U} \tfrac{h^4}{32} \{0 \quad 0 \quad 0 \quad 1 \quad 0\}^T \underline{T}_{MG} \tag{B.10k}$$

$$\frac{\partial \underline{E}_4}{\partial \xi_4^E} = \underline{T}_{MG}^T \underline{U} \tfrac{h^4}{32} \{0 \quad 0 \quad 0 \quad 0 \quad 1\}^T \underline{T}_{MG} \tag{B.10l}$$

B.1.5 Sensitivity w.r.t Lamination Parameters ξ_i^F

$$\frac{\partial \underline{k}_e}{\partial \xi_i^F} = \int_{-1}^{1}\int_{-1}^{1}\Bigg(\underline{B}_1^T \frac{\partial \underline{E}_3}{\partial \xi_i^F}\underline{B}_3 + \underline{B}_2^T \frac{\partial \underline{E}_3}{\partial \xi_i^F}\underline{B}_2 + \underline{B}_2^T \frac{\partial \underline{E}_4}{\partial \xi_i^F}\underline{B}_3 + \underline{B}_3^T \frac{\partial \underline{E}_3}{\partial \xi_i^F}\underline{B}_1 + \underline{B}_3^T \frac{\partial \underline{E}_4}{\partial \xi_i^F}\underline{B}_2 + \underline{B}_3^T \frac{\partial \underline{E}_5}{\partial \xi_i^F}\underline{B}_3\Bigg)\frac{2}{h}\Delta_A^2 \, dr\,ds \tag{B.11}$$

where

$$\frac{\partial \underline{E}_3}{\partial \xi_1^F} = \underline{T}_{MG}^T \underline{U}\gamma^2 \frac{h^5}{80}\{0 \quad 1 \quad 0 \quad 0 \quad 0\}^T \underline{T}_{MG} \tag{B.12a}$$

$$\frac{\partial \underline{E}_3}{\partial \xi_2^F} = \underline{T}_{MG}^T \underline{U}\gamma^2 \frac{h^5}{80}\{0 \quad 0 \quad 1 \quad 0 \quad 0\}^T \underline{T}_{MG} \tag{B.12b}$$

$$\frac{\partial \underline{E}_3}{\partial \xi_3^F} = \underline{T}_{MG}^T \underline{U}\gamma^2 \frac{h^5}{80}\{0 \quad 0 \quad 0 \quad 1 \quad 0\}^T \underline{T}_{MG} \tag{B.12c}$$

$$\frac{\partial \underline{E}_3}{\partial \xi_4^F} = \underline{T}_{MG}^T \underline{U}\gamma^2 \frac{h^5}{80}\{0 \quad 0 \quad 0 \quad 0 \quad 1\}^T \underline{T}_{MG} \tag{B.12d}$$

$$\frac{\partial \underline{E}_4}{\partial \xi_1^F} = \underline{T}_{MG}^T \underline{U}2\gamma \frac{h^5}{80}\{0 \quad 1 \quad 0 \quad 0 \quad 0\}^T \underline{T}_{MG} \tag{B.12e}$$

$$\frac{\partial \underline{E}_4}{\partial \xi_2^F} = \underline{T}_{MG}^T \underline{U}2\gamma \frac{h^5}{80}\{0 \quad 0 \quad 1 \quad 0 \quad 0\}^T \underline{T}_{MG} \tag{B.12f}$$

$$\frac{\partial \underline{E}_4}{\partial \xi_3^F} = \underline{T}_{MG}^T \underline{U}2\gamma \frac{h^5}{80}\{0 \quad 0 \quad 0 \quad 1 \quad 0\}^T \underline{T}_{MG} \tag{B.12g}$$

$$\frac{\partial \underline{E}_4}{\partial \xi_4^F} = \underline{T}_{MG}^T \underline{U}2\gamma \frac{h^5}{80}\{0 \quad 0 \quad 0 \quad 0 \quad 1\}^T \underline{T}_{MG} \tag{B.12h}$$

$$\frac{\partial \underline{E}_5}{\partial \xi_1^F} = \underline{T}_{MG}^T \underline{U}\frac{h^5}{80}\{0 \quad 1 \quad 0 \quad 0 \quad 0\}^T \underline{T}_{MG} \tag{B.12i}$$

$$\frac{\partial \underline{E}_5}{\partial \xi_2^F} = \underline{T}_{MG}^T \underline{U}\frac{h^5}{80}\{0 \quad 0 \quad 1 \quad 0 \quad 0\}^T \underline{T}_{MG} \tag{B.12j}$$

$$\frac{\partial \underline{E}_5}{\partial \xi_3^F} = \underline{T}_{MG}^T \underline{U}\frac{h^5}{80}\{0 \quad 0 \quad 0 \quad 1 \quad 0\}^T \underline{T}_{MG} \tag{B.12k}$$

$$\frac{\partial \underline{E}_5}{\partial \xi_4^F} = \underline{T}_{MG}^T \underline{U}\frac{h^5}{80}\{0 \quad 0 \quad 0 \quad 0 \quad 1\}^T \underline{T}_{MG} \tag{B.12l}$$

B.1.6 Sensitivity w.r.t Lamination Parameters ξ_i^G

$$\frac{\partial \underline{k}_e}{\partial \xi_i^G} = \int_{-1}^{1}\int_{-1}^{1} \left(\underline{B}_2^T \frac{\partial \underline{E}_4}{\partial \xi_i^G} \underline{B}_3 + \underline{B}_3^T \frac{\partial \underline{E}_4}{\partial \xi_i^G} \underline{B}_2 + \underline{B}_3^T \frac{\partial \underline{E}_5}{\partial \xi_i^G} \underline{B}_3 \right) \tfrac{2}{h} \Delta_A^2 \, dr\,ds \tag{B.13}$$

where

$$\frac{\partial \underline{E}_4}{\partial \xi_1^G} = \underline{T}_{MG}^T \underline{U} \gamma^2 \tfrac{h^6}{192} \{0 \quad 1 \quad 0 \quad 0 \quad 0\}^T \underline{T}_{MG} \tag{B.14a}$$

$$\frac{\partial \underline{E}_4}{\partial \xi_2^G} = \underline{T}_{MG}^T \underline{U} \gamma^2 \tfrac{h^6}{192} \{0 \quad 0 \quad 1 \quad 0 \quad 0\}^T \underline{T}_{MG} \tag{B.14b}$$

$$\frac{\partial \underline{E}_4}{\partial \xi_3^G} = \underline{T}_{MG}^T \underline{U} \gamma^2 \tfrac{h^6}{192} \{0 \quad 0 \quad 0 \quad 1 \quad 0\}^T \underline{T}_{MG} \tag{B.14c}$$

$$\frac{\partial \underline{E}_4}{\partial \xi_4^G} = \underline{T}_{MG}^T \underline{U} \gamma^2 \tfrac{h^6}{192} \{0 \quad 0 \quad 0 \quad 0 \quad 1\}^T \underline{T}_{MG} \tag{B.14d}$$

$$\frac{\partial \underline{E}_5}{\partial \xi_1^G} = \underline{T}_{MG}^T \underline{U} 2\gamma \tfrac{h^6}{192} \{0 \quad 1 \quad 0 \quad 0 \quad 0\}^T \underline{T}_{MG} \tag{B.14e}$$

$$\frac{\partial \underline{E}_5}{\partial \xi_2^G} = \underline{T}_{MG}^T \underline{U} 2\gamma \tfrac{h^6}{192} \{0 \quad 0 \quad 1 \quad 0 \quad 0\}^T \underline{T}_{MG} \tag{B.14f}$$

$$\frac{\partial \underline{E}_5}{\partial \xi_3^G} = \underline{T}_{MG}^T \underline{U} 2\gamma \tfrac{h^6}{192} \{0 \quad 0 \quad 0 \quad 1 \quad 0\}^T \underline{T}_{MG} \tag{B.14g}$$

$$\frac{\partial \underline{E}_5}{\partial \xi_4^G} = \underline{T}_{MG}^T \underline{U} 2\gamma \tfrac{h^6}{192} \{0 \quad 0 \quad 0 \quad 0 \quad 1\}^T \underline{T}_{MG} \tag{B.14h}$$

B.1.7 Sensitivity w.r.t Lamination Parameters ξ_i^H

$$\frac{\partial \underline{k}_e}{\partial \xi_i^H} = \int_{-1}^{1}\int_{-1}^{1} \left(\underline{B}_3^T \frac{\partial \underline{E}_5}{\partial \xi_i^H} \underline{B}_3 \right) \tfrac{2}{h} \Delta_A^2 \, dr\,ds \tag{B.15}$$

where

$$\frac{\partial \underline{E}_5}{\partial \xi_1^H} = \underline{T}_{MG}^T \underline{U} \gamma^2 \tfrac{h^7}{448} \{0 \quad 1 \quad 0 \quad 0 \quad 0\}^T \underline{T}_{MG} \tag{B.16a}$$

$$\frac{\partial \underline{E}_5}{\partial \xi_2^H} = \underline{T}_{MG}^T \underline{U} \gamma^2 \tfrac{h^7}{448} \{0 \quad 0 \quad 1 \quad 0 \quad 0\}^T \underline{T}_{MG} \tag{B.16b}$$

$$\frac{\partial \underline{E}_5}{\partial \xi_3^H} = \underline{T}_{MG}^T \underline{U} \gamma^2 \tfrac{h^7}{448} \{0 \quad 0 \quad 0 \quad 1 \quad 0\}^T \underline{T}_{MG} \tag{B.16c}$$

$$\frac{\partial \underline{E}_5}{\partial \xi_4^H} = \underline{T}_{MG}^T \underline{U} \gamma^2 \tfrac{h^7}{448} \{0 \quad 0 \quad 0 \quad 0 \quad 1\}^T \underline{T}_{MG} \tag{B.16d}$$

Appendix

C

CD

The following content is provided on the CD:

- Electronic copy of the report.
- Electronic copies of the following articles/reports:
  - [Kann and Sørensen, 2010]
  - [Tsai and Pagano, 1968]
  - [Miki, 1982]
  - [Grenestedt and Gudmundson, 1993]
  - [Lipton, 1994]
  - [Hammer et al., 1997]
  - [Foldager, 1999]
  - [Bloomfield et al., 2009]
  - [Svanberg, 1984]
  - [Fukunaga and Sekine, 1992]
  - [Setoodeh et al., 2006]
- The developed edition of MUST. The software is provided both as executable files as well as source code.
- Relevant FE-examples used in the report.